Interaction between retroviral Gag proteins and membranes

A dissertation presented to the faculty of the Graduate School of Cornell University In partial fulfillment of the requirements for the degree of doctor of philosophy

By

Robert Alfred Dick

August 2013

INTERACTION BETWEEN RETROVIRAL GAG PROTEINS AND MEMBRANES

Robert A Dick, Ph. D.

Cornell University 2013

Assembly of an infectious retroviral particle (virion) involves a set of events, including multimerization of thousands of Gag proteins, packaging of two copies of genomic RNA, and Gag interaction with the plasma membrane. While each of these events can be thought of as discrete, they are dependent on one another. The Gag polyprotein has three major domains: the N-terminal membrane-binding domain (MA), the central assembly domain (CA), and the C-terminal nucleic acid (or genomic RNA) binding domain (NC). According to one model for formation of virions, NC binds to genomic RNA, which promotes Gag multimerization, which in turn enhances membrane interactions. The work described in this thesis focuses on two aspects of this model, the response of Gag to lipids with different head groups and acyl chains, and the effect of multimerization of Gag on its interaction with membranes.

In a comparative study of Rous sarcoma virus (RSV) and human immunodeficiency virus type-1 (HIV-1) Gag, we found that, unlike HIV-1 Gag, RSV Gag was not dependent on the lipid phosphatidylinositol-4,5-phosphate (PI(4,5)P2) for membrane interaction and virus release *in vivo*. However, both Gag proteins had a similar response to mono-, di, and tri-phosphorylated phosphatidylinositols (PIPs) by an *in vitro* liposome flotation assay. I interpret these findings to suggest that in addition to

the specific interaction reported for HIV-1 Gag, PIPs enhance Gag membrane binding electrostatically. In a follow-up study I found that increasing the concentration of phosphatidylserine (PS) in the membrane resulted in dramatically more HIV-1 Gag binding, and this response to PS was modulated by the lipid acyl chains. Also, the presence of cholesterol in the membrane significantly increased the amount of Gag associated with the liposomes. I interpret these results to mean that Gag can sense the hydrophobic core of the lipid bilayer. To determine the effect of Gag multimerization on its binding to membranes, monomeric, dimeric, and hexameric MA chimeras were tested. *In vivo* and *in vitro,* increasing the multimeric state of MA increased its localization to the plasma membrane and to liposomes. These findings suggest that Gag binding to the plasma membrane is enhanced by multimerization.

BIOGRAPHICAL SKETCH

I haven't always known that science was right for me. In fact, I graduated High school with grades so low that going to college wasn't even an option. It wasn't that opportunities weren't available or that my parents didn't impress upon me the importance of education, but that I just lost my way. After high school graduation it was a struggle to pay my bills. Working multiple part time and full time jobs at once was barely enough. I wanted more out of life, so I enrolled in the local community college and two years later transferred to Iowa State University. The plan was to earn a degree in genetics and then go to law school. Patent law in an emerging industry seemed the best way to a six-figured salary from my point of view. But goals change. During the summer of my first research internship I was seduced by science. My new aim was to attend graduate school and pursue a career in scientific research.

As an undergrad I earned two NSF REU summer internship awards, one in the lab of Dr. Dan Voytas at Iowa State University and the second in the lab of Dr. Jian-Kang Zhu at the University of California Riverside. My summer project in the Voytas lab focused on Arabidopsis. I worked to characterize tissue expression of a family of light chain dynein motor proteins. The following summer, in the lab of Dr. Zhu, I worked to identify genes involved in DNA de-methylation. I also studied abiotic stress in plants by identifying mutants with decreased abscisic acid (ABA), a key component of stress response signaling.

Following my summer internship in the Voytas lab, Dr. Voytas asked me to join his group as an undergraduate researcher. I jumped at the opportunity. My

undergraduate research project, which was related to my master's thesis project, was the study of the yeast retrotransposable element Ty5. I performed yeast-two-hybrid analysis to identify amino acids that were important for the interaction between the retroelement's integrase protein and the yeast protein Sir4, a chromatin silencing complex protein. This research led to the identification of a cellular analog, Esc1, which had a domain homologous to Ty5 integrase.

After completion of my MS I moved to NY where I had been accepted to Cornell University's Biochemistry, Molecular and Cell Biology PhD program. Following the first year of course work and research rotations I joined the lab of Dr. Volker Vogt to study retroviral genomic RNA packaging. For about a year I worked to characterize the interaction between the genomic RNA packaging signal (Psi) and the C-terminal end of the retroviral structural protein, Gag. During this time I not only learned about RNA structure and function, I also learned many techniques necessary to handle, prepare and study both RNA and protein. However, as I worked on this project, I became interested in something else, the interaction between Gag and membranes. For the remainder of my PhD I worked to characterize this interaction.

ACKNOWLEDGEMENTS

I would like to start by thanking Volker Vogt. My success would not have been possible without his continuous support and mentorship. I would also like to thank Jerry Feigenson. His enthusiasm for science is contagious, and always welcome. Thanks also to all my committee members for their advice and guidance over the years.

Volker's lab is small, making each interaction with fellow lab mates that much more important. Over the years I have learned from each member of the Vogt lab: Bob Suran, Judy Phillips, Kari Dilley, Jany Chan, and Di Luo Bush. Thank you all.

A graduate school experience is not complete without the responsibility of mentoring undergrads. Thank you Steven Chen and Katherine Konvinse for your hard work and willingness to learn from me. I wish you both the greatest success.

I would like to thank my mother, Dara, my father, Robert, and my sister, Laura. You have supported and encouraged me in ways only a loving family can.

Lastly, thank you Megan Cox. I could not have wished for a more excellent partner in crime.

TABLE OF CONTENTS

LIST OF FIGURES

LIST OF TABLES

Chapter 3

LIST OF ABBREVIATIONS

Lipids

16-DSA: 16-DOXYL-stearic acid
DOPC: dioleoyl phosphatidylcholine
DPPS: dipalmitoyl phosphatidylserine
DSPC: distearoyl phosphatidylcholine
GM3: monosialodihexosylganglioside
PA: phosphatidic acid
PC: phosphatidylcholine
PE: phosphatidylethanolamine
PI: phosphatidylinositol
PI(3,4,5)P3: phosphatidylinositol-(3,4,5)-trisphosphate
PI(3,5)P2: phosphatidylinositol-(3,5)-bisphosphate
PI(4,5)P2: phosphatidylinositol-(4,5)-bisphosphate
PI(4)P: phosphatidylinositol-(4)-phosphate
PIP: phosphatidylinositol-phosphate
pl-PE: plasmalogen phosphatidylethanolamine
POPC: palmitoyl, oleoyl phosphatidylcholine
PS: phosphatidylserine
SM: sphingomyelin

Proteins

5ptase: inositol polyphosphate-5-phosphatase E
5PtaseIV: polyphosphoinositide 5-phosphatase IV
Alix: ALG-2-interacting protein X; also called AIPI
CA: capsid, a domain of Gag
CHMP: charged multivesicular body protein, part of ESCRT III complex
CRM1: chromosome region maintenance 1
ENTH/ANTH: epsin N-terminal homology domains/AP180 N-terminal homology
Env: envelope protein in retroviruses
FKBP: FK506-binding protein
Gag: group specific antigen, the internal structural protein in retroviruses
GFP: green fluorescent protein
IN: integrase
LDLR: low-density lipoprotein receptors
LEDGF/p75: lens Epithelium-derived Growth factor
MA: matrix, a domain of Gag
MARKS: myristoylated alanine-rich C kinase substrate
MBD: membrane binding domain
MβCD: methyl-β-cyclodextrin
NC: nucleocapsid, a domain of Gag
Nedd4: neural precursor cell expressed developmentally down-regulated protein 4
PH-GFP: pleckstrin homology domain-green fluorescent protein

Pol: polymerase
PR: retroviral protease
RT: reverse transcriptase
Sir4p: silent information regulator protein
SM: super-M or super membrane binder
SP or SP1: spacer peptide, a small segment of RSV and HIV Gag
Src: protein product of RSV oncogene
SU: surface component of the retroviral Env protein
TEM: tetraspanin-enriched microdomain
TGN: trans-Golgi network
Thy-1 (CD90): thymocyte differentiation antigen 1 (Cluster of differentiation 90)
TIP47: 47-kDa tail interacting protein, putative binding partner of HIV Env and MA
TM: transmembrane component of the retroviral Env protein
TSG101: tumor susceptibility gene 101
Znk: zinc knuckle

Viruses
ASLV: avian sarcoma leukosis virus
EIAV: equine infectious anemia virus
HIV: human immunodeficiency virus
HTLV: human T-cell leukemia virus type 1
MLV: murine leukemia virus
MPMV: Mason-Pfizer monkey virus
RSV: Rous sarcoma virus
SFV: simian foamy virus
SIV: simian immunodeficiency virus
Ty3 and Ty5: Transposons of yeast 3 and 5

Other
-sssDNA: minus-strand strong-stop DNA
+sssDNA: plus-strand strong-stop DNA
AIDS: acquired immunodeficiency syndrome
BB: dimerization chemical AP20187
cEMT: cryo-electron microscope tomography
CMS: cell membrane spheres
CTD: C-terminal domain, here referring to the CA protein
DIS: dimerization initiation site
DRM: detergent resistant membranes
dsDNA: double stranded DNA
D_T : rate of lateral diffusion (translational diffusion coefficient)
ESCRT: endosomal-sorting complex required for transport
ESR: electron spin resonance
FCS: fluorescent correlation spectroscopy
FRET: Förster resonance energy transfer

GPMV: giant plasma membrane derived vesicle
GUV: giant unilamellar vesicle
HAART: highly active antiretroviral therapy
IP6: inositolhexakisphosphate
LANR: low angle neutron reflectometry
LAT: linker for activation of T cells
L_d : liquid-disordered
L_o : liquid-ordered
LUV: large unilamellar vesicle
L_β : solid-gel
MVB: multivesicular bodies
myr: myristoylation or myristate
NLS: nuclear localization signals
NMR: nuclear magnetic resonance
NTD: N-terminal domain, here refers to CA protein
PBS: primer-binding site
PIC: pre-integration complex
PM: plasma membrane
PPT: polypurine track
Psi: packaging sequence
RBL-2H3: rat peripheral blood cells
RSE: rapid solvent exchange
S: order, or degree of movement, of segmented acyl chains
SAXS: small angle x-ray scattering
SEC: size exclusion chromatography
SLD: scattering length densities
TIRF: total internal reflection fluorescence microscopy
UTR: untranslated regions
vgRNA: viral genomic RNA
VLP: viral like particle
WT: wild type
$\Delta\Theta$: The space the acyl chain samples

CHAPTER 1

INTRODUCTION

ENVELOPED VIRUSES

All retroviruses are enveloped, a common characteristic of many animal viruses. The viral envelope is a lipid bilayer derived from the host cell. The acquisition of a viral envelope is a strategy employed by both RNA and DNA viruses to protect their genome. Many enveloped viruses are linked to human pathogenicity including the RNA virus influenza, a member of the family *Orthomyxoviridae*, the DNA virus smallpox, a member of the family *Poxviridae*, and the retrovirus responsible for acquired immunodeficiency syndrome (AIDS), human immunodeficiency virus (HIV-1). The viral envelope is not only composed of lipids but also has embedded in it the viral fusion glycoproteins and small amounts of cellular membrane-associated proteins. The glycoproteins serve to direct viruses to the correct host cell by specific interactions with receptor proteins, and to mediate fusion. This interaction leads to structural changes in the glycoprotein that provide some of the energy required for fusion between viral and host cell membranes.

Acquisition of the viral envelope is a coordinated process that involves viral and cellular proteins. Most retroviruses acquire their envelope from the plasma membrane (PM) of the host cell. The Simian foamy virus (SFV), from the genus Spumarirus, is an exception to the rule. Foamy viruses, named because of the characteristic foamy appearance of infected cells, bud into the endoplasmic reticulum and are then likely

exocytosed into the extracellular space. Membrane acquisition from cellular membranes other than the PM is not uncommon for non-retroviruses.

Because enveloped viruses are more sensitive to desiccation and heat than are non-enveloped viruses, they typically require host-host contact for transmission. For example, HIV-1 requires fluid-fluid contact between hosts. The most common transmission routes for HIV are sexual contact, blood transfusions, and sharing of needles between intravenous drug users. Decreasing the spread of HIV-1 has been accomplished by increasing the use of condoms, blood screening, and clean needle programs. However, in developing countries, these simple measures have proven to be difficult to implement, and therefore HIV-1 continues to be a major threat to human health.

RETROVIRAL PATHOGENESIS

According to the world health organization, while the number of deaths is on a steady decline, approximately thirty four million people are currently infected with HIV-1 and two and a half million new infections are added annually. HIV-1 accounts for more than a million deaths a year. In comparison, flu accounts for one quarter to one half that number of deaths (151). Retroviruses cause many diseases including malignancies, immunodeficiencies, and neurologic disorders (54). It is clear that retroviruses represent a severe risk to human health, which is why it is so important that we study how they function. By understanding how retroviruses function we can better design drugs that minimize their spread.

The lentivirus HIV-1 is the prime example of a retrovirus that causes immunodeficiency. In humans, HIV-1 infects and kills CD4-positive T-cells, which over the course of many years leads to severe impairment of the host's immune system, a condition known as AIDS. AIDS is characterized by a low T cell count and an increase in the number of opportunistic infections not common in people with a healthy immune system, such as pneumonia. While a vaccine for HIV-1 remains elusive, extensive study into the molecular biology of HIV-1 has led to a number of different classes of antiretrovirals that, when used together (highly active antiretroviral therapy, HAART), have proven effective in preventing HIV-1 infection from progressing to AIDS. HAART is a cocktail of drugs that can include inhibitors of entry, reverse transcription, integration, and maturation. The cocktail is necessary because HIV rapidly escapes single blocks to its spread by having a large amount of genetic diversity. This diversity is a hallmark of retroviruses, and is caused by the error prone reverse transcriptase (RT), which generates roughly one mutation per viral genome.

Because of the threat to human health that retroviruses represent, it is important to continue to develop new strategies to combat them. By studying HIV-1 and model retroviruses like Rous sarcoma virus (RSV) and murine leukemia virus (MLV) we can characterize critical steps in the retroviral lifecycle that could be new targets for antiretrovirals.

RETROVIRAL GENOME

The retroviral genome is a single stranded RNA molecule between seven and twelve thousand bases in length (Fig. 1.1). The 5' and 3' ends of the genome are composed of untranslated regions (UTRs), which contain multiple elements critical to the virus. The primer-binding site (PBS), the packaging sequence (Psi), and the dimerization initiation site (DIS) are located in the 5'UTR. The PBS is a stretch of nucleotides that binds to a host cell tRNA which is required for initiation of reverse transcription. Psi and DIS direct genome packaging and dimerization, and both will be discussed in detail in a later section.

Retroviruses can be split into two categories, simple or complex. The genomes of simple retroviruses, RSV for example, code for three genes: *gag*, *pol*, and *env*. *Gag* codes for the structural protein Gag and, in the case of RSV, protease (PR). *Pol* encodes the enzymatic proteins, integrase (IN), RT, and for most retroviruses, PR. *Env* encodes the transmembrane envelope glycoprotein Env, which is processed in the Golgi to yield the two subunits, the surface protein (SU) and the transmembrane protein (TM). In addition to the three major genes, complex retroviruses code for multiple accessory proteins that are involved in the trafficking of retroviral components in the cell and adaptation to cellular restriction factors that act to prevent viral spread.

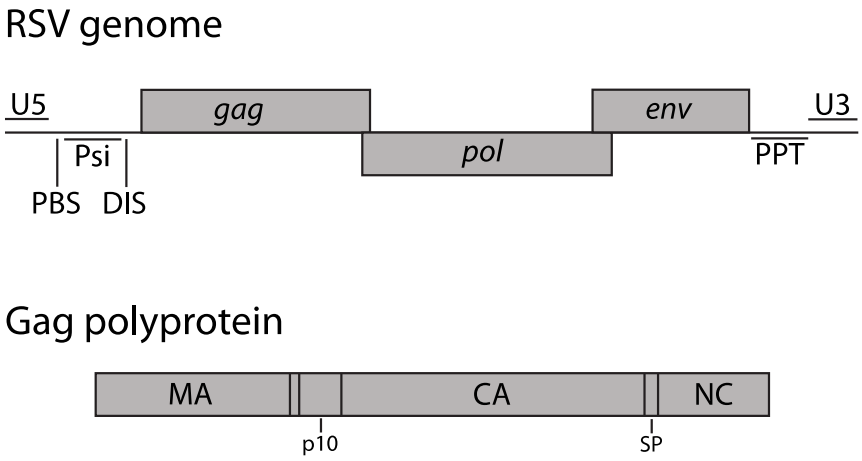

Fig 1.1 RSV genome and the Gag polyprotein. The RSV genome codes for three genes and a 5' and 3' UTR, which contains elements required for reverse transcription and packaging. The Gag polyprotein is shown with protease cleavage sites indicated by vertical lines. The three major domains, MA, CA, and NC, common to all retroviruses are shown. Minor cleavage products for RSV Gag, p10 and SP are also shown. The UTRs are not drawn to scale.

RETROVIRAL LIFECYCLE

The retroviral lifecycle is a complex process that can be split into multiple steps, including fusion of the virus with the host cell, reverse transcription of the RNA genome into double stranded DNA (dsDNA), uncoating the viral core, integration of the dsDNA genome into the host's genome, and assembly, budding and maturation of the new virion (virus particle) (Fig. 1.2). Each one of these steps is critical to successful propagation of the retrovirus.

The retroviral life cycle begins with the fusion of an infectious virus particle with a target cell. Also known as viral entry, fusion involves the interaction between the viral glycoprotein and a specific receptor protein located on the extracellular side of a target cell's plasma membrane. Different retroviruses recognize different receptors.

Following interaction between the viral glycoprotein and the host cell receptor, fusion can proceed down one of two pathways. For some viruses, including RSV and influenza, the acidic environment of the endosome is required to activate the fusogenic properties of their glycoprotein complexes (54). However, most retroviruses undergo fusion without being endocytosed. Conformational changes in the viral glycoprotein lead to contact and fusion between the viral and cellular membrane.

The next step of viral entry is the release of the viral core into the cell's cytoplasmic space, which is followed by reverse transcription of the viral genomic RNA (vgRNA) by RT into dsDNA.

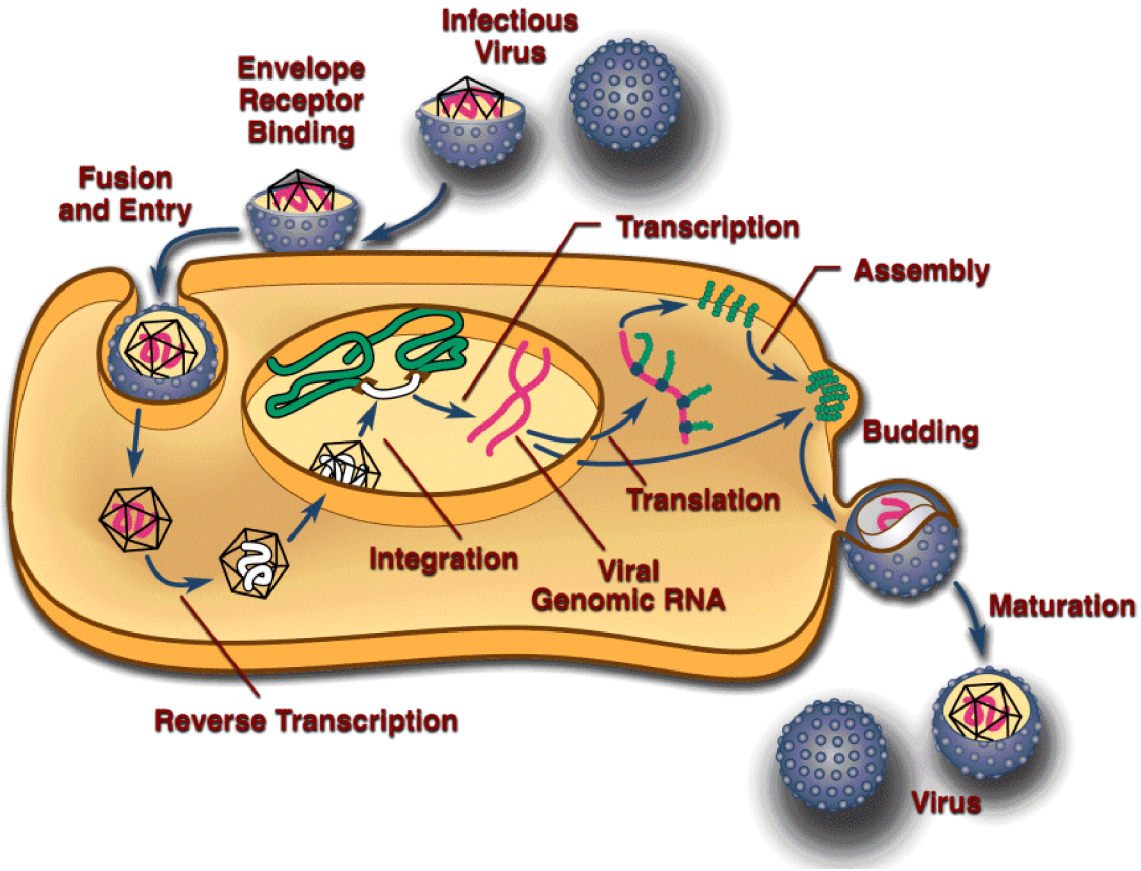

Fig 1.2 The retroviral life cycle (adapted from (54)). Viral entry is mediated by interaction of the viral Env to a specific cellular receptor protein. Reverse transcription results in a dsDNA that is integrated into the host DNA. Cell protein-mediated transcription and translation of viral RNA and protein lead to assembly of viral components at the inner leaflet of the plasma membrane. Recruitment of cellular ESCRT proteins to the budding site aids in the fission event that releases the virus particle into the extracellular space. The final step, known as maturation occurs during or following fission. Viral protease becomes active cleaving the viral Gag protein at multiple locations resulting in rearrangement of the Gag domain CA. CAs make new contacts forming the viral core.

It should be noted that the discovery of RT upended the central dogma of molecular biology, namely that DNA is always transcribed into RNA (and never the reverse), which is translated into protein. Because the process of reverse transcription is unique to retroviruses and retrotransposable elements, it is a prime target for antiretroviral therapy.

Reverse transcription is a complex process that involves multiple steps. The retroviral RNA enters the cytoplasm as part of a nucleoprotein complex, and reverse transcription is initiated at the 3' end of a cellular tRNA, which is bound to the genome's 5' PBS. This first round of RT activity results in the minus-strand strong-stop DNA (-sssDNA) (54). Following RNase H degradation (RNase H is part of the reverse transcriptase enzyme) of the -sssDNA duplexed RNA, the -sssDNA segment transfers to the 3' end of the genome mediated by identical sequence repeats in both the 5' and 3' ends of the viral genome. The second round of reverse transcription results in the generation of a complete minus strand DNA. Next, RNase H degrades the template RNA except for a resistant short region, the polypurine tract (PPT). The PPT serves as the initiation site for the RT-generated plus-strand strong-stop DNA (+sssDNA). Following RNase H removal of the tRNA, –sssDNA circularizes and serves as a template for making +sssDNA resulting in dsDNA.

The next step of infection is the integration of the dsDNA into the host genome. Integration begins when the retroviral IN cleaves two nucleotides from each end of the dsDNA viral genome generating two 3'OH groups. The IN-dsDNA complex (or pre-integration complex (PIC)) is then trafficked into the nucleus of the host cell where the

viral DNA 3'OH groups attack the phosphodiester backbone of the host genome. The integration generates a staggered break in the host DNA, which is then filled in by cellular proteins resulting in a short repeats of the host's genome (54). Integration of the viral genome can be considered the last step in the establishment of viral infection. If an integrated genome does not disrupt essential coding sequences, and is never transcribed into mRNA, a host may suffer no consequences.

The site of retroviral genome integration is important both to the host and the virus. If the integration occurs in a region of the host's genome that is transcriptionally inactive, the viral DNA may not be transcribed into mRNA. Viruses avoid dead-end integration by targeting transcriptionally active regions of the genome. For example, HIV-1 integrates preferentially into transcriptionally active genes throughout the cell's DNA, and MLV insertion is directed towards promoter regions (102, 112, 142, 146). Avian sarcoma leukosis virus (ASLV) shows less targeted integration behavior, with only a slight preference for integration into transcriptionally active regions detected (11, 112). Human T-lymphotropic virus (HTLV) is similar to ASLV, showing little to no preference for targeted site insertion (61).

To achieve targeted integration, HIV-1 IN interacts with the cellular protein LEDGF/p75. This interaction directs HIV-1 integration to regions of the host cell DNA that LEDGF/p75 interacts with (49). Cellular co-factors that direct integration of other retroviruses have yet to be identified. However, excellent examples of targeted integration do exist for the yeast retrotransposable elements Ty3 and Ty5. Retrotransposable elements are closely related to retroviruses, coding for proteins with

similar functions to Gag and Pol. However, they do not leave the host cell, and so they do not code for the envelope glycoprotein. Ty3 integrates selectively into regions adjacent to RNA Pol III start sites near the front of tRNA genes (54). Ty5 integrates preferentially into silenced regions of the yeast chromosome owing to interaction between IN and the chromatin silencing complex protein Sir4p (27, 161).

VIRAL PARTICLE PRODUCTION

In order for a virus to spread to other cells and host organisms it must form an infectious virus particle. Successful assembly of the virus particle requires the convergence of multiple viral components within the cell. These spatially and temporally controlled events include Gag trafficking to and interacting with the PM, Gag interacting with other Gag proteins, and Gag interacting with vgRNA. If any of these events is disrupted infectious virus particles will not be produced. The one component common to all of these events is the Gag polyprotein, which is the only retroviral protein required to form a virus particle.

Function of Gag polyprotein domains

The retroviral Gag polyprotein is a long, rod-like protein with three independently folded structures or domains. These three domains are common to all retroviruses, sharing a large degree of structural and functional, but not sequence, homology. The N-terminal domain is matrix (MA), followed by capsid (CA), and at the C-terminus, nucleocapsid (NC) (Fig. 1.1). During virus particle maturation, cleavage of the Gag

polyprotein by the retroviral protease results in genus-specific cleavage products. These specific regions are important for assembly and trafficking of Gag.

Viral assembly and maturation

Viral particle assembly is driven by interactions between Gag proteins, often referred to as Gag multimerization. In cells, efficient particle assembly only takes place when Gag has a membrane-binding domain, and membrane binding of Gag is only efficient when Gag multimerization takes place. What regions of Gag drive Gag-Gag interactions and how do these interactions lead to particle assembly?

Before Gag cleavage by PR, the virus particle contains a lattice of Gag hexamers named the immature lattice. Gag-Gag interactions in the immature lattice, common to most retroviruses, occur via contacts between CAs. CA folds into two domains, the N-terminal domain (NTD) and the C-terminal domain (CTD). Based on the mature CA lattice, people expected that the NTD-NTD contacts would hold the immature hexamer together, but actually a recent paper on MPMV electron cryotomography (Briggs et al), implies that it is primarily CTD-CTD contacts that hold the hexamer together, and NTD-NTD and CTD-NTD contacts bridge between the hexamers, as if the molecular contacts are very different in CA and Gag (3). It has been proposed that the region immediately following CA, the spacer peptide (SP), is alpha helical and forms a six-helix bundle, which further stabilizes each hexamer (21, 159). While MLV Gag does not have a spacer peptide, it does have a domain that appears to be analogous to the SP helix, named the “charged assembly helix” or “electric wire” owing to its high number of charged residues (50). Mutational analysis and modeling strongly suggest that this

domain also forms a helix (50). Whether or not the putative helical domain immediately downstream or at the C-terminus of the CA domain forms a six helix bundle remains to be determined. However, this domain is clearly a conserved structural component with a function that is critical to the formation of the immature virus particle.

During or immediately following viral budding, PR becomes activated and cleaves the Gag polyprotein beginning the process named maturation. Maturation causes the rearrangement of contacts between CAs, which dramatically changes the lattice resulting in the formation of the viral core. The viral core is a lattice of CA hexamers and pentamers. The lattice has been well studied by electron cryo-tomography (cEMT) (17, 28, 30, 103), electron crystallography (76). These studies provide low-resolution data about the contacts required to form the lattice. The low-resolution data were used to identify interfaces that could be stabilized by di-sulfide crosslinking. Crosslinking was then used to generate stable mature CA hexamers and pentamers which, when crystallized, resulted in high resolution structures of 2Å (129, 130) and 2.5Å resolution (131). Taken together, these studies reveal that CA hexamers are held together by CA-CTD dimers and the lattice is stabilized by an interface between the CA-CTD and CA-NTD (29, 129-131). Just as the assembly of the viral particle is required to form infectious virus particles, maturation is also required. Because these key steps are essential, they are both targets for antiretrovirals. One difference between immature and mature assembly is that only the former requires interactions with the plasma membrane.

Nucleocapsid and genome packaging

Initiation of Gag-Gag interactions and multimerization may occur when Gag proteins bind their vgRNA in the cellular cytoplasm. Disruption of NC-RNA interactions disrupts localization of Gag to the plasma membrane. Because multimerization is linked to interaction with the PM it is important to have an understanding of the process of packaging.

NC of most retroviruses, except spumaretroviruses, has one or two zinc knuckles (Znk,), similar to Zn-finger domains, characterized by a CCHC amino acid motif and a tightly bound Zn (57). Other than the Znk, the NC is unstructured. NC also contains multiple basic residues centered between and after the Znks. Disruption of the Znks does not abolish particle assembly *in vivo* or *vitro* but it does prevent vgRNA packaging (18). Packaging of vgRNA is a tightly controlled step late in the viral life cycle. Amino acids between or immediately following the second Znk interact with specific vgRNA secondary structures and nucleotides. These specific interactions ensure that retroviruses select their own RNA from the milieu of cellular RNA (reviewed in (57)). Interestingly, one way that NC and packaging sequences were characterized was the generation of Gag chimeras with the NC domain of a different retrovirus. For example, when the NC domain of MLV is replaced with that of HIV, the HIV vgRNA is preferentially packaged and vice versa (20, 164). A similar result is also obtained when the NC of RSV is swapped with that of MLV (69). Therefore, NC is the major domain required to ensure that a budding virus selects its vgRNA.

Successful genome packaging requires NC recognition of unique features of the target viral genome. The packaging sequence, or Psi for short, is generally defined as the minimal sequence that supports incorporation of vgRNA into the viral particle, and is located in the 5' untranslated region of the viral genome (57). Originally, a 160 nucleotide minimal packaging sequence for RSV (named MPsi or MΨ) was identified that is capable of packaging RNA into virus particles at efficiencies that are only 2.6-fold lower than the intact genome (9). However, other studies showed that the third stem-loop of MPsi was not important for packaging (8, 67) and a new 82 nucleotide minimal packaging sequence was defined, named μPsi (8). The structure of the μPsi sequence in complex with NC was elucidated by nuclear magnetic resonance (NMR), which identified key nucleotide and amino acid interactions (165). Many tools have been used to define the secondary structure and nucleotides of RSV Psi that are critical for packaging, including computer simulation, NMR analysis, and multiple binding and packaging assays (67, 98, 165).

NC also has chaperone activity that plays a role in reverse transcription of the vgRNA into dsDNA, and that is also important for genome dimerization (101, 136). Retroviral genome dimerization is initiated at the DIS. Genome dimerization spreads through the genome and one resulting stable structure is the dimer linkage structure (DLS) located downstream of Psi in the *gag* gene (16). The chaperone activity of NC lowers the activation energy required to fold nucleic acid into secondary structures that have a high number of nucleotide base pairs (135, 136). A series of assays aimed at tracking genome dimerization and packaging found that both were dependent on the

DIS, and 90% of budded virus particles contain vgRNA, which was always dimeric (48, 64). Packaging is also not dependent on the size of the RNA but instead on the presence of two copies of the genome (116). An example of how retroviruses select a dimerized genome comes from work with MLV. MLV NC preferentially binds to single stranded UCUG sequences. Upon genome dimerization, there is a rearrangement of RNA secondary structure exposing multiple UCUG sites in and around Psi (58). This result suggests that in general Psi function will boil down to multiple binding sites, maybe with different affinities for NC.

Other Gag cleavage products

Smaller cleavage products of Gag are not as conserved as the three major ones. However, these domains serve critical functions for the viruses that do have them. For example, RSV Gag codes two regions, p2 and p10 before CA, and SP after CA. These domains are discussed in greater detail in other sections but briefly here. The p2 and p10 cleavage products each contain a late domain (63, 158, 160). P10 is also critical for viral particle assembly, by participating in and stabilizing the immature Gag lattice (127). The SP region (called SP1 in HIV-1), as previously discussed, which is inferred to be helical in the Gag lattice, is essential for particle formation, and may act to regulate maturation of the CA lattice.

GAG INTERACTION WITH THE PLASMA MEMBRANE

How does Gag select the PM as the site of assembly and not the endoplasmic reticulum (ER) or Golgi? The answer likely lies in a series of signals that drive Gag

membrane binding. These signals include electrostatic interactions, binding pockets in MA that specifically recognize unique phospholipids, hydrophobic interactions with the core of membranes by post-translational modification of MA with fatty acid chains, and multimerization of Gag.

The MA domains of retroviruses share a high degree of structural homology. The NTD of MA is composed of 5-6 major alpha helices that fold into a globular shape (86, 113). The globular head of MA positions a number of basic amino acids on one surface resulting in a basic patch that is oriented towards the PM. This basic patch interacts electrostatically with the positively charged inner leaflet of the PM. Most genera of retrovirus have a basic patch, with the net surface charge of MA domains differing from neutral to positive three or six, as in the case of equine infectious anemia virus (EIAV), RSV, and HIV-1, respectively (113).

The inner leaflet of cellular plasma membranes is negatively charged owing to twenty to thirty molar percent of the net negative lipid phosphatidylserine (PS). The negative charge is increased by minor (1-2%) levels of the highly negative lipid phosphatidylinositol-4,5-bisphosphate (PI(4,5)P2). In addition to phospholipids the plasma membrane contains high levels of cholesterol, neutral lipids, and by mass is roughly 50% cellular proteins (55).

RSV MA binding to membranes

The MA domain of RSV Gag is not myristoylated and does not appear to have a phosphatidylinositol-phosphate (PIP) binding pocket but instead likely relies on electrostatics to maintain protein-membrane interactions. Single and double mutations

of basic to acidic amino acids in RSV MA result in a decrease or a loss, respectively, of Gag localization to the PM and virion release (37). In the background of a double basic to acidic mutant, mutations elsewhere in MA that return the net surface charge to positive three restore virion release (37). Interestingly, mutating two acidic amino acids to basic amino acids, results in increased viral release (37). This mutant Gag protein, dubbed super-M or super membrane binder (SM), does not traffic through the nucleus of the cell, packages 1/10th the vgRNA of wild type (wt) particles, releases virus particles more rapidly than wt, and is non-infectious (36). It remains unclear if the decrease in vgRNA packaging is due to the rapid viral release or to the defect in nuclear trafficking (36).

One of the most common ways used to study RSV MA and Gag membrane binding in vitro is a liposome flotation assay. In a typical flotation the protein of interest is mixed with liposomes, which are lipid membrane bilayers that may be uni- or multi-lamellar depending on the method of preparation. The liposome-protein mix is subjected to sucrose equilibrium sedimentation, and any protein bound to a liposome will float to the top of the sucrose gradient owing to the low density of the liposome compared to the sucrose. By taking fractions of the gradient following flotation one can determine the percent of the total protein associated with liposomes by SDS PAGE analysis.

Liposome flotation analysis of RSV MA and Gag strengthens the hypothesis that its membrane binding is driven by electrostatics. RSV MA binding to liposomes composed of physiological amounts of the negatively charged phospholipid PS decreases to undetectable levels as salt is increased from 75 to 500mM NaCl (59). A

MA mutant with two basic lysine residues mutated to the neutral asparagine is significantly defective in membrane binding (59). Increasing the lipid concentration of PS increases the amount of protein that associates with liposomes (45, 59). While some retroviral MAs bind specifically to PIPs, RSV MA has no known PIP binding pocket. However, RSV MA responds strongly to the presence of PIPs as measured by liposome flotation (chapter 4). This apparent discrepancy may be due to the high charge density of PIPs at physiological pH.

It is difficult to disrupt the overall electrostatic charge of the inner leaflet of the PM without the possibility of generating experimental artifacts. However, it is possible to deplete the highly charged lipid, PI(4,5)P2 from the PM. If RSV Gag is dependent on PI(4,5)P2 for specific interactions, or for its charge, it is possible to detect this *in vivo* by PIP depletion. PI(4,5)P2 depletion from the PM is accomplished by overexpression of the polyphosphoinositide 5-phosphatase IV (5PtaseIV) protein. Depletion is observed indirectly by the relocalization of a PI(4,5)P2-specific binding protein domain from phospholipase-C, the pleckstrin homology domain, fused to the green fluorescent protein (PH-GFP) (45, 162). PH binding to PI(4,5)P2 is mediated by a basic patch oriented by three variable loops (14, 79, 99). *In vivo*, PI(4,5)P2 depletion does not cause a change in RSV Gag membrane association, as detected by GFP labeled Gag, or a change in the amount of virus particle release (45). Under equivalent conditions, HIV-1 Gag does respond to PI(4,5)P2 depletion (45). However, under different conditions, RSV Gag shows slight sensitivity to PI(4,5)P2 depletion (114). Based on the conflicting

in vivo results it is difficult to assign a role to PI(4,5)P2 in RSV Gag membrane association.

HTLV-1 and MLV MA binding to membranes

Like RSV MA, HTLV-1 MA has no known PIP binding pocket, and PIP depletion in cells does not significantly alter Gag localization or virus release (92). HTLV-1 also does not respond to the presence of PI(4,5)P2 in liposomes but does respond to increased PS concentrations (92). The authors propose that HTLV-1 MA membrane binding is electrostatic, similar to RSV MA (92). RNase-mediated degradation of RNA from the liposome binding reaction does not increase HTLV-1 Gag binding to liposomes, similar to what is reported here in this thesis for RSV Gag (92).

The MA domain of MLV Gag, similar to the MA domains of RSV and HIV Gag, has many clustered basic residues oriented so that they can interact with the PM. *In vivo*, virus production of MLV is significantly decreased by 5PtaseIV mediated depletion of PI(4,5)P2, despite there being no known MA PIP binding pocket (84). *In vitro*, MLV MA membrane binding is enhanced when the membrane contains any of the PIPs tested, but membranes containing PI(4,5)P2 enhances binding the most. Interestingly, the strong response to PI(4,5)P2 is not observed if the membrane does not contain PS (84). These results are difficult to interpret since the *in vitro* work was performed with a non-myristoylated purified MA protein, and myristoylation is known to be essential for MLV Gag function *in vivo*.

HIV-1 MA binding to membranes

If RSV MA represents a simple model of membrane binding then HIV-1 MA could be placed at the opposite end of the spectrum. Also, because of the link of HIV-1 to human health, much more effort has been made to characterize it compared to the simpler virus RSV. HIV-1 MA contains as many as four membrane binding signals: a highly basic patch, a PIP binding pocket, an N-terminal fatty acid modification, and hydrophobic grooves that have been reported to bind to lipid acyl-chains (113, 138, 141, 155) (Fig. 1.3). The highly basic patch is composed of multiple lysine and arginine residues in the front half of MA. These residues result in a plus six charge (compared to RSV's plus three). The first thirty-one residues of MA can function independently as a membrane-binding region, dependent on the basic residues and the myristate, as demonstrated by the membrane binding of a MA-Src chimera (166).

Increasing the number of basic residues in HIV-1 MA increases membrane binding. For example, mutation I18K/L20K results in nearly double the amount of membrane-associated Gag protein compared to wt as measured by liposome flotation (123). The mutation K29T/K31T results in a three-fold reduction of virus release and K29E/K31E results in Gag accumulation at the Golgi in cells (73, 123). Individual mutation of the basic residues K18, R20, and R22 each results in a dramatic decrease in viral infectivity. However, these mutants still produce virions but with lower levels of Env incorporation, which may account for the decreased infectivity (22). Interestingly, mutations K29T/K31T and K29E/K31E do not significantly reduce binding to phosphatidylcholine/PS (PC/PS) membranes in a standard liposome flotation assay, but

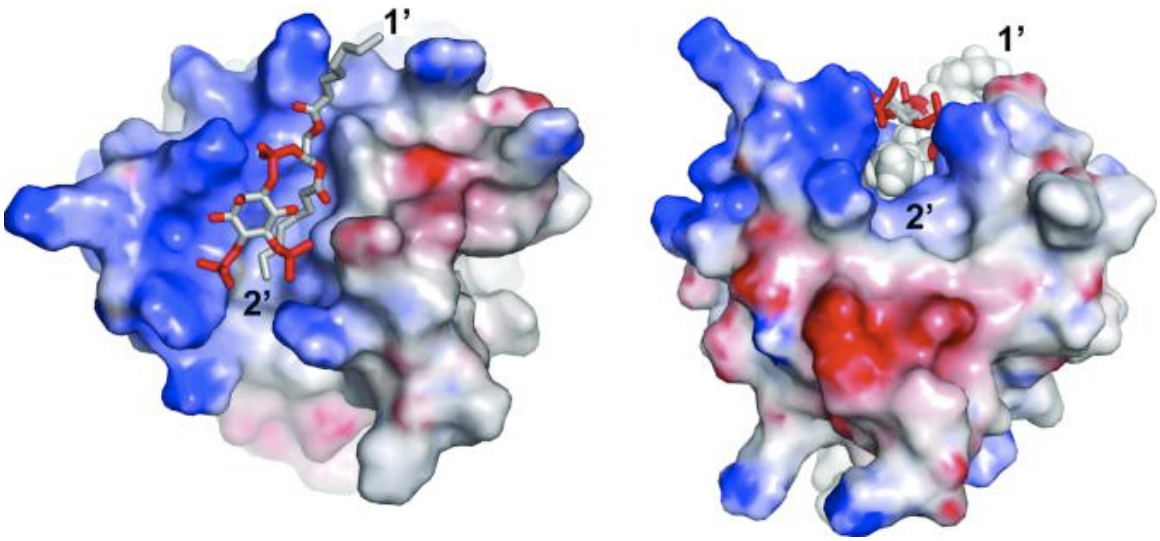

Fig 1.3 HIV-1 MA binding to C8-PI(4,5)P2 (adapted from (141)). Structure of the N-terminus membrane-binding domain colored according to electrostatic surface potential with basic areas in blue and acidic areas in red. The PI(4,5)P2 headgroup is shown with acidic phosphate groups in red and the 2' lipid acyl chain, in grey, sequestered into a hydrophobic groove.

they decrease binding to membranes that contain PI(4,5)P2 (51). Taken together, these results show that electrostatics are a key driving force in HIV-1 Gag's interaction with membranes.

Mass spectrometric protein footprinting found that of the twenty one modifiable lysines in Gag, only K29 and K31 (published as K30 and K32 due to a difference in annotation) bound well to PI(4,5)P2 (147). This indicates that some of the basic residues in HIV MA are positioned to respond specifically to PIP and are not required for electrostatic interactions.

The binding of HIV MA to the phospholipid PI(4,5)P2 has been confirmed by multiple lines of investigation including NMR solution structure, *in vivo* depletion of PIP2, *in vitro* liposome binding assays, and the previously mentioned mutagenic studies. X-ray crystal structures of HIV-1 MA reveal a pocket that by NMR studies binds to PIPs. NMR solution structures show that HIV MA binds to the PIP headgroup of a soluble short chain PI(4,5)P2 but not to closely related phosphatidylinositol-3-phosphate (PI(3)P), phosphatidylinositol-4-phosphate (PI(4)P), or phosphatidylinositol-5-phosphate (PI(5)P) (141). Surprisingly, the NMR structure revealed that not only does the PIP head group bind to MA, but also the lipid's sn-2 acyl chain binds to a hydrophobic pocket on MA (Fig. 1.3). Cellular PIP acyl chains vary in length and saturation. Generally speaking, the sn-2 acyl chain is highly unsaturated, containing as many as four double bonds, which results in a high degree of chain disorder. It is possible that this chain samples the head group region of the bilayer and under the right conditions "pops-out" of the bilayer and, if MA is present, into MA's hydrophobic groove. This model is supported by a second

NMR study in which two additional hydrophobic grooves in MA were identified and shown to be capable of binding the sn-2 chain of PS, PC, or phosphatidylethanolamine (PE) lipids (155). A role for acyl chain involvement in MA binding to membranes is suggested by the results of a surface plasmon resonance study that found that the contribution of the lipid acyl chain provides more energy for binding to MA than the PIP head group (6). But because NMR studies of HIV-1 MA binding to lipid acyl chains have been performed with short-chain, soluble PIPs, it remains unclear if the binding is biologically relevant.

Liposome flotation assays of HIV Gag and purified HIV MA also show that PIPs strongly enhance binding of the proteins to liposomes (45, 51, 62). However, the enhancement of binding is not limited to PI(4,5)P2. PI(4)P, PI(3)P, and phosphatidyinositiol-3,4,5-phosphate (PI(3,4,5)P3) also enhance membrane binding of HIV Gag and RSV Gag, suggesting that the electrostatic affects of PI(4,5)P2 may not be easily separated from specific head group recognition. Surprisingly, phosphatidylinositol-3,5-phosphate (PI(3,5)P2) only weakly enhances the binding of RSV or HIV Gag to membranes *in vitro* (45, 51).

HIV-1 Gag clearly shows sensitivity to PI(4,5)P2 *in vitro*, similar to RSV Gag, but is it sensitive to PI(4,5)P2 *in vivo*? Co-expression of 5PtaseIV with HIV-1 Gag, tested in multiple cell types, results in both a loss of Gag localization to the PM and loss of virus release (51, 92, 121).

A model of HIV-1 MA binding to membranes has emerged based largely on NMR data (139-141, 153, 155) and reviewed in (81) (Fig. 1.4). In this model, not only does

MA bind to PIPs but this binding also promotes structural changes in MA that increase myristate exposure. Also by NMR, purified MA is in a monomer-trimer equilibrium and trimerization causes structural changes that expose the myristate, perhaps increasing its insertion into a membrane (137, 153). Another line of investigation that fits the MA-trimerization model comes from the Barklis lab, which showed that MA-CA forms hexamers of trimers on a supported bilayer containing PIP2 (2).

In addition to HIV-1, HIV-2, EIAV, and Mason-Pfizer monkey virus (MPMV) also have PIP binding pockets (70, 132, 139). Unlike HIV-1, HIV-2 (139) and MPMV (132) binding to PIP2 does not promote myristate exposure. EIAV Gag responds to decreased levels of PIP in cellular membranes when a broadly acting phosphatase, synaptojanin-2, is expressed (70). By NMR EIAV binds more tightly to PI(3)P than to PI(4,5)P2 and in cells Gag is localized to cellular compartments enriched in PI(3)P in addition to localization to the PM (70).

Another membrane binding signal found in nearly all retroviruses is myristoylation, an N-terminal post-translational modification that strengthens interactions with membranes. Most retroviral MAs are myristoylated, except RSV and EIAV (138). Addition of myristic acid, a fourteen-carbon fatty acid, occurs at a glycine residue located at the second amino acid position, i.e. following the initiating methionine. Myristoylation of HIV-1 MA is critical to MA's ability to bind to membranes. Mutation of glycine to alanine, which abolishes myristoylation, results in a loss of Gag localization to the PM and loss of virus release (118). *In vitro*, abrogation of myristoylation results in a significant decrease in Gag and MA binding to liposomes (51, 53, 60). Myristoylation is

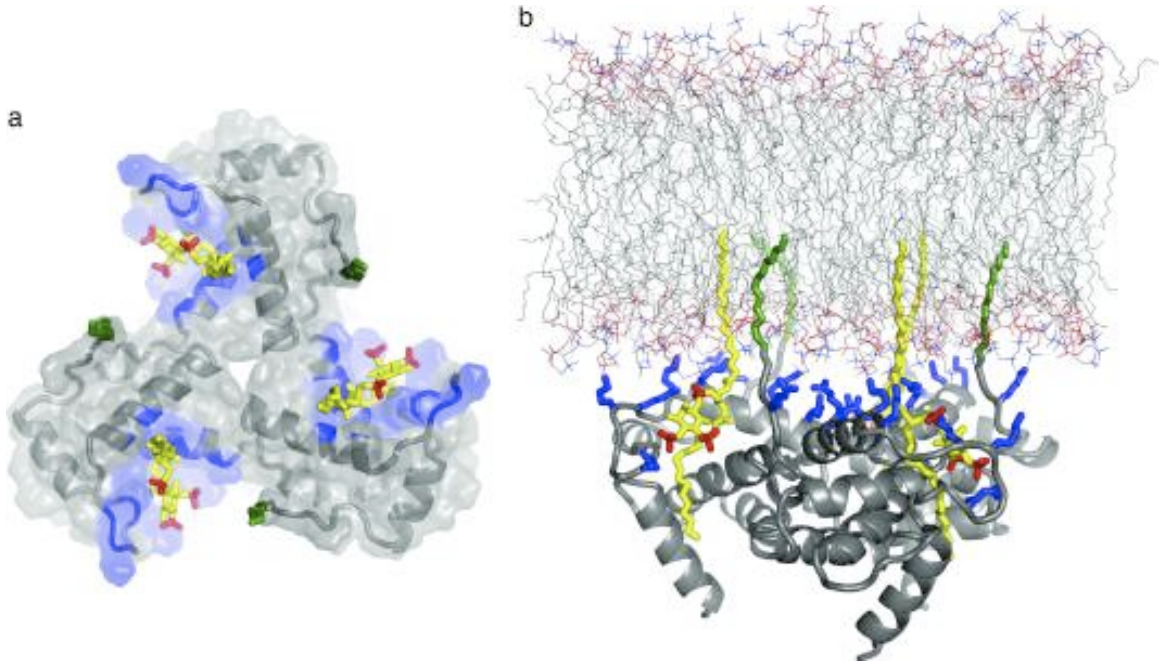

Fig 1.4 HIV-1 MA trimer model of membrane binding (adapted from (71)) . This model shows how trimerized-MA binds to the bilayer and extracts the 2' acyl chain of PI(4,5)P2 lipids. PIP is shown in yellow and myristic acid is shown in green.

arguably the most important membrane-binding signal as evidenced by a study in which the basic region of MA was deleted, including the PIP binding pocket (134). The only remaining membrane binding signal was the myristate, which was sufficient to localize Gag to the PM, and only modest reductions in viral particle production were measured (25, 134). Non-myristoylated Gag is dominant negative when co-expressed with wt Gag. This result may be partially dependent on NC mediated Gag-Gag dimerization (95).

Clearly the binding of retroviral Gag proteins to the PM represents a complex interaction. HIV-1 Gag is arguably more complex than RSV Gag. By studying both viral Gag proteins, and making comparisons of them, we can better interpret results. For example, the finding that RSV Gag, which has no known PIP binding pocket, responds to PIPs in vitro but not in vivo calls into question the original interpretation of HIV-1 Gag binding to PIPs. Instead of a strong specific interaction between HIV-1 MA and the PIP head group, perhaps the stimulatory effect of PIPs on MA membrane-binding has more to do with electrostatic interactions.

A role for nucleic acid in Gag membrane binding?

The study of HIV MA membrane binding is complicated by the observation that HIV-1 MA also binds to nucleic acid. The nucleic acid binding has been proposed to be a regulatory mechanism that restricts MA from binding promiscuously to cellular membranes other than the PM (53). Flotations performed on Gag translated in rabbit reticulocyte reactions have the advantage of containing physiological concentrations of protein and nucleic acid. Following translation, RNA can be depleted from the reticulocyte reaction by treatment with RNase. This results in increased Gag membrane

interactions (52, 53). It should be noted that these binding experiments were performed at ionic strengths approximately 1/3 to 1/5 of physiological. The effect of RNA on MA binding is not dependent on the presence of the highly basic NC domain and occurs for both reticulocyte translated and purified MA (data from chapter 4 and (52, 53)). In an alternative approach, to test the effect of PIP and nucleic acid on membrane binding, Barklis et al. bound purified MA to agarose beads and tested the affinity of the MA-coated beads to liposomes containing trace amounts of fluorescently labeled lipids (4). In this assay, liposomes containing PI(4,5)P2 were able to outcompete nucleic acid for MA binding but liposomes without PI(4,5)P2 were unable to do so (4). In summary, while nucleic acid does bind to MA under certain conditions, this binding has not been shown to be biologically relevant.

TRAFFICKING OF GAG TO THE PLASMA MEMBRANE

In principle there are two ways that Gag can reach the site of viral particle assembly, the PM, by diffusion or by a directed pathway. One hypothesis that has gained some traction suggests that Gag uses parts of the endosomal trafficking pathway to reach the PM. Multiple lines of evidence support this model for HIV-1 Gag trafficking (reviewed in (119)). Gag interacts with adapter complexes AP1, AP2, and AP3. Each complex plays a role in cellular transport between membrane compartments. Knockdown of AP1, which is involved in the transport of endosomes to the Golgi, results in a decrease in viral budding for both MLV and HIV-1, while overexpression of the AP1 complex enhances release of HIV-1 Gag (42). AP2, which is involved in endocytosis, interacts with the MA domain of HIV-1 Gag and may act to restrict viral egress to Env

containing PM microdomains (12). The AP3 complex, which is involved in trafficking from early endosomes to late endosomes, has also been reported to interact with the MA domain of HIV Gag. Disruption of the interaction between HIV-1 Gag and AP3 results in a decrease in particle production (66). However, NMR results suggest that AP3 may not interact directly with HIV MA (97).

Env trafficking to the PM also involves endosomal trafficking. Env mainly resides in the trans-Golgi network (TGN) and interacts directly with an endosome-to-TGN transporter, TIP47 (24). TIP47 also interacts with the MA domain of HIV-1 Gag which would suggest that TIP47 acts as an adaptor between Gag and Env (106). Depletion of TIP47 abolishes Env incorporation into virus particles (13, 106). However, published reports of TIP47 are not all consistent. Checkley et al found that while MA does interact with TIP47, as measured by NMR, TIP47 overexpression or depletion in Jurkat T and HeLa cells does not affect incorporation of Env into virions (47). Based on these studies, it seems likely that TIP47 plays a role in the incorporation of Env into virus particles, but this function may be cell-type dependent.

Another example of Gag trafficking comes from studies that show that RSV Gag is trafficked into the nucleus, owing to two nuclear localization signals (NLS) located in the MA and NC domains, which bind to import receptors importin-11 and importin-alpha, respectively (35, 83, 144). Gag is exported out of the nucleus through the CRM1 nuclear export pathway by a nuclear export signal located in the p10 region (144, 145). What does Gag do while it is in the nucleus? When RSV Gag is mutated so that it is myristoylated, it bypasses trafficking through the nucleus resulting in decreased levels

of vgRNA packaging (78). This observation has led to the hypothesis that nuclear transport of RSV Gag is related to packaging. However, when RSV MA is replaced with the MA of HIV-1 Gag, cycling through the nucleus is lost but at least some viral infectivity is maintained (7). It remains unclear what role nuclear trafficking of RSV Gag may play.

GAG MULTIMERIZATION

The formation of the retroviral Gag lattice likely begins with one or multiple Gag dimerization events. Gag dimerization is critical to viral particle formation and requires interactions between NC and nucleic acid. *In vitro* assembly of RSV virus-like particles (VLPs) requires nucleic acid long enough to support the binding of at least two Gag proteins (40, 108, 109). For HIV-1, the addition of nucleic acid and inositol phosphates (IPs) or PIPs is required to obtain regularly sized (VLPs) (38, 39). Abrogating the nucleic acid binding capacity of NC by mutation or deletion prevents *in vitro* and *vivo* assembly for RSV (93) but only modestly reduces virus particle production *in vivo* for HIV-1 (118, 125). However, if NC is swapped for a naturally dimerizing leucine zipper, VLP formation is similar to that of wt Gag (56, 93). Chemical or oxidation-induced dimerization of Gag, whose NC domain is replaced with cysteines, also supports VLP formation (3).

Does Gag multimerization occur prior to PM binding or do Gag monomers bind to the PM and than begin to multimerize? Because HIV-1 MA is in a monomer-trimer equilibrium, determined by NMR (153), it is possible to study the effect of MA

multimerization in cells without complicating results by using Gag. It should be noted that trimeric MA has never been observed in the context of the full length Gag protein. One group found HIV-1 MA monomers, dimers, and trimers in the cytoplasm of cells and associated with the PM (150). However, other studies using monomeric or dimeric chimeras of MA, observed monomeric HIV-1 MA to be entirely cytoplasmic and dimeric MA to be partially localized to the plasma membrane (60). Differences between results may be attributed to cell type or levels of protein production. Monomeric HIV-1 Gag is found at intracellular membranes and the plasma membrane indicating that it can reach sites of assembly although not efficiently enough for assembly (68). In the cell cytoplasm, Gag is monomeric and dimeric owing to a dimer interface in CA (75). However, monomeric Gag is not found associated with the PM; only Gag multimers are found associated with the PM (96). In addition, Gag is associated with genomic RNA in the cytoplasm (96). According to Hogue et al., increasing the membrane binding affinity of MA relieves reduced viral particle production caused by deletion of NC (87). Collectively, the data can be interpreted to mean that there is cooperation between assembly, RNA binding by NC, and membrane binding by MA.

Because RSV Gag has no known dimerization interface like the one found in HIV-1 Gag, and is monomeric at concentrations consistent with cellular levels, it is difficult to test cellular localization of monomeric vs dimeric RSV Gag. However, prevention of RSV Gag assembly by disrupting nucleic acid binding results in a diffuse cytoplasmic localization (93). Additionally, RSV MA is cytoplasmic and nuclear due to a

NLS in MA (77, 78). The cellular localization of RSV MA multimers will be covered in detail in chapter four.

LATE DOMAINS

Enveloped virus particles derive their membrane from the host cell in which they are replicated. Retroviruses like RSV and HIV-1 bud from the site of particle assembly, the plasma membrane. Following assembly of Gag and incorporation of the vgRNA, the viral particle undergoes a scission event, which separates the virus from the host cell membrane (also referred to as fission). The process of fission requires multiple cellular proteins that are part of the endosomal-sorting complexes required for transport (ESCRT) pathway. The ESCRT proteins' normal cellular function is the biogenesis of multivesicular bodies (MVB) and cellular abscission (23, 72, 90, 91).

Late domains in the Gag polyprotein recruit cellular proteins to assembly sites at the PM. There are three classes of late domains with the consensus sequences PS/TAP, PPXY, and LYPXnL. The viral late domain PTAP found in the p6 domain of HIV-1 Gag recruits the ESCRT-1 complex through interactions with TSG101 (23, 90). PS/TAP is encoded by many budding viruses other than HIV-1, including Ebola, HTLV and simian immunodeficiency virus (SIV) (26, 63, 110, 156). The PPXY late domain, encoded by RSV Gag in the p2B region, interacts with WW domains of the Nedd4 family of ubiquitin ligases (63). The third domain, LYPXnL, which RSV Gag codes for as a secondary domain five amino acids downstream of its PPXY domain, interacts with Alix (63, 74).

Generally late domains recruit ESCRT-I and/or ESCRT-II complexes with the ultimate goal of recruiting the ESCRT-III complex (90, 91). ESCRT-III includes the CHMP proteins, which are key to membrane scission (91). Two pathways for ESCRT-III assembly at the virus bud-neck have been proposed: the first is ESCRT-1-dependent and the second is Alix-dependent (43) (Fig. 1.5). In the ESCRT-1 dependent scission, ESCRT-1 interacts with Gag and ESCRT-II, which interacts with ESCRT-III components. The Alix-dependent model eliminates ESCRT-I and –II with Alix interacting with Gag and ESCRT-III directly.

BUDDING FROM MEMBRANE RAFTS

Membranes can form more than one liquid domain, often referred to as raft behavior. A membrane raft is typically composed of high Tm lipids and cholesterol. This domain is more ordered than the surrounding membrane. A hypothesis has emerged that suggests that the Gag proteins select the plasma membrane to assemble and bud by binding to rafts. Two lines of investigation suggest that viral particles bud from lipid rafts. First, multiple studies have found that the viral envelope has a lipid composition different than the bulk plasma membrane. While the studies do differ in degree and type of lipid enrichment, they generally find that in HIV-1 virus particles, cholesterol, ceramide, GM3, PIPs, PS, and plasmalogen-PE (pl-PE) are enriched (5, 32, 46, 126). However, the most recent of these studies found that virions have roughly two fold more pl-PE, PS, and sphingomyelin (SM) than the PM but found no enrichment of cholesterol (107). It should be noted that cholesterol is a critical component of raft formation (or

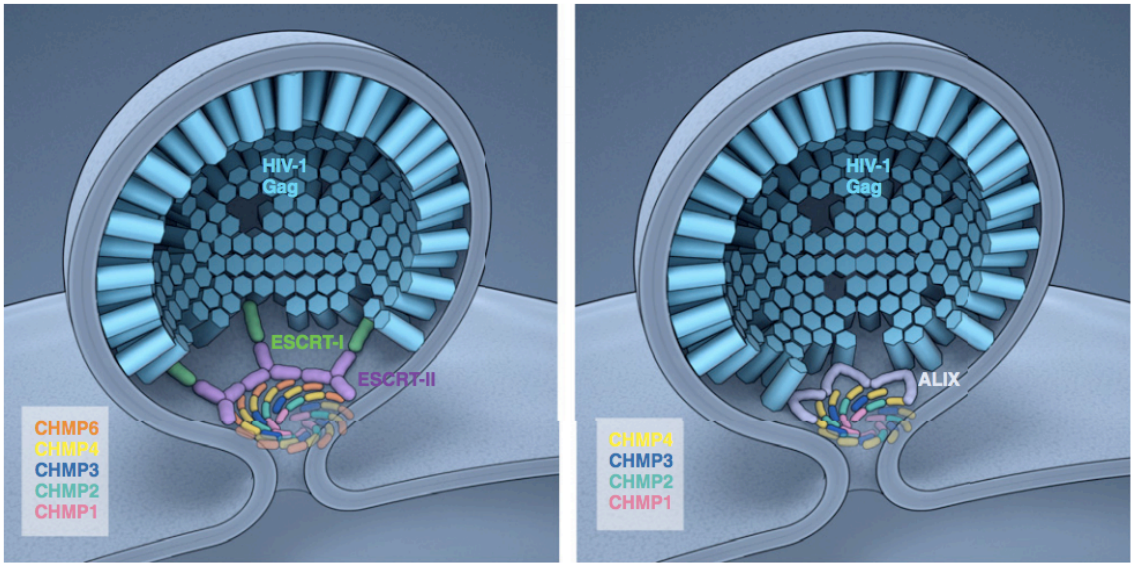

Fig 1.5 ESCRT-1 dependent and independent models of virion fission (adapted from (43)). Rod-like Gag proteins form an incomplete lattice in the forming virion. A subset of Gag interacts with either ESCRT-1 (panel 1) or ALIX (panel 2) to form the CHMP complex required for completing fission of the bud neck.

membrane phase behavior). Comparison of these studies reveals a range of cholesterol enrichment, from none to two-fold. Inconsistencies between studies may be due to variations in the methods used to measure cholesterol concentrations, techniques used to isolate the PM fraction from the cell, or the cell type used. In summary, these studies strongly suggest that the viral envelope has a lipid composition that differs from the bulk PM.

Depletion of cholesterol from the plasma membrane of cells transfected with HIV-1 Gag by methyl-β-cyclodextrin (MβCD) results in a reduction of Gag membrane binding and a reduction of higher order Gag multimerization (124). Cholesterol depletion also decreases viral budding of other enveloped viruses such as influenza (10) and West Nile virus (111). Cholesterol also enhances membrane binding of Gag *in vitro* (62).

Not only is cholesterol enriched in, but also it is an essential component of, the virus particle envelope. Removal of cholesterol from the viral envelope decreases infectivity of enveloped arboviruses (149) and influenza virus (152). Cholesterol may play an important role in maintaining the integrity of the viral enveloped core as evidenced in a study with HIV-1 and SIV that found cholesterol depletion resulted in abrogation of enzymatic properties of IN and RT (82). Viral infectivity can be restored by adding cholesterol back into the membrane of virus particles (41). However, EM analysis of cholesterol-depleted virions revealed that their membranes had holes (82) so it is possible that cholesterol depletion wrecks the viral membrane.

Cellular cholesterol is also important for virus entry into cells. For example, HIV-1 virions bind well to the surface of cholesterol depleted macrophage cells but their entry

is blocked (44). Taken together these results clearly show that cholesterol is a critical component of viral budding and entry.

Since cholesterol is one major component of lipid rafts it has become common to cite these studies as evidence that lipid rafts are important for viral function. This hypothesis is further supported by the observation that HIV-1 Gag is found in detergent resistant membrane (DRM) fractions, and this localization is dependent on Gag multimerization (104). DRMs are membrane fractions that are enriched in cholesterol and sphingolipids, and are often identified as evidence for the presence of membrane rafts in the cellular PM. However, the process of DRM isolation may induce lipid segregation. Interestingly, fatty acid modification of Gag with unsaturated myristic acid analogs decreases Gag's localization to the DRM membrane fraction, and blocks budding (104, 105).

Other evidence for a role of lipid rafts in viral budding comes from studies that show that sites of Gag assembly co-localize with proteins found in DRMs, and DRM-proteins are found in budded virus particles (reviewed in (88, 119, 122)). Virions collected from T-cells contain GPI-linked proteins Thy-1 and CD59 which are known to partition to DRM fractions (115). HIV-1 Gag also co-localizes with these DRM proteins in the uropods of T-cells (115). Interestingly, sites of Gag assembly do not contain proteins that are not found in DRM fractions (115).

In addition to the inclusion of DRM proteins into viral particles, HIV-1 Gag co-localizes with tetraspanin enriched microdomains (TEMs) at the PM, and TEMs have been found in virions (120). TEMs contain short, transmembrane proteins that have four

membrane spanning sequences, and are one of many membrane structures that inhibit random mixing of membrane proteins and lipids (117, 163). Virion-associated TEMs modulate infectivity by inhibiting Env mediated fusion with cells (143). TEMs also act to inhibit Env-induced cell-cell fusion which interestingly requires the presence of Gag (157).

Based on mounting evidence, it seems clear that viral budding from cells is a tightly controlled process that includes selection of specific lipid types and the incorporation of non-randomly distributed proteins. Cellular protein incorporation may occur because Gag assembly occurs at sites enriched in the proteins or because Gag induces the formation of a membrane domain to which these proteins preferentially distribute. Alternatively, studies of TEMs suggest that the cell may act to restrict viral entry by incorporating specific membrane proteins into the viral envelope (157). Whether the presence of cholesterol or increased levels of pl-PE represent the formation of or recognition of a raft by the virus, or if these lipids are enriched due to virion-induced curvature, needs to be resolved.

While extensive work has been done to characterize raft behavior for biologically relevant lipid mixtures, no raft behavior has been observed for mixtures that mimic the inner leaflet of the plasma membrane. It is possible that raft behavior on the outer leaflet of the bilayer is transmitted to the inner leaflet through the interdigitation of the lipid acyl chains but this has yet to be determined. Clearly current models do not satisfy the existing data and so further work is required to develop a more complete picture of Gag binding to and budding from the PM.

LIPIDS AND MEMBRANES

To better understand the role lipids play in Gag membrane interactions and the formation of the viral envelope it is necessary to have an understanding of lipid behavior. Lipids represent a diverse group of molecules involved in energy storage, signaling, and the structure of cellular membranes. Glycerophospholipids, characterized by a glycerol head group and two fatty acid chains, represent the predominant group of polar membrane lipids in eukaryotic cells (154) (Fig. 1.6). The most common cellular glycerophospholipids are PC, PS, PE, phosphatidylinositol (PI), and phosphatidic acid (PA). The sterol cholesterol is the most common non-polar membrane lipid.

The plasma membrane of cells is an asymmetric bilayer approximately 30 Angstroms thick and represents only 2-3 percent of total cellular lipids (1). Approximately 50% of the plasma membrane mass is protein, so the study of retroviral protein interaction with membranes prepared from pure lipids must be considered incomplete. However, *in vitro* characterization of lipid mixtures has yielded many breakthroughs in the understanding of membranes and so these studies are useful.

Lipids can be characterized by a number of measurements including their rate of lateral diffusion (translational diffusion coefficient (D_T)) and the order, or degree of movement, of their segmented acyl chains (S). Defining the characteristics of lipids in a membrane bilayer can also be thought of as defining the phase behavior of the membrane bilayer. Membrane phase behavior refers to the solid or liquid state of individual lipids and mixtures, and how this state changes as temperature changes

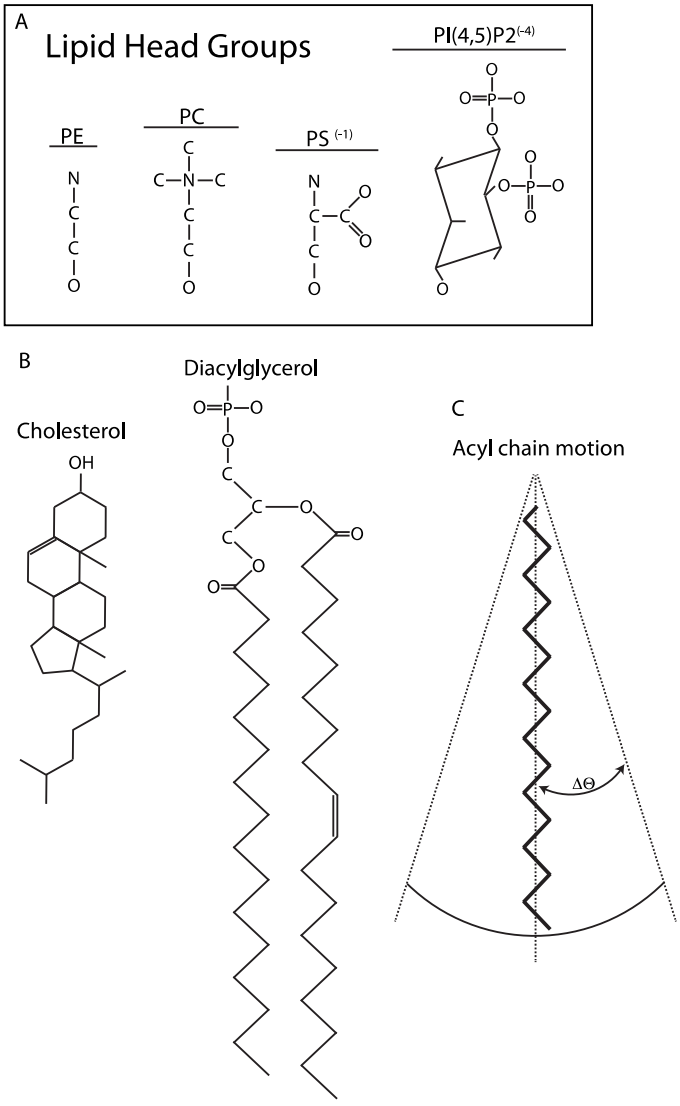

Fig 1.6 Key lipid characteristics. A) Some common lipid head groups shown without hydrogen atoms. The smallest PE is enriched on the inner leaflet of the PM with the net negative PS and PI(4,5)P2 lipids. PC is found primarily on the outer leaflet of the PM. B) Cholesterol and lipid acyl chains occupy the hydrophobic core of the membrane bilayer. Lipid acyl chains can be saturated (no double bonds) as pictured for the chain in the sn-1 position, or unsaturated as pictured for the chain in the sn-2 position. C) The order parameter of a segmented acyl chain (S) is a measure of the space the lipid sweeps out (ΔΘ).

(154). Membrane phases include liquid-disordered (L_d), liquid-ordered (L_o), and solid-gel (L_β) (Fig. 1.7). Liquid-disordered lipid bilayers generally have low concentrations or no cholesterol and lipids with unsaturated acyl chains (154). The lipids are loosely packed with their chains sampling a large cone of space below the lipid's head group. The space the acyl chain samples is ΔΘ. Due to the packing density of lipids the L_d bilayer is thin. Solid-gel bilayers are composed of lipids that pack closely to each other with a low ΔΘ (154). Additionally, the rate that lipids exchange with each other in the solid-gel bilayer is about a thousand-times slower than in liquid-disordered bilayers. Liquid-ordered bilayers typically contain a mix of saturated and unsaturated acyl chain lipids and cholesterol, and while the bilayer has a ΔΘ similar to solid-gel its D_T is similar to liquid disordered (154).

Similar to lipid acyl chains, cholesterol must be shielded from the aqueous environment, but unlike lipids cholesterol does not contain a hydrophilic head group. Shielding of cholesterol in the bilayer is accomplished by straightening of lipid acyl chains (a decrease in ΔΘ) so the lipid head group can shield both its own acyl chains and cholesterol (89).

Membrane phase behavior can be determined for up to three and four component lipid mixtures. These data can be displayed in a phase diagram. A typical three-component phase diagram displays the membrane phase behavior for mixtures of cholesterol, a high Tm (saturated) lipid, and a low Tm (unsaturated) lipid (Fig. 1.8). These diagrams can be used to determine if a given mixture is one, two, or three phase,

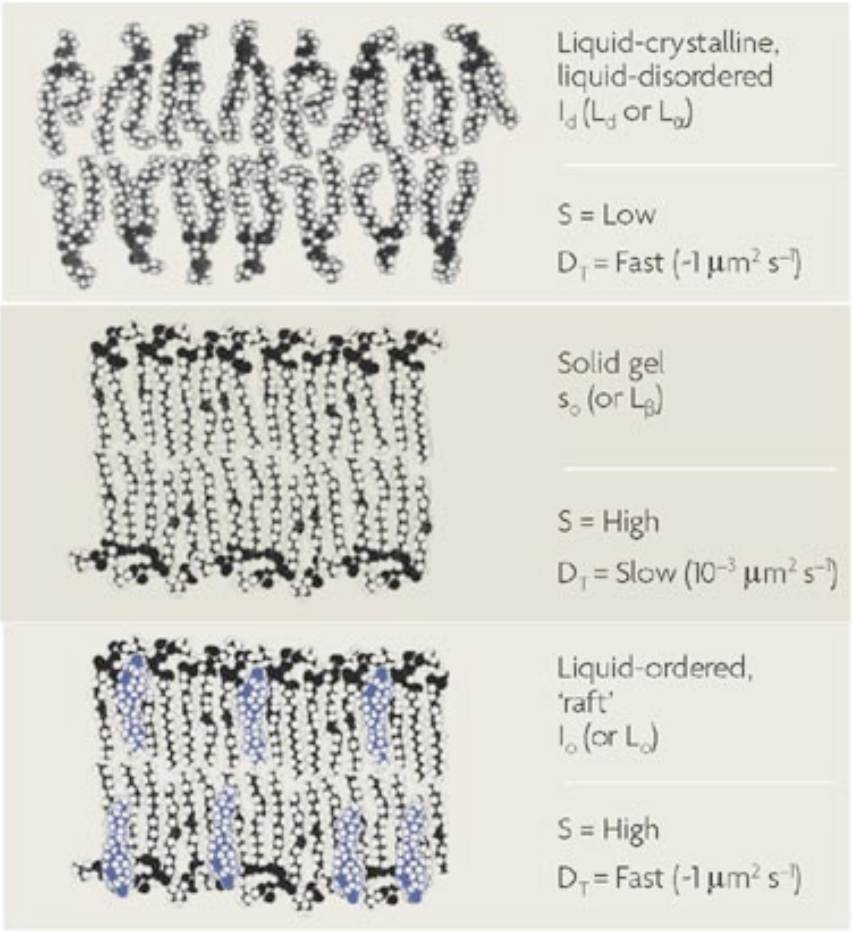

Fig 1.7 Membrane phase behavior (Figure adapted from (154)). Three phases, liquid-disordered, solid gel, and liquid-ordered are pictured from top to bottom. Phases are defined by the order of the order parameter of the segmented acyl chains (low S when the chains have a high ΔΘ, and high S when the chains have a low ΔΘ). The rate of the average lipid latter diffusion D_T is fast for liquid-disordered and liquid-ordered membranes, but slow for solid gel membranes.

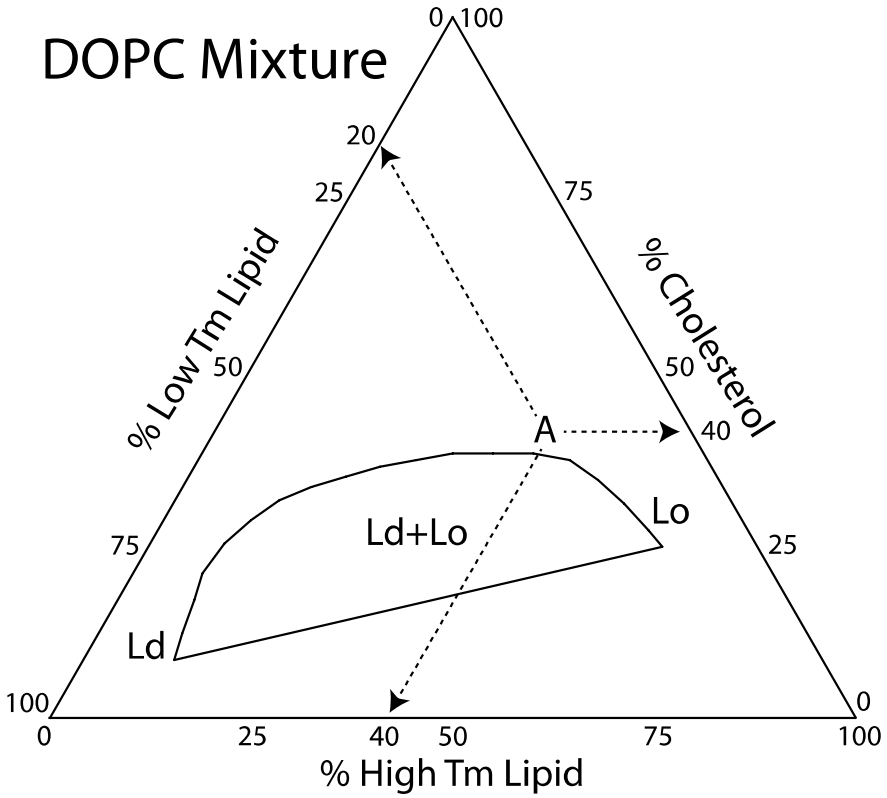

Fig 1.8 Three component phase diagram. The vertices of the triangle represent pure components: 100% cholesterol, 100% low Tm lipid, and 100% high Tm lipid. Each side of the triangle represents a binary mixture. This particular phase diagram displays a two-phase coexistence region, Ld+Lo, surrounded by one-phase regions Ld or Lo, and a three-phase coexistence region (unlabeled) below. To read a composition, choose any point within the triangle, e.g. point “A”. From point “A”, draw three lines towards each binary axis that are parallel to each sides of the triangle. The mole % of each component for “A” is read directly from where the lines intersect with the binary axes. In this example, the composition is 40% high Tm lipid, 20% low Tm lipid, and 40% cholesterol.

and if those phases are L_o, L_d, or L_β. Phase diagrams also define the composition of mixtures that are near critical points between two phase and one-phase mixtures.

Membrane phases can be nanoscopic or microscopic. Nanoscopic domains are typically characterized using Förster resonance energy transfer (FRET) while macroscopic domains can be observed with a microscope by employing giant unilamellar vesicles (GUVs) prepared with fluorescent dyes that partition into different phases (85). FRET also measures the partitioning of lipid dyes in bilayers (33). An advantage of FRET is that preparation of the membranes by rapid solvent exchange (RSE) does not require lipids to transition through a dry phase, a step that is required in GUV preparation that may introduce artifacts (34). The use of GUVs to study membrane phase behavior yields striking and convincing evidence for the presence of lipid phases.

Formation of distinct membrane phases has never been observed in living or fixed cells. This does not mean that it does not occur. The phases may be nanoscopic and so not observable by microscopic techniques. There is indirect evidence for the existence of phase behavior in cellular membranes. For example, treating cells with cold detergent results in the isolation of a highly ordered, raft-like lipid and protein fraction dubbed detergent resistant membranes (DRMs). DRMs are enriched in cholesterol and sphingolipids (31, 148) and one study found enrichment of arachidonic acid (20:4) and PE (128). Electron spin resonance (ESR), a method that measures the order of lipid bilayers, found that DRMs isolated from rat peripheral blood cells (RBL-2H3) were liquid ordered (80). While the behavior of DRMs has convincingly been defined as raft-like, it

remains unclear if DRMs represent a phase present in living cells or an artifact generated during cold detergent treatment of cells.

Further evidence for cell membrane phase behavior comes from microscopic based studies that characterize GUV-like membranes isolated from the PM of cells. The first study collected giant plasma membrane derived vesicles (GPMV) from cells by treating them with paraformaldehyde which induces membrane blebbing (15). At room temperature GPMVs demonstrate lipid dye partitioning similar to that observed for model membranes with well defined L_o and L_d phases (15). The second study collected GUVs by the paraformaldehyde method and an alternative method which involves the swelling of cell membrane spheres (CMS) with PBS buffer (94). The CMSs demonstrated phase separation similar to GPMVs, and the inclusion of a PM protein, the transmembrane protein linker for activation of T cells (LAT) in the Lo phase was also detected (94). Perhaps owing to the inclusion of the LAT transmembrane protein, the L_o phase of CMSs is significantly less ordered than that of model membrane mixes (94). This is an important observation given that cellular membranes contain equivalent amounts of lipids and proteins. If rafts are present in cellular membranes it is likely that they are associated with or perhaps induced by membrane associated cellular proteins (133).

While a role for PM phase behavior has not been identified for viral assembly and budding, as has previously been discussed, that does not mean that understanding membrane behavior is not important to understanding Gag membrane binding. As will

be presented in Chapter 3, the presence of cholesterol and the types of lipid acyl chains in a membrane have dramatic effects on the interaction of Gag with a membrane.

THESIS OUTLINE

The binding of the retroviral Gag protein to the PM is a critical step in the virus life cycle. The signals that govern both components of this interaction, the membrane and the protein, are many. Characterizing the signals and how they overlap each other is difficult. While the field has made significant progress in this endeavour there are still gaps in our knowledge. In chapters 2, 3, and 4 I present my work to address some of these gaps.

Does the binding of RSV Gag to membranes require the presence of the lipid PI(4,5)P2? In chapter 2 I present data from a comparative study of RSV and HIV-1 Gag proteins and their sensitivity to PI(4,5)P2. I found that unlike HIV-1, RSV was not sensitive to PI(4,5)P2 depletion in cells. Interestingly, both RSV and HIV-1 Gag responded similarly to the presence of PI(4,5)P2 as measured by *in vitro* flotation. These results are interpreted to mean that the effect of PI(4,5)P2 may be at least in part due to its electrostatic contribution to the membrane and that this contribution may be difficult to untangle from the effect of specific recognition of the PIP head.

The observation that HIV-1 Gag responds strongly to increasing PS concentrations and the popular hypothesis that retroviruses bud from membrane rafts motivated me to address the effect of membrane order and PS on Gag binding. In chapter 3 I present data from a study of these two factors. I found that while increasing

concentrations of membrane PS does stimulate membrane binding, the effect was strongly influenced by the acyl chains of the PS lipid. I also determined that the presence of cholesterol in the membrane also increased Gag binding. However, both the effect of cholesterol and lipid acyl chains was independent of the overall order of the membrane.

It is known that Gag assembly occurs at the PM but it is not known what the role of Gag multimerization is on Gag's ability to bind the PM. In chapter 4 I present data from a study which addresses this gap in our understanding. One striking result from this study is the difference between the level of MA-multimerization required to localize RSV MA and HIV-1 MA to the PM *in vivo*. In addition to determining the effect of multimerization on binding of MA to membranes, I also studied the effect of RNA on inhibiting this interaction. I found that HIV-1 MA binding to membranes, at physiologic ionic conditions, is inhibited by RNA, but RSV MA is not.

While we have made advances in our understanding of Gag-membrane interactions there are still a great number of things we do not know. In chapter 5 I present some of the interesting questions remaining in this field and propose some methods that could be used to begin to answer them.

CHAPTER 1 REFERENCES

1. **Alberts, B.** 2002. Molecular biology of the cell, 4th ed. Garland Science, New York.

2. **Alfadhli, A., R. L. Barklis, and E. Barklis.** 2009. HIV-1 matrix organizes as a hexamer of trimers on membranes containing phosphatidylinositol-(4,5)-bisphosphate. Virology **387:**466-72.

3. **Alfadhli, A., T. C. Dhenub, A. Still, and E. Barklis.** 2005. Analysis of human immunodeficiency virus type 1 Gag dimerization-induced assembly. J Virol **79:**14498-506.

4. **Alfadhli, A., A. Still, and E. Barklis.** 2009. Analysis of human immunodeficiency virus type 1 matrix binding to membranes and nucleic acids. J Virol **83:**12196-203.

5. **Aloia, R. C., H. Tian, and F. C. Jensen.** 1993. Lipid composition and fluidity of the human immunodeficiency virus envelope and host cell plasma membranes. Proc Natl Acad Sci U S A **90:**5181-5.

6. **Anraku, K., R. Fukuda, N. Takamune, S. Misumi, Y. Okamoto, M. Otsuka, and M. Fujita.** 2010. Highly sensitive analysis of the interaction between HIV-1 Gag and phosphoinositide derivatives based on surface plasmon resonance. Biochemistry **49:**5109-16.

7. **Baluyot, M. F., S. A. Grosse, T. D. Lyddon, S. K. Janaka, and M. C. Johnson.** 2012. CRM1-dependent trafficking of retroviral Gag proteins revisited. J Virol **86:**4696-700.

8. **Banks, J. D., and M. L. Linial.** 2000. Secondary structure analysis of a minimal avian leukosis-sarcoma virus packaging signal. J Virol **74:**456-64.

9. **Banks, J. D., A. Yeo, K. Green, F. Cepeda, and M. L. Linial.** 1998. A minimal avian retroviral packaging sequence has a complex structure. J Virol **72:**6190-4.

10. **Barman, S., and D. P. Nayak.** 2007. Lipid raft disruption by cholesterol depletion enhances influenza A virus budding from MDCK cells. J Virol **81:**12169-78.

11. **Barr, S. D., J. Leipzig, P. Shinn, J. R. Ecker, and F. D. Bushman.** 2005. Integration targeting by avian sarcoma-leukosis virus and human immunodeficiency virus in the chicken genome. J Virol **79:**12035-44.

12. **Batonick, M., M. Favre, M. Boge, P. Spearman, S. Honing, and M. Thali.** 2005. Interaction of HIV-1 Gag with the clathrin-associated adaptor AP-2. Virology **342:**190-200.

13. **Bauby, H., S. Lopez-Verges, G. Hoeffel, D. Delcroix-Genete, K. Janvier, F. Mammano, A. Hosmalin, and C. Berlioz-Torrent.** 2010. TIP47 is required for the production of infectious HIV-1 particles from primary macrophages. Traffic **11:**455-67.

14. **Baumann, M. K., M. J. Swann, M. Textor, and E. Reimhult.** 2011. Pleckstrin homology-phospholipase C-delta1 interaction with phosphatidylinositol 4,5-bisphosphate containing supported lipid bilayers monitored in situ with dual polarization interferometry. Anal Chem **83:**6267-74.

15. **Baumgart, T., A. T. Hammond, P. Sengupta, S. T. Hess, D. A. Holowka, B. A. Baird, and W. W. Webb.** 2007. Large-scale fluid/fluid phase separation of proteins and lipids in giant plasma membrane vesicles. Proc Natl Acad Sci U S A **104:**3165-70.

16. **Bender, W., and N. Davidson.** 1976. Mapping of poly(A) sequences in the electron microscope reveals unusual structure of type C oncornavirus RNA molecules. Cell **7:**595-607.

17. **Benjamin, J., B. K. Ganser-Pornillos, W. F. Tivol, W. I. Sundquist, and G. J. Jensen.** 2005. Three-dimensional structure of HIV-1 virus-like particles by electron cryotomography. J Mol Biol **346:**577-88.

18. **Berkowitz, R., J. Fisher, and S. P. Goff.** 1996. RNA packaging. Curr Top Microbiol Immunol **214:**177-218.

19. **Berkowitz, R. D., M. L. Hammarskjold, C. Helga-Maria, D. Rekosh, and S. P. Goff.** 1995. 5' regions of HIV-1 RNAs are not sufficient for encapsidation: implications for the HIV-1 packaging signal. Virology **212:**718-23.

20. **Berkowitz, R. D., A. Ohagen, S. Hoglund, and S. P. Goff.** 1995. Retroviral nucleocapsid domains mediate the specific recognition of genomic viral RNAs by chimeric Gag polyproteins during RNA packaging in vivo. J Virol **69:**6445-56.

21. **Bharat, T. A., N. E. Davey, P. Ulbrich, J. D. Riches, A. de Marco, M. Rumlova, C. Sachse, T. Ruml, and J. A. Briggs.** 2012. Structure of the immature retroviral capsid at 8 A resolution by cryo-electron microscopy. Nature **487:**385-9.

22. **Bhatia, A. K., N. Campbell, A. Panganiban, and L. Ratner.** 2007. Characterization of replication defects induced by mutations in the basic domain and C-terminus of HIV-1 matrix. Virology **369:**47-54.

23. **Bieniasz, P. D.** 2006. Late budding domains and host proteins in enveloped virus release. Virology **344:**55-63.

24. **Blot, G., K. Janvier, S. Le Panse, R. Benarous, and C. Berlioz-Torrent.** 2003. Targeting of the human immunodeficiency virus type 1 envelope to the trans-Golgi network through binding to TIP47 is required for env incorporation into virions and infectivity. J Virol **77:**6931-45.

25. **Borsetti, A., A. Ohagen, and H. G. Gottlinger.** 1998. The C-terminal half of the human immunodeficiency virus type 1 Gag precursor is sufficient for efficient particle assembly. J Virol **72:**9313-7.

26. **Bouamr, F., J. A. Melillo, M. Q. Wang, K. Nagashima, M. de Los Santos, A. Rein, and S. P. Goff.** 2003. PPPYVEPTAP motif is the late domain of human T-cell leukemia virus type 1 Gag and mediates its functional interaction with cellular proteins Nedd4 and Tsg101 [corrected]. J Virol **77:**11882-95.

27. **Brady, T. L., P. G. Fuerst, R. A. Dick, C. Schmidt, and D. F. Voytas.** 2008. Retrotransposon target site selection by imitation of a cellular protein. Mol Cell Biol **28:**1230-9.

28. **Briggs, J. A., K. Grunewald, B. Glass, F. Forster, H. G. Krausslich, and S. D. Fuller.** 2006. The mechanism of HIV-1 core assembly: insights from three-dimensional reconstructions of authentic virions. Structure **14:**15-20.

29. **Briggs, J. A., J. D. Riches, B. Glass, V. Bartonova, G. Zanetti, and H. G. Krausslich.** 2009. Structure and assembly of immature HIV. Proc Natl Acad Sci U S A **106:**11090-5.

30. **Briggs, J. A., T. Wilk, R. Welker, H. G. Krausslich, and S. D. Fuller.** 2003. Structural organization of authentic, mature HIV-1 virions and cores. EMBO J **22:**1707-15.

31. **Brown, D. A., and J. K. Rose.** 1992. Sorting of GPI-anchored proteins to glycolipid-enriched membrane subdomains during transport to the apical cell surface. Cell **68:**533-44.

32. **Brugger, B., B. Glass, P. Haberkant, I. Leibrecht, F. T. Wieland, and H. G. Krausslich.** 2006. The HIV lipidome: a raft with an unusual composition. Proc Natl Acad Sci U S A **103:**2641-6.

33. **Buboltz, J. T.** 2007. Steady-state probe-partitioning fluorescence resonance energy transfer: a simple and robust tool for the study of membrane phase behavior. Phys Rev E Stat Nonlin Soft Matter Phys **76:**021903.

34. **Buboltz, J. T., and G. W. Feigenson.** 1999. A novel strategy for the preparation of liposomes: rapid solvent exchange. Biochim Biophys Acta **1417:**232-45.

35. **Butterfield-Gerson, K. L., L. Z. Scheifele, E. P. Ryan, A. K. Hopper, and L. J. Parent.** 2006. Importin-beta family members mediate alpharetrovirus gag nuclear entry via interactions with matrix and nucleocapsid. J Virol **80:**1798-806.

36. **Callahan, E., and J. Wills.** 2003. Link between genome packaging and rate of budding for Rous sarcoma virus. J Virol **77:**9388-98.

37. **Callahan, E., and J. Wills.** 2000. Repositioning basic residues in the M domain of the Rous sarcoma virus gag protein. J Virol **74:**11222-9.

38. **Campbell, S., R. J. Fisher, E. M. Towler, S. Fox, H. J. Issaq, T. Wolfe, L. R. Phillips, and A. Rein.** 2001. Modulation of HIV-like particle assembly in vitro by inositol phosphates. Proc Natl Acad Sci U S A **98:**10875-9.

39. **Campbell, S., and A. Rein.** 1999. In vitro assembly properties of human immunodeficiency virus type 1 Gag protein lacking the p6 domain. J Virol **73:**2270-9.

40. **Campbell, S., and V. M. Vogt.** 1997. In vitro assembly of virus-like particles with Rous sarcoma virus Gag deletion mutants: identification of the p10 domain as a morphological determinant in the formation of spherical particles. J Virol **71:**4425-35.

41. **Campbell, S. M., S. M. Crowe, and J. Mak.** 2002. Virion-associated cholesterol is critical for the maintenance of HIV-1 structure and infectivity. AIDS **16:**2253-61.

42. **Camus, G., C. Segura-Morales, D. Molle, S. Lopez-Verges, C. Begon-Pescia, C. Cazevieille, P. Schu, E. Bertrand, C. Berlioz-Torrent, and E. Basyuk.** 2007. The clathrin adaptor complex AP-1 binds HIV-1 and MLV Gag and facilitates their budding. Mol Biol Cell **18:**3193-203.

43. **Carlson, L. A., and J. H. Hurley.** 2012. In vitro reconstitution of the ordered assembly of the endosomal sorting complex required for transport at membrane-bound HIV-1 Gag clusters. Proc Natl Acad Sci U S A **109:**16928-33.

44. **Carter, G. C., L. Bernstone, D. Sangani, J. W. Bee, T. Harder, and W. James.** 2009. HIV entry in macrophages is dependent on intact lipid rafts. Virology **386:**192-202.

45. **Chan, J., R. A. Dick, and V. M. Vogt.** 2011. Rous sarcoma virus gag has no specific requirement for phosphatidylinositol-(4,5)-bisphosphate for plasma membrane association in vivo or for liposome interaction in vitro. J Virol **85:**10851-60.

46. **Chan, R., P. Uchil, J. Jin, G. Shui, D. Ott, W. Mothes, and M. Wenk.** 2008. Retroviruses human immunodeficiency virus and murine leukemia virus are enriched in phosphoinositides. J Virol **82:**11228-38.

47. **Checkley, M. A., B. G. Luttge, P. Y. Mercredi, S. K. Kyere, J. Donlan, T. Murakami, M. F. Summers, S. Cocklin, and E. O. Freed.** 2013. Reevaluation of the requirement for TIP47 in human immunodeficiency virus type 1 envelope glycoprotein incorporation. J Virol **87:**3561-70.

48. **Chen, J., O. Nikolaitchik, J. Singh, A. Wright, C. E. Bencsics, J. M. Coffin, N. Ni, S. Lockett, V. K. Pathak, and W. S. Hu.** 2009. High efficiency of HIV-1 genomic RNA packaging and heterozygote formation revealed by single virion analysis. Proc Natl Acad Sci U S A **106:**13535-40.

49. **Cherepanov, P., G. Maertens, P. Proost, B. Devreese, J. Van Beeumen, Y. Engelborghs, E. De Clercq, and Z. Debyser.** 2003. HIV-1 integrase forms stable tetramers and associates with LEDGF/p75 protein in human cells. J Biol Chem **278:**372-81.

50. **Cheslock, S. R., D. T. Poon, W. Fu, T. D. Rhodes, L. E. Henderson, K. Nagashima, C. F. McGrath, and W. S. Hu.** 2003. Charged assembly helix motif in murine leukemia virus capsid: an important region for virus assembly and particle size determination. J Virol **77:**7058-66.

51. **Chukkapalli, V., I. B. Hogue, V. Boyko, W. S. Hu, and A. Ono.** 2008. Interaction between the human immunodeficiency virus type 1 Gag matrix domain and phosphatidylinositol-(4,5)-bisphosphate is essential for efficient gag membrane binding. J Virol **82:**2405-17.

52. **Chukkapalli, V., J. Inlora, G. C. Todd, and A. Ono.** 2013. Evidence in support of RNA-mediated inhibition of phosphatidylserine-dependent HIV-1 Gag membrane binding in cells. J Virol.

53. **Chukkapalli, V., S. J. Oh, and A. Ono.** 2010. Opposing mechanisms involving RNA and lipids regulate HIV-1 Gag membrane binding through the highly basic region of the matrix domain. Proc Natl Acad Sci U S A **107:**1600-5.

54. **Coffin, J. M., S. H. Hughes, and H. Varmus.** 1997. Retroviruses. Cold Spring Harbor Laboratory Press, Plainview, N.Y.

55. **Cooper, G.** 2000. Structure of the Plasma Membrane. The Cell: A Molecular Approach **2nd edition**.

56. **Crist, R. M., S. A. Datta, A. G. Stephen, F. Soheilian, J. Mirro, R. J. Fisher, K. Nagashima, and A. Rein.** 2009. Assembly properties of human immunodeficiency virus type 1 Gag-leucine zipper chimeras: implications for retrovirus assembly. J Virol **83:**2216-25.

57. **D'Souza, V., and M. F. Summers.** 2005. How retroviruses select their genomes. Nat Rev Microbiol **3:**643-55.

58. **D'Souza, V., and M. F. Summers.** 2004. Structural basis for packaging the dimeric genome of Moloney murine leukaemia virus. Nature **431:**586-90.

59. **Dalton, A., P. Murray, D. Murray, and V. Vogt.** 2005. Biochemical characterization of rous sarcoma virus MA protein interaction with membranes. J Virol **79:**6227-38.

60. **Dalton, A. K., D. Ako-Adjei, P. S. Murray, D. Murray, and V. M. Vogt.** 2007. Electrostatic interactions drive membrane association of the human immunodeficiency virus type 1 Gag MA domain. J Virol **81:**6434-45.

61. **Derse, D., B. Crise, Y. Li, G. Princler, N. Lum, C. Stewart, C. F. McGrath, S. H. Hughes, D. J. Munroe, and X. Wu.** 2007. Human T-cell leukemia virus type 1 integration target sites in the human genome: comparison with those of other retroviruses. J Virol **81:**6731-41.

62. **Dick, R. A., S. L. Goh, G. W. Feigenson, and V. M. Vogt.** 2012. HIV-1 Gag protein can sense the cholesterol and acyl chain environment in model membranes. Proc Natl Acad Sci U S A **109:**18761-6.

63. **Dilley, K. A., D. Gregory, M. C. Johnson, and V. M. Vogt.** 2010. An LYPSL late domain in the gag protein contributes to the efficient release and replication of Rous sarcoma virus. J Virol **84:**6276-87.

64. **Dilley, K. A., N. Ni, O. A. Nikolaitchik, J. Chen, A. Galli, and W. S. Hu.** 2011. Determining the frequency and mechanisms of HIV-1 and HIV-2 RNA copackaging by single-virion analysis. J Virol **85:**10499-508.

65. **Ding, L., A. Derdowski, J. J. Wang, and P. Spearman.** 2003. Independent segregation of human immunodeficiency virus type 1 Gag protein complexes and lipid rafts. J Virol **77:**1916-26.

66. **Dong, X., H. Li, A. Derdowski, L. Ding, A. Burnett, X. Chen, T. R. Peters, T. S. Dermody, E. Woodruff, J. J. Wang, and P. Spearman.** 2005. AP-3 directs the intracellular trafficking of HIV-1 Gag and plays a key role in particle assembly. Cell **120:**663-74.

67. **Doria-Rose, N. A., and V. M. Vogt.** 1998. In vivo selection of Rous sarcoma virus mutants with randomized sequences in the packaging signal. J Virol **72:**8073-82.

68. **Dou, J., J. J. Wang, X. Chen, H. Li, L. Ding, and P. Spearman.** 2009. Characterization of a myristoylated, monomeric HIV Gag protein. Virology **387:**341-52.

69. **Dupraz, P., and P. F. Spahr.** 1992. Specificity of Rous sarcoma virus nucleocapsid protein in genomic RNA packaging. J Virol **66:**4662-70.

70. **Fernandes, F., K. Chen, L. S. Ehrlich, J. Jin, M. H. Chen, G. N. Medina, M. Symons, R. Montelaro, J. Donaldson, N. Tjandra, and C. A. Carter.** 2010. Phosphoinositides Direct Equine Infectious Anemia Virus Gag Trafficking and Release. Traffic.

71. **Freed, E. O.** 2006. HIV-1 Gag: flipped out for PI(4,5)P(2). Proc Natl Acad Sci U S A **103:**11101-2.

72. **Freed, E. O.** 2002. Viral late domains. J Virol **76:**4679-87.

73. **Freed, E. O., G. Englund, and M. A. Martin.** 1995. Role of the basic domain of human immunodeficiency virus type 1 matrix in macrophage infection. J Virol **69:**3949-54.

74. **Fujii, K., J. H. Hurley, and E. O. Freed.** 2007. Beyond Tsg101: the role of Alix in 'ESCRTing' HIV-1. Nat Rev Microbiol **5:**912-6.

75. **Gamble, T. R., S. Yoo, F. F. Vajdos, U. K. von Schwedler, D. K. Worthylake, H. Wang, J. P. McCutcheon, W. I. Sundquist, and C. P. Hill.** 1997. Structure of the carboxyl-terminal dimerization domain of the HIV-1 capsid protein. Science **278:**849-53.

76. **Ganser-Pornillos, B. K., A. Cheng, and M. Yeager.** 2007. Structure of full-length HIV-1 CA: a model for the mature capsid lattice. Cell **131:**70-9.

77. **Garbitt, R. A., K. R. Bone, and L. J. Parent.** 2004. Insertion of a classical nuclear import signal into the matrix domain of the Rous sarcoma virus Gag protein interferes with virus replication. J Virol **78:**13534-42.

78. **Garbitt-Hirst, R., S. P. Kenney, and L. J. Parent.** 2009. Genetic evidence for a connection between Rous sarcoma virus gag nuclear trafficking and genomic RNA packaging. J Virol **83:**6790-7.

79. **Garcia, P., R. Gupta, S. Shah, A. J. Morris, S. A. Rudge, S. Scarlata, V. Petrova, S. McLaughlin, and M. J. Rebecchi.** 1995. The pleckstrin homology domain of phospholipase C-delta 1 binds with high affinity to phosphatidylinositol 4,5-bisphosphate in bilayer membranes. Biochemistry **34:**16228-34.

80. **Ge, M., K. A. Field, R. Aneja, D. Holowka, B. Baird, and J. H. Freed.** 1999. Electron spin resonance characterization of liquid ordered phase of detergent-resistant membranes from RBL-2H3 cells. Biophys J **77:**925-33.

81. **Ghanam, R. H., A. B. Samal, T. F. Fernandez, and J. S. Saad.** 2012. Role of the HIV-1 Matrix Protein in Gag Intracellular Trafficking and Targeting to the Plasma Membrane for Virus Assembly. Front Microbiol **3:**55.

82. **Graham, D. R., E. Chertova, J. M. Hilburn, L. O. Arthur, and J. E. Hildreth.** 2003. Cholesterol depletion of human immunodeficiency virus type 1 and simian immunodeficiency virus with beta-cyclodextrin inactivates and permeabilizes the virions: evidence for virion-associated lipid rafts. J Virol **77:**8237-48.

83. **Gudleski, N., J. M. Flanagan, E. P. Ryan, M. C. Bewley, and L. J. Parent.** 2010. Directionality of nucleocytoplasmic transport of the retroviral gag protein depends on sequential binding of karyopherins and viral RNA. Proc Natl Acad Sci U S A **107:**9358-63.

84. **Hamard-Peron, E., F. Juillard, J. Saad, C. Roy, P. Roingeard, M. Summers, J. Darlix, C. Picart, and D. Muriaux.** 2010. Targeting of murine leukemia virus gag to the plasma membrane is mediated by PI(4,5)P2/PS and a polybasic region in the matrix. J Virol **84:**503-15.

85. **Heberle, F. A., and G. W. Feigenson.** 2011. Phase separation in lipid membranes. Cold Spring Harb Perspect Biol **3**.

86. **Hill, C. P., D. Worthylake, D. P. Bancroft, A. M. Christensen, and W. I. Sundquist.** 1996. Crystal structures of the trimeric human immunodeficiency virus type 1 matrix protein: implications for membrane association and assembly. Proc Natl Acad Sci U S A **93:**3099-104.

87. **Hogue, I. B., A. Hoppe, and A. Ono.** 2009. Quantitative fluorescence resonance energy transfer microscopy analysis of the human immunodeficiency virus type 1 Gag-Gag interaction: relative contributions of the CA and NC domains and membrane binding. J Virol **83:**7322-36.

88. **Hogue, I. B., G. N. Llewellyn, and A. Ono.** 2012. Dynamic Association between HIV-1 Gag and Membrane Domains. Mol Biol Int **2012:**979765.

89. **Huang, J.** 2009. Model membrane thermodynamics and lateral distribution of cholesterol: from experimental data to Monte Carlo simulation. Methods Enzymol **455:**329-64.

90. **Hurley, J. H., E. Boura, L. A. Carlson, and B. Rozycki.** 2010. Membrane budding. Cell **143:**875-87.

91. **Hurley, J. H., and P. I. Hanson.** 2010. Membrane budding and scission by the ESCRT machinery: it's all in the neck. Nat Rev Mol Cell Biol **11:**556-66.

92. **Inlora, J., V. Chukkapalli, D. Derse, and A. Ono.** 2011. Gag Localization and Virus-like Particle Release Mediated by the Matrix Domain of Human T-Lymphotropic Virus Type-1 Gag are Less Dependent on Phosphatidylinositol-(4,5)-bisphosphate than Those Mediated by the Matrix Domain of Human Immunodeficiency Virus Type-1 Gag. J Virol.

93. **Johnson, M. C., H. M. Scobie, Y. M. Ma, and V. M. Vogt.** 2002. Nucleic acid-independent retrovirus assembly can be driven by dimerization. J Virol **76:**11177-85.

94. **Kaiser, H. J., D. Lingwood, I. Levental, J. L. Sampaio, L. Kalvodova, L. Rajendran, and K. Simons.** 2009. Order of lipid phases in model and plasma membranes. Proc Natl Acad Sci U S A **106:**16645-50.

95. **Kawada, S., T. Goto, H. Haraguchi, A. Ono, and Y. Morikawa.** 2008. Dominant negative inhibition of human immunodeficiency virus particle production by the nonmyristoylated form of gag. J Virol **82:**4384-99.

96. **Kutluay, S. B., and P. D. Bieniasz.** 2010. Analysis of the initiating events in HIV-1 particle assembly and genome packaging. PLoS Pathog **6:**e1001200.

97. **Kyere, S. K., P. Y. Mercredi, X. Dong, P. Spearman, and M. F. Summers.** 2012. The HIV-1 matrix protein does not interact directly with the protein interactive domain of AP-3delta. Virus Res **169:**411-4.

98. **Lee, E. G., and M. L. Linial.** 2000. Yeast three-hybrid screening of rous sarcoma virus mutants with randomly mutagenized minimal packaging signals reveals regions important for gag interactions. J Virol **74:**9167-74.

99. **Lemmon, M. A., K. M. Ferguson, R. O'Brien, P. B. Sigler, and J. Schlessinger.** 1995. Specific and high-affinity binding of inositol phosphates to an isolated pleckstrin homology domain. Proc Natl Acad Sci U S A **92:**10472-6.

100. **Lever, A., H. Gottlinger, W. Haseltine, and J. Sodroski.** 1989. Identification of a sequence required for efficient packaging of human immunodeficiency virus type 1 RNA into virions. J Virol **63:**4085-7.

101. **Levin, J. G., J. Guo, I. Rouzina, and K. Musier-Forsyth.** 2005. Nucleic acid chaperone activity of HIV-1 nucleocapsid protein: critical role in reverse transcription and molecular mechanism. Prog Nucleic Acid Res Mol Biol **80:**217-86.

102. **Lewinski, M. K., M. Yamashita, M. Emerman, A. Ciuffi, H. Marshall, G. Crawford, F. Collins, P. Shinn, J. Leipzig, S. Hannenhalli, C. C. Berry, J. R.**

Ecker, and F. D. Bushman. 2006. Retroviral DNA integration: viral and cellular determinants of target-site selection. PLoS Pathog **2:**e60.

103. **Li, S., C. P. Hill, W. I. Sundquist, and J. T. Finch.** 2000. Image reconstructions of helical assemblies of the HIV-1 CA protein. Nature **407:**409-13.

104. **Lindwasser, O. W., and M. D. Resh.** 2001. Multimerization of human immunodeficiency virus type 1 Gag promotes its localization to barges, raft-like membrane microdomains. J Virol **75:**7913-24.

105. **Lindwasser, O. W., and M. D. Resh.** 2002. Myristoylation as a target for inhibiting HIV assembly: unsaturated fatty acids block viral budding. Proc Natl Acad Sci U S A **99:**13037-42.

106. **Lopez-Verges, S., G. Camus, G. Blot, R. Beauvoir, R. Benarous, and C. Berlioz-Torrent.** 2006. Tail-interacting protein TIP47 is a connector between Gag and Env and is required for Env incorporation into HIV-1 virions. Proc Natl Acad Sci U S A **103:**14947-52.

107. **Lorizate, M., T. Sachsenheimer, B. Glass, A. Habermann, M. J. Gerl, H. G. Krausslich, and B. Brugger.** 2013. Comparative lipidomics analysis of HIV-1 particles and their producer cell membrane in different cell lines. Cell Microbiol **15:**292-304.

108. **Ma, Y. M., and V. M. Vogt.** 2004. Nucleic acid binding-induced Gag dimerization in the assembly of Rous sarcoma virus particles in vitro. J Virol **78:**52-60.

109. **Ma, Y. M., and V. M. Vogt.** 2002. Rous sarcoma virus Gag protein-oligonucleotide interaction suggests a critical role for protein dimer formation in assembly. J Virol **76:**5452-62.

110. **Martin-Serrano, J., T. Zang, and P. D. Bieniasz.** 2001. HIV-1 and Ebola virus encode small peptide motifs that recruit Tsg101 to sites of particle assembly to facilitate egress. Nat Med **7:**1313-9.

111. **Medigeshi, G. R., A. J. Hirsch, D. N. Streblow, J. Nikolich-Zugich, and J. A. Nelson.** 2008. West Nile virus entry requires cholesterol-rich membrane microdomains and is independent of alphavbeta3 integrin. J Virol **82:**5212-9.

112. **Mitchell, R. S., B. F. Beitzel, A. R. Schroder, P. Shinn, H. Chen, C. C. Berry, J. R. Ecker, and F. D. Bushman.** 2004. Retroviral DNA integration: ASLV, HIV, and MLV show distinct target site preferences. PLoS Biol **2:**E234.

113. **Murray, P., Z. Li, J. Wang, C. Tang, B. Honig, and D. Murray.** 2005. Retroviral matrix domains share electrostatic homology: models for membrane binding function throughout the viral life cycle. Structure **13:**1521-31.

114. **Nadaraia-Hoke, S., D. V. Bann, T. L. Lochmann, N. Gudleski-O'Regan, and L. J. Parent.** 2013. Alterations in the MA and NC domains modulate phosphoinositide-dependent plasma membrane localization of the Rous sarcoma virus Gag protein. J Virol **87:**3609-15.

115. **Nguyen, D. H., and J. E. Hildreth.** 2000. Evidence for budding of human immunodeficiency virus type 1 selectively from glycolipid-enriched membrane lipid rafts. J Virol **74:**3264-72.

116. **Nikolaitchik, O. A., K. A. Dilley, W. Fu, R. J. Gorelick, S. H. Tai, F. Soheilian, R. G. Ptak, K. Nagashima, V. K. Pathak, and W. S. Hu.** 2013. Dimeric RNA Recognition Regulates HIV-1 Genome Packaging. PLoS Pathog **9:**e1003249.

117. **Nydegger, S., S. Khurana, D. N. Krementsov, M. Foti, and M. Thali.** 2006. Mapping of tetraspanin-enriched microdomains that can function as gateways for HIV-1. J Cell Biol **173:**795-807.

118. **O'Carroll, I. P., F. Soheilian, A. Kamata, K. Nagashima, and A. Rein.** 2012. Elements in HIV-1 Gag contributing to virus particle assembly. Virus Res.

119. **Ono, A.** 2009. HIV-1 Assembly at the Plasma Membrane: Gag Trafficking and Localization. Future Virol **4:**241-257.

120. **Ono, A.** 2012. Relationships between plasma membrane microdomains and HIV-1 assembly. Biol Cell **102:**335-50.

121. **Ono, A., S. D. Ablan, S. J. Lockett, K. Nagashima, and E. O. Freed.** 2004. Phosphatidylinositol (4,5) bisphosphate regulates HIV-1 Gag targeting to the plasma membrane. Proc Natl Acad Sci U S A **101:**14889-94.

122. **Ono, A., and E. O. Freed.** 2001. Plasma membrane rafts play a critical role in HIV-1 assembly and release. Proc Natl Acad Sci U S A **98:**13925-30.

123. **Ono, A., J. Orenstein, and E. Freed.** 2000. Role of the Gag matrix domain in targeting human immunodeficiency virus type 1 assembly. J Virol **74:**2855-66.

124. **Ono, A., A. A. Waheed, and E. O. Freed.** 2007. Depletion of cellular cholesterol inhibits membrane binding and higher-order multimerization of human immunodeficiency virus type 1 Gag. Virology **360:**27-35.

125. **Ott, D. E., L. V. Coren, E. N. Chertova, T. D. Gagliardi, K. Nagashima, R. C. Sowder, 2nd, D. T. Poon, and R. J. Gorelick.** 2003. Elimination of protease activity restores efficient virion production to a human immunodeficiency virus type 1 nucleocapsid deletion mutant. J Virol **77:**5547-56.

126. **Pessin, J. E., and M. Glaser.** 1980. Budding of Rous sarcoma virus and vesicular stomatitis virus from localized lipid regions in the plasma membrane of chicken embryo fibroblasts. J Biol Chem **255:**9044-50.

127. **Phillips, J. M., P. S. Murray, D. Murray, and V. M. Vogt.** 2008. A molecular switch required for retrovirus assembly participates in the hexagonal immature lattice. EMBO J **27:**1411-20.

128. **Pike, L. J., X. Han, K. N. Chung, and R. W. Gross.** 2002. Lipid rafts are enriched in arachidonic acid and plasmenylethanolamine and their composition is independent of caveolin-1 expression: a quantitative electrospray ionization/mass spectrometric analysis. Biochemistry **41:**2075-88.

129. **Pornillos, O., B. K. Ganser-Pornillos, S. Banumathi, Y. Hua, and M. Yeager.** 2010. Disulfide bond stabilization of the hexameric capsomer of human immunodeficiency virus. J Mol Biol **401:**985-95.

130. **Pornillos, O., B. K. Ganser-Pornillos, B. N. Kelly, Y. Hua, F. G. Whitby, C. D. Stout, W. I. Sundquist, C. P. Hill, and M. Yeager.** 2009. X-ray structures of the hexameric building block of the HIV capsid. Cell **137:**1282-92.

131. **Pornillos, O., B. K. Ganser-Pornillos, and M. Yeager.** 2011. Atomic-level modelling of the HIV capsid. Nature **469:**424-7.

132. **Prchal, J., P. Srb, E. Hunter, T. Ruml, and R. Hrabal.** 2012. The structure of myristoylated Mason-Pfizer monkey virus matrix protein and the role of phosphatidylinositol-(4,5)-bisphosphate in its membrane binding. J Mol Biol **423:**427-38.

133. **Rajendran, L., and K. Simons.** 2005. Lipid rafts and membrane dynamics. J Cell Sci **118:**1099-102.

134. **Reil, H., A. A. Bukovsky, H. R. Gelderblom, and H. G. Gottlinger.** 1998. Efficient HIV-1 replication can occur in the absence of the viral matrix protein. EMBO J **17:**2699-708.

135. **Rein, A.** 2010. Nucleic acid chaperone activity of retroviral Gag proteins. RNA Biol **7:**700-5.

136. **Rein, A., L. E. Henderson, and J. G. Levin.** 1998. Nucleic-acid-chaperone activity of retroviral nucleocapsid proteins: significance for viral replication. Trends Biochem Sci **23:**297-301.

137. **Resh, M. D.** 2004. A myristoyl switch regulates membrane binding of HIV-1 Gag. Proc Natl Acad Sci U S A **101:**417-8.

138. **Resh, M. D.** 1999. Fatty acylation of proteins: new insights into membrane targeting of myristoylated and palmitoylated proteins. Biochim Biophys Acta **1451:**1-16.

139. **Saad, J., S. Ablan, R. Ghanam, A. Kim, K. Andrews, K. Nagashima, F. Soheilian, E. Freed, and M. Summers.** 2008. Structure of the myristylated human immunodeficiency virus type 2 matrix protein and the role of phosphatidylinositol-(4,5)-bisphosphate in membrane targeting. J Mol Biol **382:**434-47.

140. **Saad, J., E. Loeliger, P. Luncsford, M. Liriano, J. Tai, A. Kim, J. Miller, A. Joshi, E. Freed, and M. Summers.** 2007. Point mutations in the HIV-1 matrix protein turn off the myristyl switch. J Mol Biol **366:**574-85.

141. **Saad, J., J. Miller, J. Tai, A. Kim, R. Ghanam, and M. Summers.** 2006. Structural basis for targeting HIV-1 Gag proteins to the plasma membrane for virus assembly. Proc Natl Acad Sci U S A **103:**11364-9.

142. **Santoni, F. A., O. Hartley, and J. Luban.** 2010. Deciphering the code for retroviral integration target site selection. PLoS Comput Biol **6:**e1001008.

143. **Sato, K., J. Aoki, N. Misawa, E. Daikoku, K. Sano, Y. Tanaka, and Y. Koyanagi.** 2008. Modulation of human immunodeficiency virus type 1 infectivity through incorporation of tetraspanin proteins. J Virol **82:**1021-33.

144. **Scheifele, L. Z., R. A. Garbitt, J. D. Rhoads, and L. J. Parent.** 2002. Nuclear entry and CRM1-dependent nuclear export of the Rous sarcoma virus Gag polyprotein. Proc Natl Acad Sci U S A **99:**3944-9.

145. **Scheifele, L. Z., E. P. Ryan, and L. J. Parent.** 2005. Detailed mapping of the nuclear export signal in the Rous sarcoma virus Gag protein. J Virol **79:**8732-41.

146. **Schroder, A. R., P. Shinn, H. Chen, C. Berry, J. R. Ecker, and F. Bushman.** 2002. HIV-1 integration in the human genome favors active genes and local hotspots. Cell **110:**521-9.

147. **Shkriabai, N., S. Datta, Z. Zhao, S. Hess, A. Rein, and M. Kvaratskhelia.** 2006. Interactions of HIV-1 Gag with assembly cofactors. Biochemistry **45:**4077-83.

148. **Simons, K., and E. Ikonen.** 1997. Functional rafts in cell membranes. Nature **387:**569-72.

149. **Sousa, I. P., Jr., C. A. Carvalho, D. F. Ferreira, G. Weissmuller, G. M. Rocha, J. L. Silva, and A. M. Gomes.** 2011. Envelope lipid-packing as a critical factor for the biological activity and stability of alphavirus particles isolated from mammalian and mosquito cells. J Biol Chem **286:**1730-6.

150. **Spearman, P., R. Horton, L. Ratner, and I. Kuli-Zade.** 1997. Membrane binding of human immunodeficiency virus type 1 matrix protein in vivo supports a conformational myristyl switch mechanism. J Virol **71:**6582-92.

151. **Statistics, H.** 2013. World Health Statistics. World Health Organization.

152. **Sun, X., and G. R. Whittaker.** 2003. Role for influenza virus envelope cholesterol in virus entry and infection. J Virol **77:**12543-51.

153. **Tang, C., E. Loeliger, P. Luncsford, I. Kinde, D. Beckett, and M. F. Summers.** 2004. Entropic switch regulates myristate exposure in the HIV-1 matrix protein. Proc Natl Acad Sci U S A **101:**517-22.

154. **van Meer, G., D. R. Voelker, and G. W. Feigenson.** 2008. Membrane lipids: where they are and how they behave. Nat Rev Mol Cell Biol **9:**112-24.

155. **Vlach, J., and J. S. Saad.** 2012. Trio engagement via plasma membrane phospholipids and the myristoyl moiety governs HIV-1 matrix binding to bilayers. Proc Natl Acad Sci U S A.

156. **Wang, H., N. J. Machesky, and L. M. Mansky.** 2004. Both the PPPY and PTAP motifs are involved in human T-cell leukemia virus type 1 particle release. J Virol **78:**1503-12.

157. **Weng, J., D. N. Krementsov, S. Khurana, N. H. Roy, and M. Thali.** 2009. Formation of syncytia is repressed by tetraspanins in human immunodeficiency virus type 1-producing cells. J Virol **83:**7467-74.

158. **Wills, J. W., C. E. Cameron, C. B. Wilson, Y. Xiang, R. P. Bennett, and J. Leis.** 1994. An assembly domain of the Rous sarcoma virus Gag protein required late in budding. J Virol **68:**6605-18.

159. **Wright, E. R., J. B. Schooler, H. J. Ding, C. Kieffer, C. Fillmore, W. I. Sundquist, and G. J. Jensen.** 2007. Electron cryotomography of immature HIV-1 virions reveals the structure of the CA and SP1 Gag shells. EMBO J **26:**2218-26.

160. **Xiang, Y., C. E. Cameron, J. W. Wills, and J. Leis.** 1996. Fine mapping and characterization of the Rous sarcoma virus Pr76gag late assembly domain. J Virol **70:**5695-700.

161. **Xie, W., X. Gai, Y. Zhu, D. C. Zappulla, R. Sternglanz, and D. F. Voytas.** 2001. Targeting of the yeast Ty5 retrotransposon to silent chromatin is mediated by interactions between integrase and Sir4p. Mol Cell Biol **21:**6606-14.

162. **Yagisawa, H.** 2006. Nucleocytoplasmic shuttling of phospholipase C-delta1: a link to Ca2+. J Cell Biochem **97:**233-43.

163. **Yanez-Mo, M., O. Barreiro, M. Gordon-Alonso, M. Sala-Valdes, and F. Sanchez-Madrid.** 2009. Tetraspanin-enriched microdomains: a functional unit in cell plasma membranes. Trends Cell Biol **19:**434-46.

164. **Zhang, Y., and E. Barklis.** 1995. Nucleocapsid protein effects on the specificity of retrovirus RNA encapsidation. J Virol **69:**5716-22.

165. **Zhou, J., R. L. Bean, V. M. Vogt, and M. Summers.** 2007. Solution structure of the Rous sarcoma virus nucleocapsid protein: muPsi RNA packaging signal complex. J Mol Biol **365:**453-67.

166. **Zhou, W., L. J. Parent, J. W. Wills, and M. D. Resh.** 1994. Identification of a membrane-binding domain within the amino-terminal region of human immunodeficiency virus type 1 Gag protein which interacts with acidic phospholipids. J Virol **68:**2556-69.

CHAPTER 2

ROUS SARCOMA VIRUS GAG HAS NO SPECIFIC REQUIREMENT FOR PHOSPHATIDYLINOSITOL-(4,5)-BISPHOSPHATE FOR PLASMA MEMBRANE ASSOCIATION IN VIVO OR FOR LIPOSOME INTERACTION IN VITRO[1]

The MA domain of the retroviral Gag protein mediates interactions with the plasma membrane, which is the site of productive virus release. HIV-1 MA has a phosphatidylinositol-(4,5)-bisphosphate [PI(4,5)P_2] binding pocket; depletion of this phospholipid from the plasma membrane compromises Gag membrane association and virus budding. We used multiple methods to examine the possible role of PI(4,5)P_2 in Gag-membrane interaction of the alpharetrovirus Rous sarcoma virus (RSV). In contrast to HIV-1, which was tested in parallel, neither membrane localization of RSV Gag-GFP nor release of virus-like particles was affected by phosphatase-mediated depletion of PI(4,5)P_2 in transfected avian cells. In liposome flotation experiments, RSV Gag required acidic lipids for binding but showed no specificity for PI(4,5)P_2. Mono-, di- and tri-phosphorylated PIP species as well as high concentrations of phosphatidylserine (PS) supported similar levels of flotation. A mutation that increases the[2] overall charge

[1] The following section is reproduced from: Chan, J., R. A. Dick, and V. M. Vogt. 2011. Rous sarcoma virus gag has no specific requirement for phosphatidylinositol-(4,5)-bisphosphate for plasma membrane association in vivo or for liposome interaction in vitro. J Virol 85:10851-60, with modifications to conform to the required format. R.A.D. perfomed liposome flotations and virus release. J.C. performed cell imaging.

of RSV MA also enhanced Gag membrane binding. Contrary to previous reports, we found that high concentrations of PS, in the absence of PIPs, also strongly promoted HIV-1 Gag flotation. Taken together, we interpret these results to mean that RSV Gag membrane association is driven by electrostatic interactions and not by any specific association with $PI(4,5)P_2$.

INTRODUCTION

Assembly and budding of retrovirus particles are complex processes mediated by the viral structural protein Gag. Several thousand Gag molecules along with two copies of the RNA genome and the viral glycoprotein Env are transported to the assembly site where Gag-lipid, Gag-Gag, and Gag-RNA interactions drive the formation of a virus particle. The assembly site is determined largely by the membrane binding domain (MBD) at the N-terminus of the Gag protein, which mediates membrane targeting and membrane binding (25, 43, 58, 59, 64, 68). For most retroviruses, productive viral assembly occurs at the plasma membrane (PM) (21, 30).

Across retroviral genera, sequence similarity among retroviral MBDs is limited; however, all previously studied retroviral MBDs fold into a small, globular domain with an alpha helical core (40). The MBD usually contains two membrane-binding signals, an N-terminal myristate, which inserts into the hydrophobic interior of lipid membranes, and a surface patch of basic residues, which interacts with acidic phospholipids. Several retroviral MBDs are not myristoylated , including those of equine infectious anemia virus (EIAV) (10, 26) and Rous sarcoma virus (RSV) (38). In contrast, the basic patch is highly conserved, suggesting that electrostatic interactions are universally

important in membrane binding of Gag (40). Depending on the type of retrovirus and the severity of the changes, mutations in the basic patch can shift Gag localization from the plasma membrane to intracellular membranes (22, 43, 60), promote promiscuous binding to cellular membranes (55), or abolish membrane binding entirely (6, 58). Mutations that increase the positive charge of the basic patch can rescue Gag localization to the PM or enhance the release of virus particles (5, 6).

Acidic phospholipids, especially phosphatidylserine (PS) and phosphatidylinositol phosphates (PIPs) are important cellular factors in mediating protein-membrane interactions (27, 35, 39, 67). PS has a single, net negative charge, while PIPs have multiple negative charges due to phosphorylation of the inositol ring at positions 3, 4 and/or 5. The location and degree of phosphorylation is determined by spatially regulated kinases and phosphatases, which results in the enrichment of specific species of PIPs at different cellular membranes [reviewed in (33)]. PS and PI(4,5)P_2 are found primarily on the inner leaflet of the PM in mammalian cells, where they account for 25-35% and 0.5-1.0% of the phospholipids, respectively (2, 9, 36, 49). Recruitment of cellular MBDs [e.g. pleckstrin homology (PH) domains (16, 19, 63), C2 domains (37), and epsin N-terminal homology domains/AP180 N-terminal homology (ENTH/ANTH) domains (28)] to the PM is dependent on direct interactions with PS and/or PI(4,5)P_2. However, the quantitative contribution of each of these acidic lipids to PM binding of proteins is uncertain since different studies have yielded conflicting results (27, 67).

As purified proteins, some retroviral MBDs (e.g. that of HIV-1 and HIV-2) bind specifically to versions of PI(4,5)P_2 that have shortened fatty acid chains required for

solubility (51, 54). Mutation of the residues involved in $PI(4,5)P_2$ interaction reduces PM affinity in vivo and also binding to artificial liposomes in vitro (3, 10, 25, 51, 54, 57). Consistent with the inferred role for this lipid in virus assembly at the PM, the membrane surrounding HIV-1 and murine leukemia virus (MLV) virions is enriched in $PI(4,5)P_2$ (9) as well as PS (2, 4, 47). Furthermore, over-expression of inositol polyphosphate-5-phosphatase E (here referred to as 5ptase), which depletes cellular levels of $PI(4,5)P_2$ (32), results in a decrease in Gag localization at the PM and a reduction in virus release (25, 42, 51, 60). In the case of HIV-1, binding to $PI(4,5)P_2$ leads to exposure of the myristate, thereby enhancing the affinity of the MBD for the PM (53, 54).

The RSV MBD is not myristoylated, nor does it contain a linear sequence of basic residues as do EIAV and MLV. However, the three-dimensional structure of the protein reveals that multiple basic residues come together to form a surface patch (38). The RSV MBD has a net positive charge of +5 (5). Small deletions or neutralization of two or more basic residues in the surface patch abolish PM localization and reduce virus release (5, 6, 41, 44, 64). Compensatory mutations that restore the net positive charge of the MBD also restore PM localization, whereas some mutations that increase the overall charge alter the intracellular trafficking of RSV Gag, enhance Gag localization at the PM, and accelerate the budding kinetics of virus-like particles (VLPs) (6). These results were interpreted to imply that RSV Gag-membrane binding is driven chiefly by electrostatic interactions (5, 6).

Using computational modeling and liposome flotation assays with purified recombinant proteins, we previously reported that RSV and HIV-1 MA membrane

binding in vitro is driven by electrostatic interactions with negatively charged lipids (13, 14). Preliminary data also suggested that $PI(4,5)P_2$ at 1% of total phospholipid does not significantly enhance MA-liposome binding in the presence of physiological levels of PS. We have now extended these studies to the RSV Gag protein, in comparison with the HIV-1 Gag protein that has been studied by others (1, 11, 12, 20, 29). By fluorescence imaging and virus release in cells and by liposome flotation of protein synthesized in a reticulocyte lysate, RSV Gag appears to have no specific requirement for $PI(4,5)P_2$ in membrane targeting and viral assembly in vivo or for liposome binding in vitro. Rather, RSV Gag membrane association relies only on electrostatic interactions.

MATERIALS AND METHODS

DNA Vectors

RSV and HIV Gag constructs used in this study are shown schematically in Fig. 2.1. All DNA constructs were generated with common subcloning techniques and were propagated in DH5α cells. The 5ptase expression vector, pcDNA4TO/Myc5ptaseIV (11) was a gift from Akira Ono. Plasmid PH-GFP, a gift from Barbara Baird, encodes the pleckstrin homology (PH) domain from human phospholipase C δ1 fused to eGFP under control of the cytomegalovirus immediate early promoter. Fluorescent Gag proteins were created by cloning RSV GagΔPR derived from the Prague C strain or HIV-1 Gag derived from the BH-10 strain into the pEGFP-N1 vector (Clontech). Plasmid PHGag-GFP was constructed by subcloning the PH domain from pPH-GFP into RSV GagΔPR-GFP between the *SacI* site (nt 255) in the leader region and the *XhoI* site in

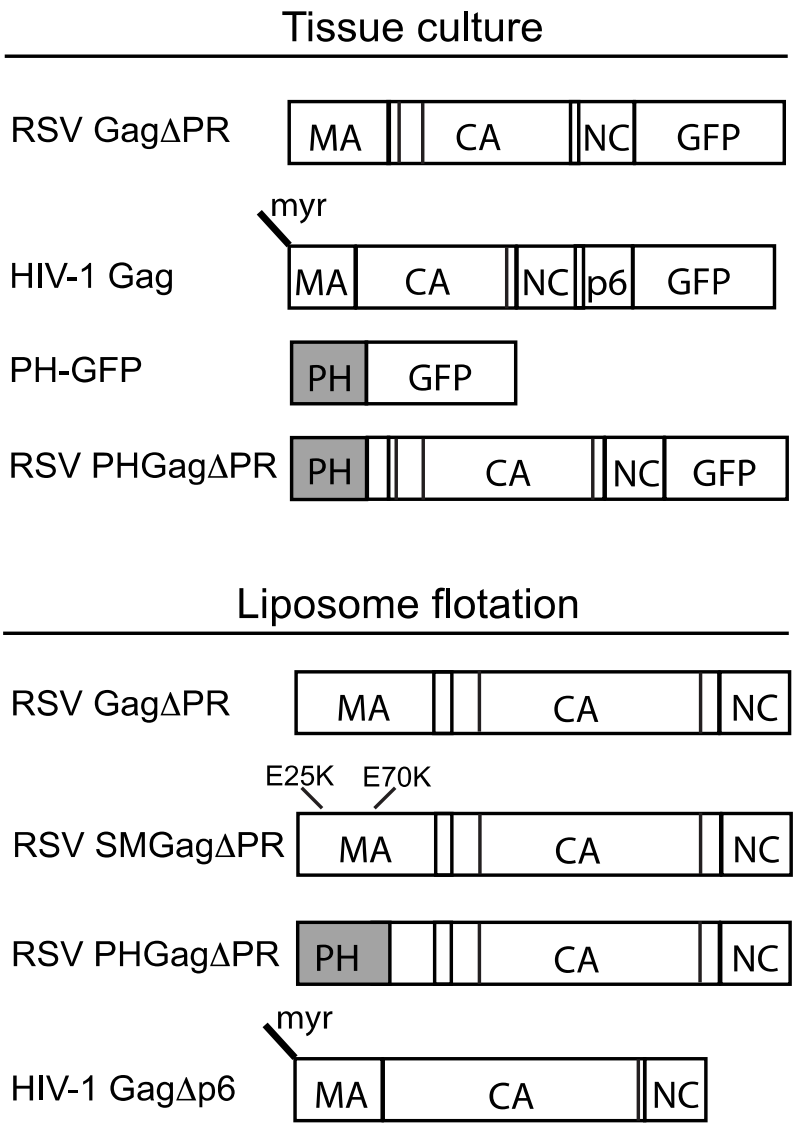

Fig. 2.1 Schematic representations of proteins. RSV and HIV-1 GFP-tagged proteins expressed in transfected cells are shown at the top along with the PH-GFP protein. Proteins translated in vitro and submitted to flotation analysis are shown at the bottom. Vertical lines in the boxes stand for protease cleavage sites.

MA (nt 630), which has traditionally been used to define the C-terminal end of the RSV MBD (38).

The previously described plasmid RSV GagΔPR (8) was used to generate SuperM (SM)GagΔPR and PHGagΔPR. The RSV SMGag construct (6) was a gift from John Wills. The region of MA containing the SM mutations E25K and E70K was PCR amplified and cloned into pET3xc RSV GagΔPR using sites *XbaI* (in the backbone of the vector and added upstream of Gag by PCR) and *XhoI* (nt 630). RSV PHGagΔPR was constructed by PCR amplifying the PH domain from PH Gag-GFP and cloning the product into RSV GagΔPR using sites *XbaI* and *XhoI*. The plasmid expressing HIV-1 GagΔp6 (strain BH10) was a gift from Alan Rein. For simplicity, in the Results and Discussion sections of this paper, RSV GagΔPR and its derivatives as well as HIV-1 GagΔp6 are referred to as RSV Gag and HIV-1 Gag, respectively. Neither of these deleted domains affects the membrane targeting properties of Gag or the first steps in assembly.

Cells and transfection

Cell cultures and transfections were performed as previously described (14). DF1 (chicken) and QT6 (quail) fibroblast cells were maintained in Dulbecco modified Eagle medium supplemented with 5% fetal bovine serum, 5% NuSerum (BD Biosciences), 1% heat-inactivated chick serum, standard vitamins, L-glutamine, penicillin and streptomycin.

DF1 and QT6 cells were seeded onto glass cover slips for imaging or six-well plates for virus release assays 24 h prior to transfection. DF1 cells at 60% confluency

were transfected with 2 µg of total DNA at a 1:1 ratio of fluorescent Gag to the 5ptase expression plasmid or to the control plasmid pBluescript SK(+) (Stratagene). QT6 cells at 30% confluency were transfected with 3 µg of total DNA at a 1:2 ratio of fluorescent Gag to 5ptase or control plasmid. Transient transfections were performed using FuGENE HD (Roche) according to manufacturer's instructions.

Virus release and immunoblotting

Medium and cells were collected 24 h post-transfection. The medium was centrifuged at 5,000 x g for 5 min to remove cellular debris. Virus-like particles (VLPs) were isolated by layering the cleared medium onto 0.50 mL virus pelleting buffer (15% sucrose in 20 mM Tris HCl [pH 7.5], 100 mM NaCl, 1 mM EDTA) and centrifuging at 90,000 rpm for 45 min in a Beckman TLA 100.4 rotor. Western blots were performed on cellular and VLP-associated Gag using rabbit anti-RSV capsid (αCA) serum diluted 1:1,000 or rabbit anti-HIV-1 p24 (NIH AIDS Research and Reference Reagent Program, Reagent 4250) diluted 1:5,000 and then probed with anti-rabbit IgG-Alkaline phosphatase (Sigma) diluted 1:30,000. Following incubation in the ECF reagent (Sigma), blots were imaged on a Storm scanner (Molecular Dynamics). Bands were quantified using Image Quant software.

Liposome binding assay

Liposomes were prepared as previously described with some modifications (13). The lipid concentrations were chosen largely based on previously published studies, to facilitate comparisons. Chloroform solutions of purified natural L-α-phosphatidylcholine (egg PC), L-α-phosphatidylserine (brain PS), L-α-phosphatidylinositol-4,5-bisphosphate

(brain PI(4,5)P_2), L-α-phosphatidylinositol-4-phosphate (brain PI(4)P), and dry unsaturated 1,2-dioleoyl-sn-glycero-3-phospho-(1'-myo-inositol-3'-phosphate) (18:1 PI(3)P), 1,2-dioleoyl-*sn*-glycero-3-phospho-(1'-myo-inositol-3',5'-bisphosphate) (18:1 PI(3,5)P_2), 1,2-dioleoyl-*sn*-glycero-3-phospho-(1'-myo-inositol-3',4',5'-trisphosphate) (18:1 PI(3,4,5)P_3) were purchased from Avanti Polar Lipids. Dry lipids were resuspended in chloroform per the manufacturer's directions. Chloroform solutions of PC and PS (67%:33%, 50%:50%, or 33%:67%), or PC, PS, and PIPs (61.75%:31%:7.25%) were mixed at the stated ratios and then dried under a stream of nitrogen and resuspended (1 hr to overnight at 4°C with occasional mixing) in 20mM HEPES (pH 7.0) to a concentration of 10 mg/mL under nitrogen gas. The resuspended lipids were passed at least 60 times through a 100 nm polycarbonate filter in an Avanti extruder to yield uniform liposomes. Liposomes were stored at 4°C under nitrogen and used no later than 10 days after preparation.

In vitro translation and liposome binding reactions were performed as previously described with modifications (11). Briefly, in vitro translation of the Gag constructs was performed using the T7 coupled TNT reticulocyte lysate system (Promega). Fifty µL reticulocyte reactions were prepared according to the manufacturer's instructions with [^{35}S]methionine-cysteine (Perkin Elmer: ExPRE35S35 protein labeling mix) for protein labeling and incubated for 90 min at 30°C. Then 100 µg of liposomes was added to the reaction, for a final liposome concentration of 1.7 mg/mL, and incubated for an additional 30 min at 30°C.

In preparation for flotation, the reticulocyte reaction with liposomes was diluted to a final volume of 0.25 mL with 20 mM HEPES (pH 7.0), mixed with 0.75 mL 67% sucrose, and then transferred to an ultracentrifuge tube. The mixture was overlaid with 1.6 mL 40% sucrose followed by 0.40 mL 4% sucrose. All sucrose solutions were prepared by dissolving sucrose (wt/wt) in 20 mM HEPES pH 7.0. The sucrose gradients were centrifuged at 90,000 rpm at 4°C for 180 min in a Beckman TLA 100.4 rotor. Four 0.75 mL fractions were collected. The top one or two fractions represented liposome-bound Gag, and the bottom two fractions represented non-liposome-bound Gag. Unless otherwise noted, 30 µL of each fraction was resolved by SDS PAGE. The gels were incubated for 30 min in 1M sodium salicylate, dried, and placed on film at -80°C for 16-36 hr. The resulting autoradiograms were scanned and quantified using Image Quant software.

Many attempts were made to resolve the persistent high molecular weight band observed on the fluorograms of RSV Gag (and derivatives of Gag) flotations with liposomes containing PIPs. These included increasing the concentration of SDS in loading buffer, adding urea to 8M, incubating with NaOH, and varying the time, pH, and temperature of samples incubated prior to gel loading. None of these treatments had a significant effect.

Immunofluoresence and confocal microscopy

Monoclonal anti-myc antibody (Covance) was diluted 1:1,000 in phosphate-buffered saline (pH 7.4) (PBS). Tetramethyl rhodamine isothiocyanate-conjugated anti-mouse antibody was diluted 1:500 in PBS with 1% non-fat milk carrier. DF1 and QT6

cells were collected 12-16h or 20-24h post-transfection, respectively, and fixed with 3.7% formaldehyde in PBS for 15 min, permeabilized with 0.1% Tween 20 in PBS for 15 min, and then blocked with 4% bovine serum albumin for 30 min. Cells were stained with primary and secondary antibodies for 30 min each at 37°C, and then mounted on glass slides with Fluoro-Gel (Electron Microscopy Sciences) for viewing on an Ultraview spinning disc confocal microscope (Perkin-Elmer) with a Nikon 100x Plan-Apochromat oil objective lens (NA 1.4). Image analysis and confocal stacks were generated with ImageJ software (v1.44d).

RESULTS

Effect of 5ptase over-expression on PI(4,5)P_2 levels at the PM

The enzyme 5ptase removes the phosphate at position 5 of the inositol ring on PIPs, converting PI(4, 5)P_2 and PI(3,4,5)P_3 to PI(4)P and PI(3,4)P_2, respectively (32). Previous studies using human 5ptase or the yeast homolog (Inp54p) reported that over-expression of this enzyme led to a significant decrease in PI(4,5)P_2 levels at the PM (42, 65). We first sought to determine if human 5ptase had a similar effect on PI(4,5)P_2 levels in avian cells. DF1 chicken fibroblasts and QT6 quail fibroblasts were co-transfected with DNAs encoding 5ptase and the PH domain of human phospholipase C δ1 (PLCδ1) fused to GFP. This well-studied PH domain binds to PI(4,5)P_2 with high specificity and is commonly used as a reporter for the presence of PI(4,5)P_2 in cells (16, 19, 63). Both cell types were initially imaged at 24h post-transfection, but DF1 cells proved to be highly sensitive to 5ptase-induced apoptosis, displaying extensive

vacuolation and blebbing at the PM (data not shown). Therefore, DF1 cells were imaged at 12-16h post-transfection when the cells were still healthy. QT6 cells were more resistant to the toxic effects of $PI(4,5)P_2$ depletion, appearing normal after 24h, and consequently were imaged at 20-24h post-transfection.

In the absence of 5ptase, PH-GFP localized primarily to the PM in both DF1 and QT6 cells (Fig. 2.2 top panels), especially to membrane ruffles and cellular protrusions expected to be enriched in $PI(4,5)P_2$. Co-transfection of the myc-tagged 5ptase abolished PM localization of PH-GFP in both cell types (Fig. 2.2 bottom panels), resulting in a diffuse signal throughout the cytoplasm. Over-expression of 5ptase also led to a nuclear accumulation of PH-GFP. PLCδ1 has been shown to shuttle between the cytoplasm and the nucleus (66), suggesting that $PI(4,5)P_2$-dependent association with membranes competes with transport into the nucleus. Our observations indicate that human 5ptase significantly depletes $PI(4,5)P_2$ at the PM in these avian cell types.

PM localization of RSV Gag after $PI(4,5)P_2$ depletion

We next wanted to determine if depletion of $PI(4,5)P_2$ affects recruitment of RSV Gag to the PM. DF1 and QT6 cells were co-transfected with DNAs expressing RSV Gag-GFP and myc-tagged 5ptase, or RSV Gag-GFP and a control plasmid (Fig. 2.3A). A second set of transfections was performed in parallel using HIV-1 Gag-GFP as a positive control (Fig. 2.3B). By themselves, HIV-1 Gag-GFP and RSV Gag-GFP were concentrated in bright puncta at the PM, commonly interpreted to be assembling or budding virions, in both DF1 and QT6 cells (Fig. 2.3A and 2.3B, top panels). Consistent

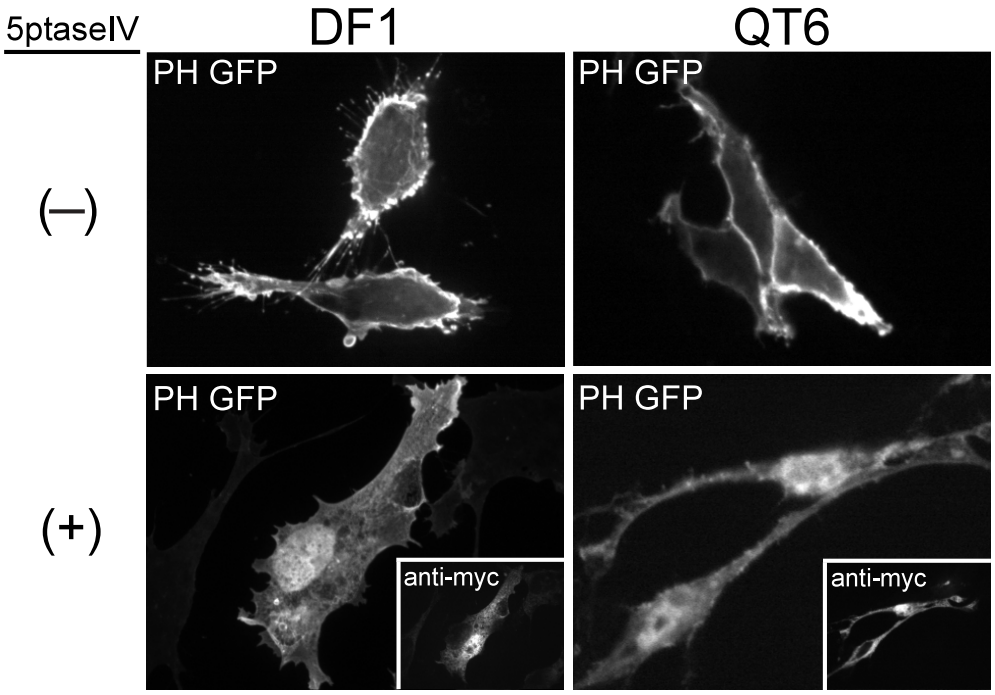

Fig. 2.2 Effect of 5ptase on PM localization of PH-GFP in avian cells. DF1 (left panels) or QT6 (right panels) cells were co-transfected with DNAs encoding PH-GFP plus a control plasmid (indicated by a minus sign, top panels), or myc-tagged 5ptase (indicated by a plus sign, bottom panels). Expression of 5ptase was detected by a monoclonal mouse anti-myc antibody (insets showing the same cells). Images are single, 0.1um confocal sections through the midbody of the cell and are representative for each condition. (n >30 cells).

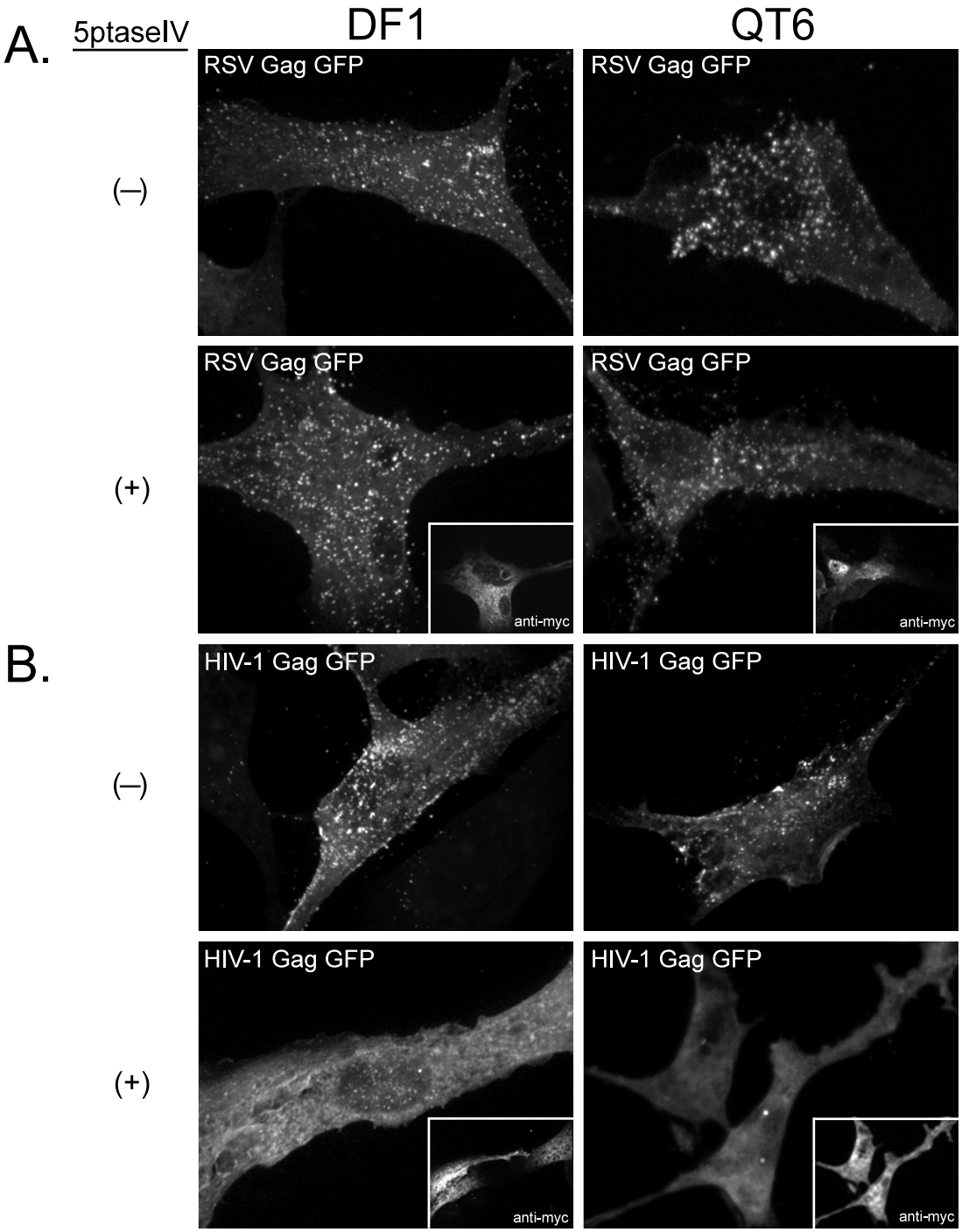
A.
5ptaseIV
DF1
QT6
RSV Gag GFP
RSV Gag GFP
(–)
RSV Gag GFP
RSV Gag GFP
(+)
anti-myc
anti-myc
B.
HIV-1 Gag GFP
HIV-1 Gag GFP
(–)
HIV-1 Gag GFP
HIV-1 Gag GFP
(+)
anti-myc
anti-myc

Fig. 2.3 Effect of 5ptase on PM localization of RSV Gag-GFP and HIV-1 Gag-GFP. DF1 (left panels) or QT6 (right panels) cells were co-transfected with DNAs encoding either RSV Gag-GFP (A) or HIV-1 Gag-GFP (B) and a control plasmid (indicated by a minus sign) or a plasmid encoding myc-tagged 5ptase (indicated by a plus sign, myc signal shown in insets). Images are projections of 10-15 confocal sections from each cell compiled by average fluorescence intensity and indicate total cellular fluorescence. Images are representative for each condition ($n > 30$).

with previous reports on mammalian cells (11, 29), expression of 5ptase prevented HIV-1 Gag-GFP from forming puncta at the PM; instead, the fluorescence signal was diffuse and primarily cytoplasmic (Fig. 2.3B, bottom panels). Occasionally the HIV-1 protein was seen in cytoplasmic accumulations, which may correspond to intracellular vesicles such as late endosomes (42). In contrast, in both types of avian cells, expression of 5ptase had no detectable effect on the punctate fluorescence signal of RSV Gag-GFP at the PM (Fig. 2.3A, bottom panels). We interpret these results to mean that, unlike HIV-1 Gag, RSV Gag does not depend on $PI(4,5)P_2$ for PM binding.

To address if the RSV MBD is responsible for the lack of 5ptase effect on PM localization of RSV Gag, we replaced the viral MBD with the PH domain from PLC δ1, a cellular $PI(4,5)P_2$-specific binding protein. The localization of this chimeric protein was examined in DF1 cells and QT6 cells as described above. In both cell types, in the absence of 5ptase, PHGag-GFP was observed primarily at the cell surface and in small vesicular structures near the cell periphery (Fig. 2.4A). Cellular and heterologous MBDs have been shown previously to support budding in the HIV-1 system (30, 56). In DF1 cells upon co-expression of RSV PHGag-GFP with 5ptase, the fluorescence signal at the PM was significantly reduced. Instead, fluorescence accumulated in large, cytoplasmic compartments (Fig. 2.4B, white arrows), similar to the late endosomal localization of HIV-1 Gag in $PI(4,5)P_2$-depleted cells (42). However, in some cells a residual fluorescence signal could be detected at the PM (Fig. 2.4A, asterisks), suggesting that depletion of this lipid was not uniform across the cell population.

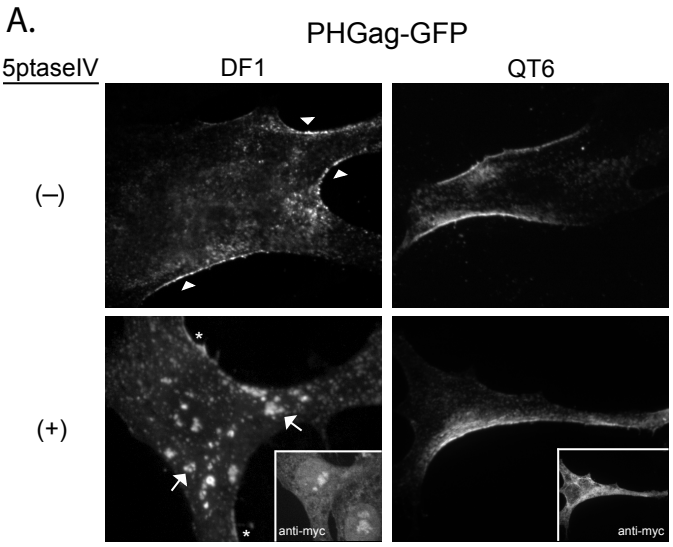
A.
PHGag-GFP
5ptaseIV
DF1
QT6
(–)
(+)
anti-myc
anti-myc

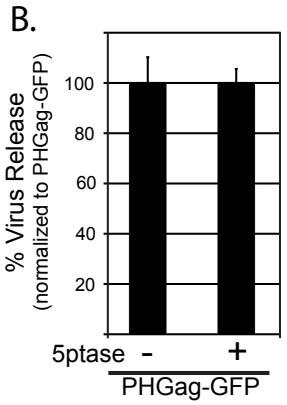
B.
% Virus Release
(normalized to PHGag-GFP)
100
80
60
40
20
5ptase -
+
PHGag-GFP

Fig 2.4 Effect of PI(4,5)P_2 depletion on RSV PHGag-GFP localization and VLP release. DF1 or QT6 cells were co-transfected with PHGag-GFP DNA and control plasmid (top panels), or PHGag-GFP DNA and 5ptase DNA (bottom panels). The cells were processed for imaging as described for Fig. 3, and for VLP release as described for Fig. 4. The 5ptase protein was detected by monoclonal mouse anti-myc Abs (insets). (A) Fuorescence imaging. In DF1 cells (left panels) expressing PHGag-GFP alone, the Gag chimera displays a strong PM localization (white arrow heads). In cells over-expressing 5ptase, PHGag-GFP is found predominantly at intracellular compartments (white arrows), although some cells display a low fluorescence signal at the PM (asterisks). In QT6 cells (right panels), PHGag-GFP appears to be unaffected by 5ptase expression. (B) VLP release from QT6 cells. These cells show little or no reduction in VLP budding.

Unexpectedly, in QT6 cells, 5ptase caused little loss of PM fluorescence when co-expressed with RSV PHGag-GFP (Fig. 2.4A).

Why might phosphatase expression lead to nearly complete removal of PH-GFP and HIV-1 Gag-GFP from the PM but only modestly affect RSV PHGag-GFP at the PM? The difference between PH-GFP and PHGag-GFP might be accounted for by Gag multimerization in the latter, which would increase membrane affinity. And the difference between RSV PHGag-GFP and HIV-1 Gag-GFP might be accounted for by the higher affinity of this PH domain for $PI(4,5)P_2$ [$K_d \sim 1.7\mu M$; (34, 62)] than the affinity of the HIV-1 MA domain for this phosphoinositide [$K_d \sim 150\mu M$, (54)], although direct comparison of these values is not possible because of the different assays used and different fatty acid lengths of the lipid molecules. According to this model, after 5ptase expression, the residual low $PI(4,5)P_2$ levels at the PM would be sufficient to bind the PH domain in PHGag, given the avidity effects due to multimerization, but not sufficient to bind the PH domains of PH-GFP, which does not multimerize, or the MA domain of HIV-1 Gag, which has a lower affinity for $PI(4,5)P_2$. Given the differences observed in the two cell types, it is likely that increasing the ratio of 5ptase to Gag in transfections or specifically targeting 5ptase to the PM would be sufficient to prevent PHGag-GFP from binding the PM in QT6 cells.

Effect of $PI(4,5)P_2$ depletion on virus release

As a second approach to address the role of $PI(4,5)P_2$ in RSV Gag PM binding, we measured the effect of 5ptase expression on the production of Gag-GFP VLPs. HIV-1 budding was previously shown to decrease by three- to five-fold upon $PI(4,5)P_2$

depletion in mammalian cells (20, 42). QT6 cells were used for these experiments because DF1 cells did not tolerate the toxic effects of 5ptase long enough for interpretable data to be obtained. VLPs were collected by centrifugation of the medium 24h post-transfection and quantified by western blotting. While HIV-1 VLP release was decreased approximately three-fold as a result of 5ptase expression, production of RSV VLPs was not affected (Fig. 2.5), which is consistent with the fluorescence imaging results. We also measured VLP release for the chimeric RSV PHGag-GFP protein in QT6 cells. Phosphatase expression had no effect (Fig. 2.4B), consistent with the imaging results for this cell type. Overall, we interpret the RSV VLP release data to support the observations from fluorescence imaging and conclude that $PI(4,5)P_2$ is not essential for PM targeting of RSV Gag.

Role of PIPs in binding of RSV Gag to liposomes

In our previously published protein flotation studies, we found that recombinant, purified RSV MA and myristoylated HIV-1 MA bound to liposomes containing physiologically relevant levels of the acidic lipid PS (13, 14). In preliminary experiments, addition of 1% $PI(4,5)P_2$ to standard PC/PS (2:1) liposomes did not lead to a significant increase in the amount of purified protein that floated. Based on these results and on computational modeling, we concluded that electrostatic interactions are the major factor in the binding of RSV and HIV-1 MA to membranes, rather than specific binding to $PI(4,5)P_2$. More recent work from other laboratories has focused on liposome interaction of the whole HIV-1 Gag protein, synthesized in vitro in a reticulocyte system (11, 12, 29). These studies showed that high levels (>5%) of PIPs, including but not

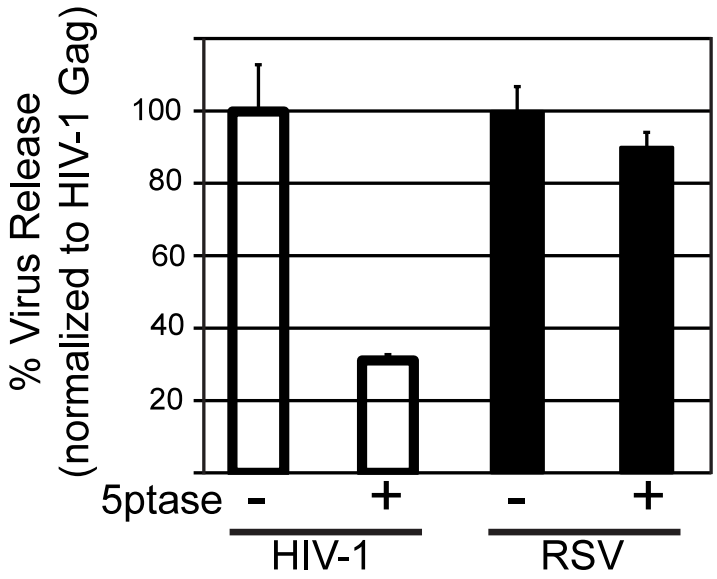

Fig. 2.5 Effect of 5ptase on virus release from QT6 cells. QT6 cells were co-transfected with DNAs encoding either HIV-1 Gag-GFP or RSV Gag-GFP, plus a control plasmid (indicated by a minus sign) or a plasmid encoding myc-tagged 5ptase (indicated by a plus sign). Twenty-four hours post transfection virus-like particles (VLPs) were collected by centrifugation from the medium and the cells were lysed. The amounts of Gag-GFP in the lysate and in the VLP fractions were measured by western blot analysis. Virus release was calculated as the amount of extracellular Gag as a fraction of total Gag. Error bars represent standard deviations from the mean from three independent experiments.

limited to $PI(4,5)P_2$ and $PI(3,4,5)P_3$, strongly augment the interaction of HIV-1 Gag with PC/PS (2:1) liposomes.

To further investigate how PIPs influence RSV Gag interaction with membranes, we performed liposome flotation reactions using a truncated version of RSV Gag that is missing the C-terminal protease domain (GagΔPR, hereafter referred to as RSV Gag). This ^{35}S-labeled protein was synthesized using a commercial reticulocyte lysate, and the crude mixture was incubated with extruded, 100 nm PC/PS (2:1) liposomes with or without added PIPs. After centrifugation in a sucrose step gradient, the percent of liposome-associated protein was quantified by SDS PAGE and fluorography. As a control, flotation reactions were carried out in parallel with HIV-1 Gag (11, 12, 29).

The presence of a high molecular weight band in the membrane fraction of RSV Gag was observed when the proteins were resolved by SDS-PAGE, which complicated the analysis of the flotation data. This band, at an apparent molecular weight greater than 250 kDa, was observed predominantly in the presence of PIPs. We infer that it corresponds to an aggregate or an assembled oligomer of RSV Gag, since the majority of total protein-associated radioactivity was in Gag, as evident when the reticulocyte reaction was analyzed in the absence of added liposomes (data not shown). All attempts to break apart this aggregate failed (see Materials and Methods). Therefore, we included the high molecular species in the quantification (Fig. 2.6B, black bars).

Compared with previous studies using purified RSV MA, RSV Gag synthesized in the reticulocyte lysate interacted weakly with PC/PS (2:1) liposomes, being barely detectable in the floated fraction (Fig. 2.6A and 2.6B). At a concentration of 7.25% of

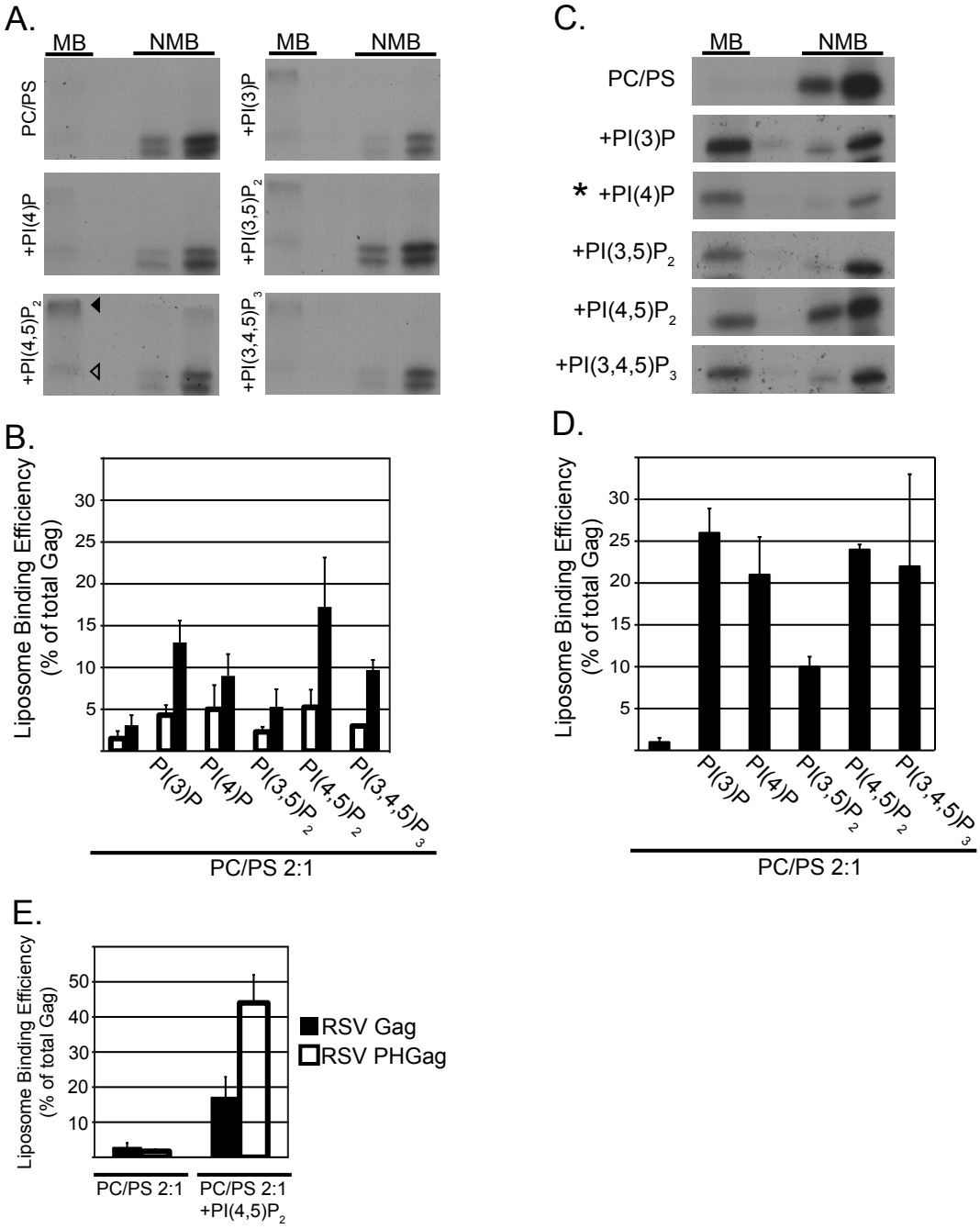
A.
MB
NMB
MB
NMB
PC/PS
+PI(3)P
+PI(4)P
+PI(3,5)P2
+PI(4,5)P2
+PI(3,4,5)P3
C.
MB
NMB
PC/PS
+PI(3)P
* +PI(4)P
+PI(3,5)P2
+PI(4,5)P2
+PI(3,4,5)P3
B.
Liposome Binding Efficiency (% of total Gag)
30
25
20
15
10
5
PI(3)P
PI(4)P
PI(3,5)P2
PI(4,5)P2
PI(3,4,5)P3
PC/PS 2:1
D.
Liposome Binding Efficiency (% of total Gag)
30
25
20
15
10
5
PI(3)P
PI(4)P
PI(3,5)P2
PI(4,5)P2
PI(3,4,5)P3
PC/PS 2:1
E.
Liposome Binding Efficiency (% of total Gag)
50
40
30
20
10
RSV Gag
RSV PHGag
PC/PS 2:1
PC/PS 2:1 +PI(4,5)P2

Fig. 2.6 Flotation analysis of RSV Gag and HIV-1 Gag binding to PC/PS and PC/PS/PIP liposomes. All liposomes were PC/PS (2:1) without or with (+) the addition of 7.25% PIPs. (A, C) Representative flotation results for RSV Gag and HIV-1 Gag, respectively. MB, membrane bound (floated liposomes); NMB, not membrane bound. The RSV autoradiograms show the Gag band (white triangle) and a higher molecular weight band (black triangle) that was consistently observed in the presence of liposomes containing PIPs. In C the (*) indicates that ¼ of the total was used for the NMB samples. (B, D) Quantification of three or more flotation reactions for each liposome composition. The RSV quantification includes values for the Gag band only (white bars) or the Gag band plus higher molecular bands (black bars). (E) Quantification of RSV PHGag and RSV Gag (data taken from Fig. 5D). Error bars represent standard deviations from the mean.

total lipids, diverse PIPs increased the fraction of protein that floated but with little evidence of specificity; mono-, di-, and tri-phosphorylated PIPs all augmented membrane binding (Fig. 2.6A and 2.6B). Although PI(4,5)P_2 appeared most effective, PI(3)P, PI(4)P, and PI(3,4,5)P_3 also increased the amount of Gag protein in the membrane fraction by at least three-fold. From these results, we conclude that the enhanced liposome interaction promoted by high concentrations of PIPs is due to electrostatics, not to specific recognition of the inositol head group by the RSV Gag protein.

To address if RSV Gag could be converted into a specific PI(4,5)P_2 binding protein, we created the chimeric protein described above, in which the MA domain is replaced by a PH domain. RSV PHGag was found to associate with PI(4,5)P_2-containing liposomes much more strongly than RSV Gag itself, while binding to PC/PS liposomes was unchanged (Fig. 2.6E). This result suggests that protein folding or other features of RSV Gag do not mask potential PIP interaction sites.

Several flotation studies reported that while HIV-1 Gag binds very poorly to PC/PS (2:1) liposomes, this interaction is strongly enhanced by inclusion of at least 5% PIPs in the artificial membranes (11, 12, 54). While PI(4,5)P_2 and PI(3,4,5)P_3 were most effective, other PIP species also augmented binding (11). We tested the ability of a collection of PIPs, all at 7.25% of total lipids in PC/PS (2:1) liposomes, to promote HIV-1 Gag flotation (Ficure 2.6C and D). The results confirm the weak interaction of Gag with PC/PS (2:1) and the strong enhancing effect of relatively high concentrations of PI(4,5)P_2 and PI(3,4.5)P_3. However, the monophosphorylated species PI(3)P and

PI(4)P, which have not been tested previously, were as potent in enhancing membrane binding as PI(4,5)P_2. Thus our flotation data for HIV-1 do not support the prevailing model that HIV-1 Gag-membrane interaction has a specific requirement for PI(4,5)P_2, as has been inferred from the properties of the phosphoinositide binding pocket in the MA domain reported in NMR studies of MA with short chain PIPs (54). Rather, the data are more consistent with a model in which the high negative charge of the PIP head group acts electrostatically to attract Gag to the PM or acts directly or indirectly to induce myristate exposure, which then enhances membrane binding through hydrophobic interactions.

In our hands, the fraction of HIV-1 Gag associated with PIP-containing liposomes was always at least two-fold greater than for RSV Gag. Previously, we reported that RSV MA and myristoylated HIV-1 MA have similar dissociation constants governing the binding to PC/PS (2:1) liposomes, and that forced dimerization of these MA proteins strengthens liposome association (13, 14), as expected on theoretical grounds. HIV-1 CA and Gag dimerize with a K_d of about 10^{-5} M (15, 24, 31, 50), an interaction that is mediated by the C-terminal domain of CA. Under similar conditions, purified RSV CA does not dimerize (31). We speculate that the stronger liposome interaction of HIV-1 Gag compared with RSV Gag is due at least in part to dimerization of the former.

Electrostatic nature of RSV Gag binding to liposomes

Purified RSV MA and HIV-1 MA interact more strongly with liposomes as the mole fraction of PS is increased (13, 14). To examine if the corresponding Gag proteins in reticulocyte lysates respond in a similar manner, we performed flotation reactions at

different PS concentrations. As the fraction of PS increased from 33% to 67%, the amount of RSV Gag that floated increased by three-fold (Fig. 2.7A, black bars). We also examined a mutant RSV Gag protein called SuperM (SMGag) (6). In this mutant, two acidic residues in the RSV MBD are replaced by two basic residues, leading to a net increase of +4 in the overall charge of the MBD. In vivo, SMGag buds more rapidly than wild type Gag, and unlike wild type Gag, does not traffic through the nucleus before localizing to the PM (5). These early in vivo studies led to the initial conclusion that RSV Gag-membrane interaction is primarily electrostatic in nature. In the present flotation experiments, SMGag and wild type Gag bound PC/PS (2:1) liposomes similarly. However, the mutant protein responded even more strongly to increased PS concentrations than the wild type protein, with more than a six-fold increase (Fig. 2.7A, open bars). SMGag also responded more strongly to the presence of $PI(4,5)P_2$ than did wild type Gag.

HIV-1 Gag liposome binding also rose dramatically at higher PS concentrations, with more than a twenty-fold increase from 33% to 67% PS (Fig. 2.7B). These very high PS concentrations promoted even stronger HIV-1 Gag-liposome interaction than 7.25% $PI(4,5)P_2$. We initially considered this result to be surprising, but it was invariably observed with different liposome batches and translation reactions. These results stand in contrast to results of previously reported experiments from the Ono laboratory, in which high PS concentrations could not supplant $PI(4,5)P_2$ (11, 29).

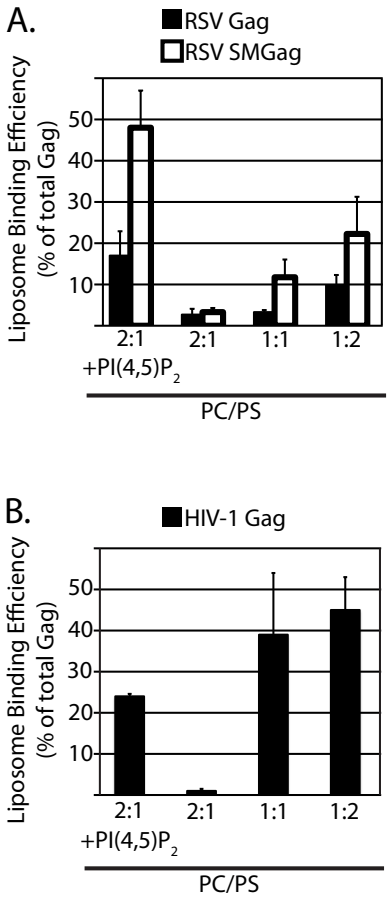

Fig. 2.7 Effect of PS concentration on binding of RSV and HIV Gag to PC/PS liposomes. The left-most bar or bars show liposome association in the presence of $PI(4,5)P_2$ as a reference point, with the data taken from Fig. 5. The other bars show liposome association at different PC:PS ratios without added PIPs. (A) RSV Gag (black bars) and RSV SMGag (white bars); (B) HIV-1 Gag.

Taken altogether, we interpret the data from the liposome flotation assays to support the model that for RSV Gag and HIV-1 Gag, membrane binding in vitro is driven primarily by charge interactions rather than by recognition of a specific phospholipid.

DISCUSSION

We have used in vivo and biochemical assays to show that RSV Gag does not have a specific requirement for $PI(4,5)P_2$ in order to associate with membranes. Cellular depletion of $PI(4,5)P_2$ by over-expression of a 5-phosphatase did not reduce RSV Gag-GFP localization to the PM nor did it compromise release of VLPs. In contrast, in parallel experiments, HIV-1 Gag-GFP localization to the PM was nearly ablated and VLP production was inhibited by $PI(4,5)P_2$ depletion, as reported previously by others (42). After synthesis in a reticulocyte lysate, RSV Gag protein bound weakly to standard PC/PS (2:1) liposomes. While this binding was augmented by inclusion of 7.25% $PI(4,5)P_2$, other PIP species were equally effective in promoting binding. High levels of PS, in the absence of added PIPs, enhanced binding similarly. All of these results are consistent with our liposome flotation analysis of the purified RSV MA domain and confirm our conclusion that Gag-membrane binding is driven primarily by electrostatic interactions in RSV. Therefore, we infer that even after in vivo depletion of $PI(4,5)P_2$ by 5ptase, the PM apparently retains enough negatively charged lipids to allow RSV Gag-PM targeting and binding.

While HIV-1 was intended primarily as a positive control, our results differ in some respects from those published previously. On the one hand, $PI(4,5)P_2$ depletion

abrogated HIV-1 Gag-GFP PM localization, as first found in the pioneering study by Ono et al (42) and later confirmed when HIV-1 was used as a control for studies on EIAV (20), MPMV (60), and HTLV (29), as well as in our own in vivo experiments. On the other hand, our biochemical results from liposome flotation assays diverged from those reported earlier (11, 29). We found no evidence of significant specificity of HIV-1 Gag for $PI(4,5)P_2$. Other PIP species as well as high levels of PS promoted similar binding to liposomes. It is important to note that lack of PIP specificity in vitro does not necessarily contradict the observation that phosphatase-mediated depletion of $PI(4,5)P_2$ leads to loss of Gag-GFP at the PM. Without a detailed understanding of the long-term effects of 5ptase on the pools of each phosphoinositide in different membrane compartments, it is not possible to directly connect biochemical data on flotation with fluorescence imaging of Gag-GFP in cells. In addition, other factors may functionally distinguish liposome binding of reticulocyte-translated proteins in vitro from PM binding in vivo, for example membrane curvature, presence of other phospholipids and cholesterol, or presence of rabbit reticulocyte proteins capable of binding to negatively charged lipids or to Gag.

What is the origin of the discrepancies between the flotation results for HIV-1 Gag reported here and the results published previously from the Ono lab (11, 29)? Our observation that PIP species other than $PI(4,5)P_2$ also strongly promote liposome binding is perhaps less significant, since for those PIP species tested by both labs [$PI(4,5)P_2$, $PI(3,5)P_2$, and $PI(3,4,5)P_3$], the raw data are not very different (11). However, our finding that high PS promotes HIV-1 Gag binding at least as strongly as 7%

$PI(4,5)P_2$ is in strikingly contrast to published results, which showed only marginal Gag binding to liposomes with 60% PS (11, 12, 29). We tested and eliminated several possible explanations for this discrepancy, including different HIV-1 strain background (BH10 versus NL4-3), different origins of lipids (brain-derived versus synthetic), and different Gag structures (lacking or including the p6 domain). Instead, the explanation appears to lie in the methods of liposome preparation and possibly the method of flotation. The previously reported experiments were carried out with liposomes that had been made by sonication in plastic tubes emersed in a water bath, conditions that are unlikely to effectively break up large multilamellar vesicles (G. Feigenson, personal communication). Our liposomes were made by repeated extrusion through a 100nm filter, which is expected to produce small unilamellar vesicles and consequently a much larger available surface area. We traded liposome preparations with the Ono lab, and in preliminary experiments confirmed the published results that for these sonicated liposomes, HIV-1 Gag floated much more extensively at 2:1 PC:PS + 7% $PI(4,5)P_2$ than at 1:1 PC: PS. In parallel, for our extruded liposomes, HIV-1 Gag bound more extensively at 1:1 PC:PS than at 2:1 PC:PS + 7% $PI(4,5)P_2$. The Ono lab observed a similar trend, although with quantitatively less flotation for the extruded than for the sonicated liposomes. We speculate that the differences in accessible membrane surface area, and perhaps also differences in liposome size and buoyant density, as well as differences in centrifugation conditions, lead to the very different measurements of ability of HIV-1 Gag in the crude reticulocyte lysate to attach to artificial membranes. For example, basic reticulocyte proteins, which might be in vast excess over the

translated radioactive HIV-1 Gag, might cover the smaller membrane surface of multilamellar liposomes and thereby prevent the weak binding of Gag to PS.

The role of $PI(4,5)P_2$ in retroviral Gag-membrane interaction has been addressed for several retroviruses but with divergent results for different experimental settings and different viruses. In HIV-1, early work on in vitro assembly of purified Gag protein, in the absence of membranes, first suggested the importance of phosphoinositides. Assembly of properly sized VLPs required inositol hexakisphosphate or pentakisphosphate (7), which were interpreted to mimic a phosphoinositide in cells, possibly $PI(3,4,5)P_3$. Some of the side chains interacting with these highly charged molecules have been mapped (57). In the original study by Ono et al (42), phosphatase-mediated depletion of $PI(4,5)P_2$ was found to redirect Gag-GFP away from the PM. A binding pocket for short chain $PI(4,5)P_2$ (54), which was later also identified for HIV-2 (51), suggested that this lipid species is responsible for HIV-1 Gag PM localization. More recently, $PI(4,5)P_2$ was found to be significantly enriched in HIV-1 virions (9).

As measured by NMR, EIAV MA also was found to bind short chain PIPs, but in this case several PIP species had higher affinities than $PI(4,5)P_2$ (20). Early experiments were interpreted to mean that EIAV MA can bind to neutral liposomes but that membrane association is strongly enhanced by acidic lipids (48). However, in a more recent report, PM fluorescence of EIAV Gag-GFP was not affected by expression of 5ptase, although a possibly more potent PIP phosphatase induced major changes in subcellular localization (20).

In the MLV system, expression of 5ptase reduced MLV VLP release (25), as in the case of HIV-1. Also, $PI(4,5)P_2$ was found to be enriched in virions (9). In vitro, PIPs in PC liposomes were found to be required for binding of MA (25), but the MA was unmyristoylated and thus the biological significance is uncertain. This stimulatory effect was quantitatively similar for diverse PIPs, and little or no binding was observed to liposomes containing only PS. However, in the presence of 20% PS, $PI(4,5)P_2$ specifically stimulated MA binding with a four-fold lower apparent K_d than other PIPs, suggesting a synergism between these two negatively charged lipids.

Finally, HTLV-1 Gag and chimeric Gag proteins bearing the HTLV-1 MA domain did not show a specific requirement for $PI(4,5)P_2$, either for PM localization in cells or for liposome binding from reticulocyte lysates. However, acidic phospholipids, including PIPs, stimulated liposome binding, similar to what we have observed for RSV Gag. Altogether, these diverse results for different retrovirus Gag proteins suggest that if a head group-specific $PI(4,5)P_2$ interaction is biologically important, it may be limited to HIV-1 Gag and its close relatives.

In overview, at least five principles underlie PM targeting of retroviral Gag proteins. First, vesicular trafficking appears to play a central role, as demonstrated by the interaction of the HIV-1 MA domain with clathrin adapter protein AP3 and the effects of knocking out this binding (17). But understanding of the trafficking pathway by which any Gag protein reaches the PM remains rudimentary and controversial, despite attempts to follow this kinetically (46).

Second, as described above, a PI(4,5)P_2 head group–specific binding pocket has been identified at the atomic level by NMR for HIV-1 and HIV-2 (51, 54). According to the myristoyl switch model proposed by these studies (23, 52-54), one of the fatty acid chains of PI(4,5)P_2 is extracted from the lipid bilayer and is bound to a hydrophobic groove in MA, just as the N-terminal myristate is extracted from its pocket in MA and becomes inserted into the membrane. In this model, it remains uncertain how the formidable energy barrier would be overcome to promote the movement of a fatty acid chain from the lipid bilayer into a hydrophobic groove in a protein. The biochemical experiments on which the model is based, as well as the NMR experiments measuring the affinities of EIAV MA protein for purified phosphoinositides (20), were necessarily carried out with short chain PIPs to maintain their solubility. A recent study using surface plasmon resonance to measure PIP binding to HIV-1 Gag concluded that the lengths of the PIP acyl chains are the major contributing factor in determining the PIP binding affinity of HIV-1 Gag, not the phosphorylation state of the inositol head group (3). Thus, the biological relevance of studies with short chain PIPs remains to be established. Finally, interpreting the effects of 5ptase-mediated depletion of PI(4,5)P_2 on Gag PM localization may be more difficult than commonly assumed. To date, all retrovirus studies on 5ptase-depletion, including ours, have been long-term, with the endpoints representing a cumulative effect of the phosphatase over many hours. Secondary effects of perturbing PIP pools are almost certain to occur and thus limit the interpretations of fluorescence imaging. All eukaryotic cells maintain tight control of the

concentrations and localization of PIPs, which probably explains why over-expression of 5ptase can trigger apoptosis in some cell types at least in some cell types.

Third, hydrophobic interactions are critical in mediating membrane interactions for those Gag proteins modified by an N-terminal myristate, like HIV-1 Gag and MLV Gag. It is widely accepted that insertion of a single fatty acid into a lipid bilayer is insufficient to lock a protein into the membrane. In the absence of other membrane binding features, a subpopulation of proteins will be cytosolic as the fatty acid moiety samples the aqueous space. In the case of retroviral Gag proteins, several factors, including multimerization of Gag (61), binding of the MA domain to PIPs (1, 51, 54), or membrane proximity, can tip this balance toward membrane attachment. By bringing the myristate into close proximity to the PM, electrostatic interactions between the MBD and acidic phospholipids favor insertion of the myristate into the lipid bilayer where it is more stable. The quantitative contributions of these factors in promoting myristate insertion are unknown. Because of the complexity in understanding the behavior of myristate and protein binding grooves for it, the nature of retroviral Gag-membrane interaction may be easiest to work out for viruses like RSV, which rely primarily on electrostatic interactions with membranes.

Fourth, multimerization of any membrane-binding protein increases its avidity for the membrane, and this property is intrinsic to Gag. Multimerization is expected to be concentration-dependent, and hence expression levels also should affect membrane binding, as found experimentally for HIV-1 MA (45). To date, the effects of multimerization on membrane binding have been modeled experimentally and

computationally only by dimerization, using RSV MA and HIV MA proteins that were induced to dimerize artificially. The behavior of higher order multimers, which might be formed in the cytoplasm or assembled on the membrane, has not been studied. Once a Gag lattice has grown beyond a minimal size, the lattice probably would remain firmly attached to the PM even after depletion of $PI(4,5)P_2$. The role of kinetics in PM binding, which is likely to be critical, has not been addressed in any study. Future work on the effects of multimerization and of $PI(4,5)P_2$ depletion in Gag PM binding may require truncated or mutated Gag proteins that do not multimerize (18).

Fifth, electrostatic interactions appear to be universal in Gag membrane targeting, perhaps providing the major force directing Gag to the PM. All MA proteins have basic patches on the membrane-proximal surface (40), and the inner leaflet of the PM is unique in its high concentration of acidic lipids. This negative charge results mainly from PS and $PI(4,5)P_2$, but the relative contributions of each of these lipids are not well understood and may depend on cell type (27, 67). In addition, clustering of lipids in membranes may result in formation of microdomains with different charges. Fluorescent protein sensors have been developed to probe for the overall negative potential of the inner leaflet. These probes are based on a positively charged segment of polypeptide plus a lipid anchor that by itself is insufficient for steady state PM localization (67). Such probes, together with PH-GFP and fluorescently marked Gag proteins, could help elucidate if the electrostatic interactions between MA domains and the PM are powered primarily by $PI(4,5)P_2$, by PS, or by a combination of the two. Different retroviruses probably lie on a gamut, with some relying more on $PI(4,5)P_2$ and

others relying more on PS. Gag proteins that rely more on $PI(4,5)P_2$ may do so in part because of a specific binding pocket for the head group or because of a local clustering of basic residues that is preferentially attracted to the multiple negative charges of this lipid. The latter effect could explain the frequently reported strong effects of PIPs in flotation analyses but without specificity for $PI(4,5)P_2$. In summary, we propose as a unified, working model that not only RSV Gag, but all retroviral Gag proteins rely primarily on electrostatic interactions to drive at least the first steps in PM binding.

ACKNOWLEDGMENTS

This work was supported by USPHS grant CA20081 to VMV. We thank David Holowka, Akira Ono, and Alan Rein for DNA clones, and Gerald Feigenson for advice on handling lipids. We are particularly appreciative of Akira Ono's willingness to trade liposomes to help resolve the discrepancies in HIV-1 Gag flotation results obtained by our two laboratories.

CHAPTER 2 REFERENCES

1. **Alfadhli, A., A. Still, and E. Barklis.** 2009. Analysis of human immunodeficiency virus type 1 matrix binding to membranes and nucleic acids. J Virol **83:**12196-203.

2. **Aloia, R. C., H. Tian, and F. C. Jensen.** 1993. Lipid composition and fluidity of the human immunodeficiency virus envelope and host cell plasma membranes. Proc Natl Acad Sci U S A **90:**5181-5.

3. **Anraku, K., R. Fukuda, N. Takamune, S. Misumi, Y. Okamoto, M. Otsuka, and M. Fujita.** 2010. Highly sensitive analysis of the interaction between HIV-1 Gag and phosphoinositide derivatives based on surface plasmon resonance. Biochemistry **49:**5109-16.

4. **Brugger, B., B. Glass, P. Haberkant, I. Leibrecht, F. T. Wieland, and H. G. Krausslich.** 2006. The HIV lipidome: a raft with an unusual composition. Proc Natl Acad Sci U S A **103:**2641-6.

5. **Callahan, E., and J. Wills.** 2003. Link between genome packaging and rate of budding for Rous sarcoma virus. J Virol **77:**9388-98.

6. **Callahan, E., and J. Wills.** 2000. Repositioning basic residues in the M domain of the Rous sarcoma virus gag protein. J Virol **74:**11222-9.

7. **Campbell, S., R. Fisher, E. Towler, S. Fox, H. Issaq, T. Wolfe, L. Phillips, and A. Rein.** 2001. Modulation of HIV-like particle assembly in vitro by inositol phosphates. Proc Natl Acad Sci U S A **98:**10875-9.

8. **Campbell, S., and V. M. Vogt.** 1997. In vitro assembly of virus-like particles with Rous sarcoma virus Gag deletion mutants: identification of the p10 domain as a morphological determinant in the formation of spherical particles. J Virol **71:**4425-35.

9. **Chan, R., P. Uchil, J. Jin, G. Shui, D. Ott, W. Mothes, and M. Wenk.** 2008. Retroviruses human immunodeficiency virus and murine leukemia virus are enriched in phosphoinositides. J Virol **82:**11228-38.

10. **Chen, K., I. Bachtiar, G. Piszczek, F. Bouamr, C. Carter, and N. Tjandra.** 2008. Solution NMR characterizations of oligomerization and dynamics of equine infectious anemia virus matrix protein and its interaction with PIP2. Biochemistry **47:**1928-37.

11. **Chukkapalli, V., I. Hogue, V. Boyko, W. Hu, and A. Ono.** 2008. Interaction between the human immunodeficiency virus type 1 Gag matrix domain and phosphatidylinositol-(4,5)-bisphosphate is essential for efficient gag membrane binding. J Virol **82:**2405-17.

12. **Chukkapalli, V., S. J. Oh, and A. Ono.** 2010. Opposing mechanisms involving RNA and lipids regulate HIV-1 Gag membrane binding through the highly basic region of the matrix domain. Proc Natl Acad Sci U S A **107:**1600-5.

13. **Dalton, A., P. Murray, D. Murray, and V. Vogt.** 2005. Biochemical characterization of rous sarcoma virus MA protein interaction with membranes. J Virol **79:**6227-38.

14. **Dalton, A. K., D. Ako-Adjei, P. S. Murray, D. Murray, and V. M. Vogt.** 2007. Electrostatic interactions drive membrane association of the human immunodeficiency virus type 1 Gag MA domain. J Virol **81:**6434-45.

15. **del Alamo, M., J. L. Neira, and M. G. Mateu.** 2003. Thermodynamic dissection of a low affinity protein-protein interface involved in human immunodeficiency virus assembly. J Biol Chem **278:**27923-9.

16. **DiNitto, J., and D. Lambright.** 2006. Membrane and juxtamembrane targeting by PH and PTB domains. Biochim Biophys Acta **1761:**850-67.

17. **Dong, X., H. Li, A. Derdowski, L. Ding, A. Burnett, X. Chen, T. Peters, T. Dermody, E. Woodruff, J. Wang, and P. Spearman.** 2005. AP-3 directs the intracellular trafficking of HIV-1 Gag and plays a key role in particle assembly. Cell **120:**663-74.

18. **Dou, J., J. Wang, X. Chen, H. Li, L. Ding, and P. Spearman.** 2009. Characterization of a myristoylated, monomeric HIV Gag protein. Virology **387:**341-52.

19. **Ferguson, K., M. Lemmon, J. Schlessinger, and P. Sigler.** 1995. Structure of the high affinity complex of inositol trisphosphate with a phospholipase C pleckstrin homology domain. Cell **83:**1037-46.

20. **Fernandes, F., K. Chen, L. S. Ehrlich, J. Jin, M. H. Chen, G. N. Medina, M. Symons, R. Montelaro, J. Donaldson, N. Tjandra, and C. A. Carter.** 2010. Phosphoinositides Direct Equine Infectious Anemia Virus Gag Trafficking and Release. Traffic.

21. **Finzi, A., A. Orthwein, J. Mercier, and E. A. Cohen.** 2007. Productive human immunodeficiency virus type 1 assembly takes place at the plasma membrane. J Virol **81:**7476-90.

22. **Freed, E., J. Orenstein, A. Buckler-White, and M. Martin.** 1994. Single amino acid changes in the human immunodeficiency virus type 1 matrix protein block virus particle production. J Virol **68:**5311-20.

23. **Freed, E. O.** 2006. HIV-1 Gag: flipped out for PI(4,5)P(2). Proc Natl Acad Sci U S A **103:**11101-2.

24. **Gamble, T. R., S. Yoo, F. F. Vajdos, U. K. von Schwedler, D. K. Worthylake, H. Wang, J. P. McCutcheon, W. I. Sundquist, and C. P. Hill.** 1997. Structure of the carboxyl-terminal dimerization domain of the HIV-1 capsid protein. Science **278:**849-53.

25. **Hamard-Peron, E., F. Juillard, J. Saad, C. Roy, P. Roingeard, M. Summers, J. Darlix, C. Picart, and D. Muriaux.** 2010. Targeting of murine leukemia virus gag to the plasma membrane is mediated by PI(4,5)P2/PS and a polybasic region in the matrix. J Virol **84:**503-15.

26. **Hatanaka, H., O. Iourin, Z. Rao, E. Fry, A. Kingsman, and D. Stuart.** 2002. Structure of equine infectious anemia virus matrix protein. J Virol **76:**1876-83.

27. **Heo, W. D., T. Inoue, W. S. Park, M. L. Kim, B. O. Park, T. J. Wandless, and T. Meyer.** 2006. PI(3,4,5)P3 and PI(4,5)P2 lipids target proteins with polybasic clusters to the plasma membrane. Science **314:**1458-61.

28. **Hom, R. A., M. Vora, M. Regner, O. M. Subach, W. Cho, V. V. Verkhusha, R. V. Stahelin, and T. G. Kutateladze.** 2007. pH-dependent binding of the Epsin ENTH domain and the AP180 ANTH domain to PI(4,5)P2-containing bilayers. J Mol Biol **373:**412-23.

29. **Inlora, J., V. Chukkapalli, D. Derse, and A. Ono.** 2011. Gag Localization and Virus-like Particle Release Mediated by the Matrix Domain of Human T-Lymphotropic Virus Type-1 Gag are Less Dependent on Phosphatidylinositol-(4,5)-bisphosphate than Those Mediated by the Matrix Domain of Human Immunodeficiency Virus Type-1 Gag. J Virol.

30. **Jouvenet, N., S. J. Neil, C. Bess, M. C. Johnson, C. A. Virgen, S. M. Simon, and P. D. Bieniasz.** 2006. Plasma membrane is the site of productive HIV-1 particle assembly. PLoS Biol **4:**e435.

31. **Kingston, R. L., T. Fitzon-Ostendorp, E. Z. Eisenmesser, G. W. Schatz, V. M. Vogt, C. B. Post, and M. G. Rossmann.** 2000. Structure and self-association of the Rous sarcoma virus capsid protein. Structure Fold Des **8:**617-28.

32. **Kisseleva, M. V., M. P. Wilson, and P. W. Majerus.** 2000. The isolation and characterization of a cDNA encoding phospholipid-specific inositol polyphosphate 5-phosphatase. J Biol Chem **275:**20110-6.

33. **Kutateladze, T.** 2010. Translation of the phosphoinositide code by PI effectors. Nat Chem Biol **6:**507-13.

34. **Lemmon, M. A., K. M. Ferguson, R. O'Brien, P. B. Sigler, and J. Schlessinger.** 1995. Specific and high-affinity binding of inositol phosphates to an isolated pleckstrin homology domain. Proc Natl Acad Sci U S A **92:**10472-6.

35. **Leventis, P. A., and S. Grinstein.** 2010. The distribution and function of phosphatidylserine in cellular membranes. Annu Rev Biophys **39:**407-27.

36. **Maldonado, R., and H. Blough.** 1980. A comparative study of the lipids of plasma membranes of normal cells and those infected and transformed by Rous sarcoma virus. Virology **102:**62-70.

37. **Manna, D., N. Bhardwaj, M. S. Vora, R. V. Stahelin, H. Lu, and W. Cho.** 2008. Differential roles of phosphatidylserine, PtdIns(4,5)P2, and PtdIns(3,4,5)P3 in plasma membrane targeting of C2 domains. Molecular dynamics simulation, membrane binding, and cell translocation studies of the PKCalpha C2 domain. J Biol Chem **283:**26047-58.

38. **McDonnell, J. M., D. Fushman, S. M. Cahill, W. Zhou, A. Wolven, C. B. Wilson, T. D. Nelle, M. D. Resh, J. Wills, and D. Cowburn.** 1998. Solution structure and dynamics of the bioactive retroviral M domain from Rous sarcoma virus. J Mol Biol **279:**921-8.

39. **McLaughlin, S., and D. Murray.** 2005. Plasma membrane phosphoinositide organization by protein electrostatics. Nature **438:**605-11.

40. **Murray, P., Z. Li, J. Wang, C. Tang, B. Honig, and D. Murray.** 2005. Retroviral matrix domains share electrostatic homology: models for membrane binding function throughout the viral life cycle. Structure **13:**1521-31.

41. **Nelle, T., and J. Wills.** 1996. A large region within the Rous sarcoma virus matrix protein is dispensable for budding and infectivity. J Virol **70:**2269-76.

42. **Ono, A., S. Ablan, S. Lockett, K. Nagashima, and E. Freed.** 2004. Phosphatidylinositol (4,5) bisphosphate regulates HIV-1 Gag targeting to the plasma membrane. Proc Natl Acad Sci U S A **101:**14889-94.

43. **Ono, A., J. Orenstein, and E. Freed.** 2000. Role of the Gag matrix domain in targeting human immunodeficiency virus type 1 assembly. J Virol **74:**2855-66.

44. **Parent, L., C. Wilson, M. Resh, and J. Wills.** 1996. Evidence for a second function of the MA sequence in the Rous sarcoma virus Gag protein. J Virol **70:**1016-26.

45. **Perez-Caballero, D., T. Hatziioannou, J. Martin-Serrano, and P. Bieniasz.** 2004. Human immunodeficiency virus type 1 matrix inhibits and confers cooperativity on gag precursor-membrane interactions. J Virol **78:**9560-3.

46. **Perlman, M., and M. Resh.** 2006. Identification of an intracellular trafficking and assembly pathway for HIV-1 gag. Traffic **7:**731-45.

47. **Pessin, J. E., and M. Glaser.** 1980. Budding of Rous sarcoma virus and vesicular stomatitis virus from localized lipid regions in the plasma membrane of chicken embryo fibroblasts. J Biol Chem **255:**9044-50.

48. **Provitera, P., F. Bouamr, D. Murray, C. Carter, and S. Scarlata.** 2000. Binding of equine infectious anemia virus matrix protein to membrane bilayers involves multiple interactions. J Mol Biol **296:**887-98.

49. **Quigley, J. P., D. B. Rifkin, and E. Reich.** 1971. Phospholipid composition of Rous sarcoma virus, host cell membranes and other enveloped RNA viruses. Virology **46:**106-16.

50. **Rose, S., P. Hensley, D. J. O'Shannessy, J. Culp, C. Debouck, and I. Chaiken.** 1992. Characterization of HIV-1 p24 self-association using analytical affinity chromatography. Proteins **13:**112-9.

51. **Saad, J., S. Ablan, R. Ghanam, A. Kim, K. Andrews, K. Nagashima, F. Soheilian, E. Freed, and M. Summers.** 2008. Structure of the myristylated human immunodeficiency virus type 2 matrix protein and the role of phosphatidylinositol-(4,5)-bisphosphate in membrane targeting. J Mol Biol **382:**434-47.

52. **Saad, J., A. Kim, R. Ghanam, A. Dalton, V. Vogt, Z. Wu, W. Lu, and M. Summers.** 2007. Mutations that mimic phosphorylation of the HIV-1 matrix protein do not perturb the myristyl switch. Protein Sci **16:**1793-7.

53. **Saad, J., E. Loeliger, P. Luncsford, M. Liriano, J. Tai, A. Kim, J. Miller, A. Joshi, E. Freed, and M. Summers.** 2007. Point mutations in the HIV-1 matrix protein turn off the myristyl switch. J Mol Biol **366:**574-85.

54. **Saad, J., J. Miller, J. Tai, A. Kim, R. Ghanam, and M. Summers.** 2006. Structural basis for targeting HIV-1 Gag proteins to the plasma membrane for virus assembly. Proc Natl Acad Sci U S A **103:**11364-9.

55. **Scheifele, L., J. Rhoads, and L. Parent.** 2003. Specificity of plasma membrane targeting by the rous sarcoma virus gag protein. J Virol **77:**470-80.

56. **Scholz, I., A. Still, T. Dhenub, K. Coday, M. Webb, and E. Barklis.** 2008. Analysis of human immunodeficiency virus matrix domain replacements. Virology **371:**322-35.

57. **Shkriabai, N., S. Datta, Z. Zhao, S. Hess, A. Rein, and M. Kvaratskhelia.** 2006. Interactions of HIV-1 Gag with assembly cofactors. Biochemistry **45:**4077-83.

58. **Soneoka, Y., S. Kingsman, and A. Kingsman.** 1997. Mutagenesis analysis of the murine leukemia virus matrix protein: identification of regions important for membrane localization and intracellular transport. J Virol **71:**5549-59.

59. **Spearman, P., J. J. Wang, N. Vander Heyden, and L. Ratner.** 1994. Identification of human immunodeficiency virus type 1 Gag protein domains essential to membrane binding and particle assembly. J Virol **68:**3232-42.

60. **Stansell, E., R. Apkarian, S. Haubova, W. E. Diehl, E. M. Tytler, and E. Hunter.** 2007. Basic residues in the Mason-Pfizer monkey virus gag matrix domain regulate intracellular trafficking and capsid-membrane interactions. J Virol **81:**8977-88.

61. **Tang, C., E. Loeliger, P. Luncsford, I. Kinde, D. Beckett, and M. F. Summers.** 2004. Entropic switch regulates myristate exposure in the HIV-1 matrix protein. Proc Natl Acad Sci U S A **101:**517-22.

62. **Uekama, N., T. Sugita, M. Okada, H. Yagisawa, and S. Tuzi.** 2007. Phosphatidylserine induces functional and structural alterations of the membrane-associated pleckstrin homology domain of phospholipase C-delta1. FEBS J **274:**177-87.

63. **Varnai, P., and T. Balla.** 1998. Visualization of phosphoinositides that bind pleckstrin homology domains: calcium- and agonist-induced dynamic changes and relationship to myo-[3H]inositol-labeled phosphoinositide pools. J Cell Biol **143:**501-10.

64. **Wills, J., R. Craven, R. J. Weldon, T. Nelle, and C. Erdie.** 1991. Suppression of retroviral MA deletions by the amino-terminal membrane-binding domain of p60src. J Virol **65:**3804-12.

65. **Wiradjaja, F., L. M. Ooms, S. Tahirovic, E. Kuhne, R. J. Devenish, A. L. Munn, R. C. Piper, P. Mayinger, and C. A. Mitchell.** 2007. Inactivation of the phosphoinositide phosphatases Sac1p and Inp54p leads to accumulation of phosphatidylinositol 4,5-bisphosphate on vacuole membranes and vacuolar fusion defects. J Biol Chem **282:**16295-307.

66. **Yagisawa, H.** 2006. Nucleocytoplasmic shuttling of phospholipase C-delta1: a link to Ca2+. J Cell Biochem **97:**233-43.

67. **Yeung, T., G. E. Gilbert, J. Shi, J. Silvius, A. Kapus, and S. Grinstein.** 2008. Membrane phosphatidylserine regulates surface charge and protein localization. Science **319:**210-3.

68. **Zhou, W., L. J. Parent, J. W. Wills, and M. D. Resh.** 1994. Identification of a membrane-binding domain within the amino-terminal region of human immunodeficiency virus type 1 Gag protein which interacts with acidic phospholipids. J Virol **68:**2556-69.

CHAPTER 3

HIV-1 GAG PROTEIN CAN SENSE THE CHOLESTEROL AND ACYL CHAIN ENVIRONMENT IN MODEL MEMBRANES[2]

Membrane binding of the HIV-1 Gag structural protein, a critical step in viral assembly at the plasma membrane, is mediated by the myristoylated, highly basic MA domain, which interacts with negatively charged lipids in the inner leaflet. According to a popular model, virus particles bud from membrane rafts, microdomains enriched in cholesterol and high-melting phospholipids with higher order than found outside of rafts. How Gag might recognize membrane rafts, if they exist in the inner leaflet, is unknown. Using a liposome flotation assay with proteins translated *in vitro*, we investigated if Gag can sense the composition of the hydrophobic part of the bilayer, by fixing lipid head group composition and varying hydrophobic properties. In liposomes composed solely of phosphatidylserine and phosphatidylcholine, and with the same overall membrane negative charge, Gag strongly preferred lipids with both acyl chains unsaturated, over those with only one chain unsaturated. Adding cholesterol increased Gag binding and led to closer p[3]acking of phospholipids. However, higher membrane order, as

[2] The following section is reproduced from: Dick, R. A., S. L. Goh, G. W. Feigenson, and V. M. Vogt. 2012. HIV-1 Gag protein can sense the cholesterol and acyl chain environment in model membranes. Proc Natl Acad Sci U S A 109:18761-6, with modifications to conform to the required format. R.A.D. performed liposome flotatation and protein purification. S.L.G. performed ESR measurements.

measured by electron spin resonance, was not correlated with increased Gag binding. Gag proteins from two other retroviruses gave similar results. These liposome binding preferences were qualitatively recapitulated by purified myristoylated HIV-1 MA. Phosphatidylinositol (4,5)bisphosphate and cholesterol enhanced binding in an additive manner. Taken together, these results show that Gag is sensitive to both the acyl chains of phosphatidylserine, as well as cholesterol concentration and other details of the membrane environment. These observations may help explain how retroviruses acquire a raft-like lipid composition.

INTRODUCTION

The retroviral structural polyprotein, Gag, drives virus assembly at the plasma membrane (PM). Gag molecules bind to the PM, and then through protein-protein interactions form a curved lattice that bulges out and eventually leads to budding and release of the enveloped virus particles. HIV-1 Gag interacts with the negatively charged inner leaflet of the PM primarily via its N-terminal MA domain. Three features of MA underlie HIV-1 Gag membrane binding: an N-terminal myristate, a highly basic patch, and a pocket for the minor lipid phosphatidylinositol bisphosphate, PI(4,5)P2 (1). Multimerization and vesicular trafficking also play roles in membrane interaction *in vivo*. PI(4,5)P2 is important *in vivo*, based on the observations that its depletion by an overexpressed phosphatase compromises budding (2), and that it is enriched in the HIV-1 envelope (3). *In vitro* and biochemical assays qualitatively support the conclusions about Gag-PM interaction *in vivo*: *In vitro* flotation assays show HIV-1 Gag

binding to liposomes to be dependent on negatively charged lipids, in particular phosphatidylserine (PS) (4), which is enriched in the inner leaflet of the PM. Liposome binding is enhanced by the addition of PI(4,5)P2 (5), although without great specificity for this particular phosphoinositide (5, 6).

HIV-1 is said to bud from rafts (reviewed in (7)). Diverse strands of evidence support this model. First, cellular proteins found in rafts are often associated with viral particles (8). Second, the envelopes of retroviruses like HIV-1 (3, 9, 10) and Rous sarcoma virus (RSV) (11, 12) are enriched in sphingomyelin (SM) and cholesterol, compared with the PM. Third, two retroviral proteins—Nef for HIV-1 and Glycogag for murine leukemia virus (MLV) —promote cholesterol incorporation into virus particles and raft association of Gag (13, 14). Fourth, cholesterol depletion from cells reduces HIV-1 release (15). But how virus particles acquire the observed high cholesterol content is unknown. For example, Gag might prefer to bind to raft-like micro-domains, or the lattice of Gag molecules might induce raft formation *de novo*, or Gag might cause coalescence of pre-existing raft domains (16). Few studies have addressed such questions *in vitro*. In chemically simple, lipid-only models of the PM outer leaflet, a large region of compositions is found in which two phases coexist, the liquid-disordered or Ld phase, and the liquid-ordered, or Lo phase. This compositional region can be termed "the raft region". The minimal lipid requirement for Ld + Lo coexistence in a mixture is a high melting temperature (Tm) lipid such as SM or distearoyl phosphatidylcholine (DSPC), a low Tm lipid such as dioleoyl phosphatidylcholine (DOPC) or palmitoyl, oleoyl

phosphatidylcholine (POPC), and cholesterol. Compared with the Ld phase, the Lo phase is enriched in the high Tm lipid and in cholesterol in these simple mixtures.

A major challenge to understanding how HIV-1 acquires a raft-like lipid composition is that rafts are known only for the outer leaflet of the PM, yet Gag interacts directly with the inner leaflet. By composition, the inner leaflet has no high Tm lipid, has lower concentrations of PC, and has high concentrations of PE, PS, and cholesterol (17). No Ld + Lo coexistence has been observed in bilayer models representing the composition of the inner leaflet (18).

Here, we investigated how cholesterol and phospholipid acyl chain type affect HIV-1 Gag binding to liposomes *in vitro*, as measured by Gag flotation in sucrose gradients. While still not a good mimic of the properties of the inner leaflet, we chose simplified model mixtures of PS/PC or PS/PC/cholesterol, because the phase behaviors of similar mixtures are relatively well understood, and accurate phase diagrams could be used to guide mixture choices (19). Results show that Gag-membrane interactions depend on phospholipid head group type, as known previously, but notably also on cholesterol concentration and on acyl chain saturation.

MATERIALS AND METHODS

Plasmids, protein purification, liposome preparation, and electron spin resonance

The plasmids encoding HIV GagΔp6 BH10 and RSV GagΔPR, and encoding myristoylated HIV-1 MA (myr-MA), as well as the purification procedure for myr-MA were previously described (4, 25) or are detailed in the Supplementary section.

Liposome preparation. Liposomes were prepared by the rapid solvent exchange (RSE) method (26) modified as described (27). Briefly, lipids in chloroform solution were dispensed into glass tubes. After the addition of buffer (20 mM HEPES, pH 7.0), the mixture was vortexed under vacuum for 90 s and sealed under argon gas, yielding 10 mg/mL hydrated liposomes. Liposome samples were stored at 4°C up to one week before extrusion. To prepare large unilamellar vesicles (LUVs), a mini-extruder block (Avanti) was heated to 45°C. Liposomes were extruded 41 times through 100 nm polycarbonate filters (Avanti) and stored at 4°C. Extruded liposomes were used within one week. Details of the methods used to handle lipids (28) and to prepare samples for ESR measurements can be found in the Supplementary section. For ESR measurements typical instrument settings were: center field = 3320 G, sweep width = 100 G, modulation frequency = 100 kHz, modulation amplitude = 1 G, time constant = conversion time = 81.92 s, resolution = 2000 points. Nine scans were averaged for each sample. A_{max} and A_{min} were determined directly from the spectra, and the order parameter of each sample was calculated according to Schorn & Marsh (29) using the hyperfine tensor (A_{xx}, A_{yy}, A_{zz}) = (5.9, 5.4, 32.9 G).

Liposome binding assay

Radioactively labeled protein was prepared by translation in the TnT coupled T7 rabbit reticulocyte reaction (Promega) in the presence of [35S] methionine-cysteine (Perkin Elmer: ExPRE35S35 protein labeling mix). The liposome binding assay used for Fig. 3.1 and 3.2, here referred to as large format assay, was previously described (6). A small format liposome binding assay was used for Fig. 3.3-3.6 as previously described

(20) with some modification. A 5 mL fraction of a 25 mL reticulocyte transcription reaction was added to 15 mL binding buffer (20mM HEPES pH 7.0) followed by 50 mg of LUVs (to a concentration of 8.5 mg/mL). The reaction mix was incubated at 22°C for 10min. Each binding reaction was mixed with 75 mL 67% sucrose, and 80 mL of this mix was placed in a TLA 100 tube followed by 120 mL 40% sucrose and 40 mL 4% sucrose. All sucrose was made w/w with binding buffer. Centrifugation was at 90k rpm in a TLA 100 rotor (Beckman) for 1 hr. Purified myr-MA flotations were performed with 15 mg of protein in place of the reticulocyte reaction, and the binding buffer and sucrose was supplemented with with NaCl so that all solutions were at a final concentration of 150 mM NaCl. Four 60 ml fractions were collected from each flotation and 40 ml of each fraction was analyzed by SDS-PAGE.

RESULTS AND DISCUSSION

We examined how membrane negative charge, cholesterol concentration, and phospholipid acyl chain properties affect HIV-1 Gag membrane binding. Radiolabeled Gag was synthesized *in vitro* in a reticulocyte translation system. Binding to 100 nm large unilamellar vesicles (LUVs) was measured by flotation in a sucrose gradient (5, 6, 20, 21).

Effects of acyl chain saturation on HIV-1 Gag binding

Increasing the ratio of PS to PC is known to increase the binding of Gag to LUVs (4-6, 20). To test if Gag is sensitive to acyl chain length and saturation, PC- and PS-containing LUVs were prepared with three acyl chain types: DOPC/DOPS, where both

lipids have two 18:1 (oleoyl) chains; POPC/POPS where one fatty acid is 16:0, the other 18:1 (palmitoyl, oleoyl); and egg PC/brain PS, a natural mixture, with the PC being 32% 16:0, 32% 18:1, 12% 18:0, and 17% 18:2, and the PS being dominated by 18:0, 18:1 chains. By keeping the PS and PC chains identical or nearly so, comparisons of each mixture focus on the behavior of the particular PS chains, rather than on the way disparate PS and PC chains might mix.

As PS concentration increased from 20% to 90%, binding of HIV-1 Gag to LUVs with mixtures of the three acyl chain types differed (Fig. 3.1). Gag binding to DOPC/DOPS increased steeply at ~30% PS, reaching a maximum at ~ 50% PS. Gag binding to POPC/POPS only gradually increased starting at ~30% PS, reaching a somewhat lower maximum. Finally, Gag binding to natural PC/PS again increased gradually starting at ~30% PS, reached a maximum at ~ 65% PS, and then gradually decreased at higher PS concentrations. The membrane charge seen by Gag is not different among these mixtures at any given PS concentration (22). Yet surprisingly, Gag behaves as if it experiences a greater effective PS concentration in the DOPC/DOPC mixtures.

Cholesterol-enhanced binding of Gag

The effect of cholesterol on membrane binding of retroviral Gag proteins *in vitro* has not been investigated systematically. We measured Gag binding to LUVs with increasing cholesterol content in four different phospholipid environments, including one that mimics Lo and Ld compositions: DSPC/DOPC/DOPS, DOPC/DOPS, POPC/POPS, and egg PC/brain PS (DSPC is distearoyl phosphatidylcholine, 18:0, 18:0-PC). In each

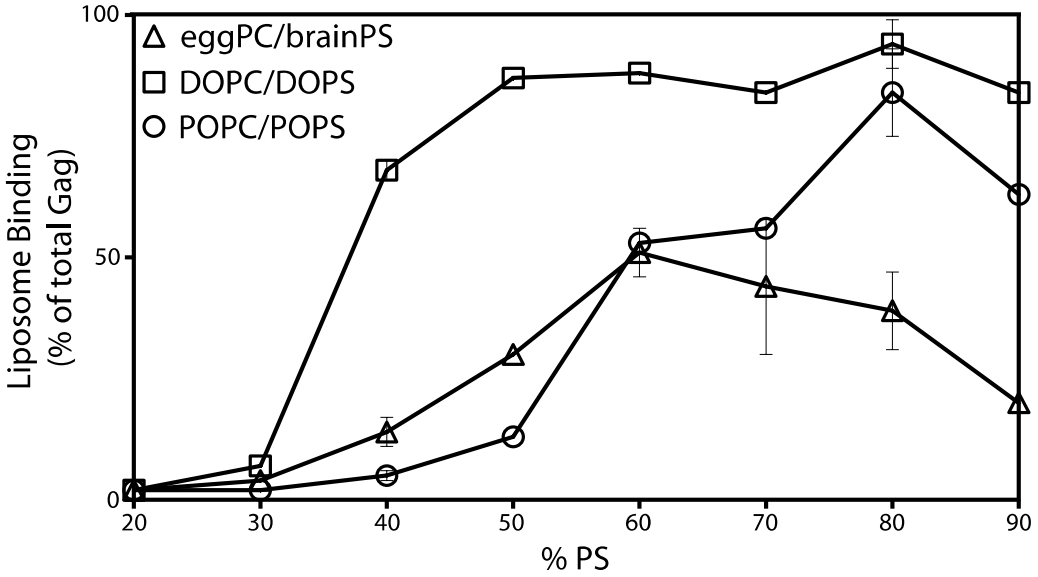

Fig. 3.1 Acyl chain saturation influences phosphatidylserine-driven HIV-1 Gag liposome binding. 35S-methionine-labeled HIV-1 Gag synthesized in a reticulocyte extract was incubated with liposomes composed of one of the following three mixtures of two phospholipids: dioleoyl-PC (DOPC) and dioleoyl-PS (DOPS); palmitoyl, oleoyl-PC (POPC) and palmitoyl, oleoyl-PS (POPS); or egg PC and brain PS. [The oleoyl acyl chain has one double bond (18:1), while the palmitoyl acyl chain has no double bonds (16:0)]. The percentage of Gag that floated with the liposomes in a sucrose gradient, as determined by SDS-PAGE and fluorography, was plotted as a function of increasing concentration of the negatively charged lipid PS. Error bars indicate standard deviation for replicas done at 40% and 80% PS for all three lipid compositions and at 60% and 70% PS for the natural phospholipids

different lipid mixture, the percentage of cholesterol was increased while the percentage of PC was decreased, keeping PS unchanged at 30%. The maximum cholesterol content, 63%, is near its solubility limit in PC mixtures (23). The resulting cholesterol concentrations cover the cholesterol concentration of plasma membranes, which can be as high as 50% (17). For all four mixtures tested, increased cholesterol concentration resulted in increased binding of Gag, as shown by the fluorograms (Fig. 3.2A) and in more detail in Fig. 3.2B. Two distinct behaviors are observed, characterized by different shapes of the binding curves: (i) In the two DOPC-containing mixtures, Gag binding increased strongly starting at the lowest cholesterol concentrations, rising to nearly maximal binding at ~36% cholesterol. This behavior occurred whether or not the mixtures contained 5% of the saturated acyl chain lipid DSPC; (ii) In egg PC/brain PS mixtures, Gag binding started to increase only at ~18% cholesterol, then rose gradually toward the same maximum found with the DOPC-containing mixtures. In POPC-containing mixtures the curve shape was similar, but with binding first detected at ~36% cholesterol, and gradually increasing to a slightly lower maximum. This cholesterol-mediated enhancement of HIV-1 Gag binding in these simple model liposomes might mimic the association of HIV-1 Gag with cholesterol-containing plasma membranes, and in particular with lipid raft microdomains in the membrane.

Adding cholesterol to phospholipid bilayers increases the packing density of phospholipid acyl chains and headgroups, the well-known “cholesterol condensing effect” (24). Closer lipid packing means increased acyl chain order, a parameter that can be measured by electron spin resonance (ESR) with spin-labeled lipid probes. We

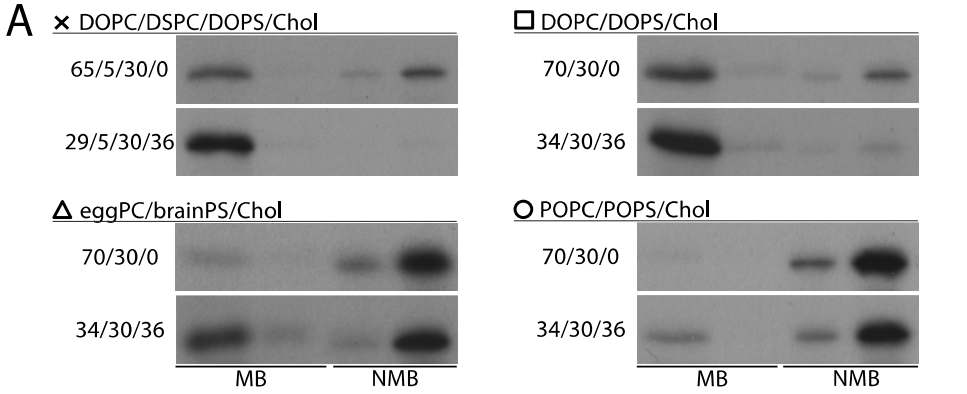
A
× DOPC/DSPC/DOPS/Chol
65/5/30/0
29/5/30/36
□ DOPC/DOPS/Chol
70/30/0
34/30/36
△ eggPC/brainPS/Chol
70/30/0
34/30/36
○ POPC/POPS/Chol
70/30/0
34/30/36
MB
NMB
MB
NMB

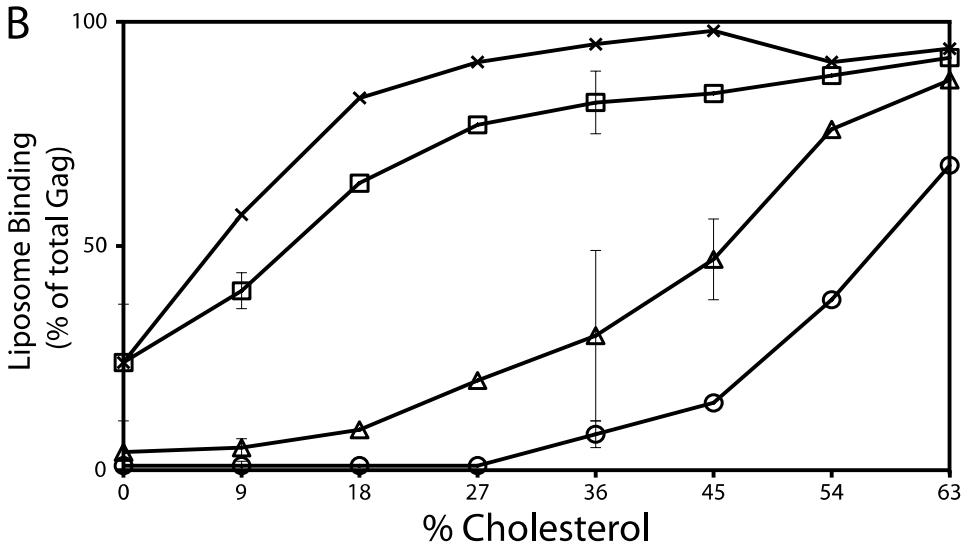
B
Liposome Binding
(% of total Gag)
100
50
0
0
9
18
27
36
45
54
63
% Cholesterol

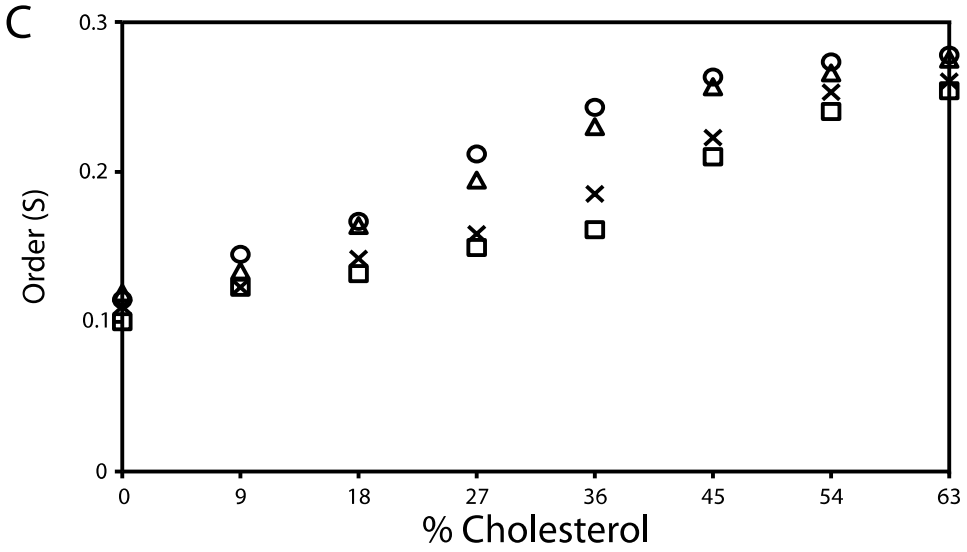
C
Order (S)
0.3
0.2
0.1
0
0
9
18
27
36
45
54
63
% Cholesterol

Fig. 3.2 Cholesterol concentration influences HIV-1 Gag binding to liposomes. Liposomes were made with a fixed 30% PS and varying ratios of cholesterol and DOPC or POPC (and in one case also containing 5% distearoyl PC (DSPC), 18:0, 18:0). HIV-1 Gag synthesis and flotation analyses were as described in Fig. 1. **A**, Examples of lipid ratios for each of the four lipid compositions used and the corresponding fluorograms. MB, membrane bound (floated liposomes); NMB, non-membrane bound (1/4 of the sample loaded compared with MB). **B**, Quantification of flotation reactions. The symbols are the same as in **A**. Error bars represent standard deviation for the three, three-component mixtures repeated in triplicate at 9% and 36% cholesterol, for DOPC/DOPS/0% cholesterol, and for eggPC/brainPS/45% cholesterol. **C**, Electron spin resonance (ESR) measurements for each of the four liposome compositions from 0% to 63% cholesterol. *S*, order parameter.

carried out ESR measurements on all four mixtures with 16-DOXYL-stearic acid (16-DSA). Increased cholesterol concentration clearly increased lipid order (Fig. 3.2C), yet the order was not correlated with the Gag binding differences seen in Fig. 3.2B. In particular, at every cholesterol concentration, Gag behaved as if it detected a higher PS concentration in DOPS-containing mixtures than in POPS or brain-PS mixtures.

Effects of lipid order on Gag membrane interaction

In order to explore more systematically the model that "viruses bud from rafts", we selected lipid mixtures that are closer in composition to actual Ld and Lo phases, based on published phase diagrams (19). We avoided phase coexistence regions by choosing cholesterol concentration just higher than the Ld + Lo coexistence region. Two kinds of mixtures were examined, one containing DOPC, the other POPC. We prepared four series of LUVs, two with constant cholesterol = 40% and PS = 20%, and two with constant cholesterol = 32% and PS = 30%. In all four mixtures, membrane order was systematically varied by changing the ratio of high-melting, saturated DSPC to low-melting, unsaturated lipids. Thereby, the LUV compositions ranged from liquid-disordered to liquid-ordered (Fig. 3.3A, 3.3B; see Table 3.1 for all lipid compositions*)*. Two sets of eight compositions were prepared for the DOPC and two for the POPC mixtures, each lying on a line of constant cholesterol concentration and extending from all low-Tm (Ld) lipid on the left to all high-Tm (Lo) lipid on the right. Because Gag binding to DOPC/DOPS/cholesterol at 40% cholesterol was nearly maximal at 30% PS (Fig. 3.2B), the PS in the DOPC-containing mixture was reduced to a fixed 20% in order to increase the dynamic range for observing Gag binding in these mixtures.

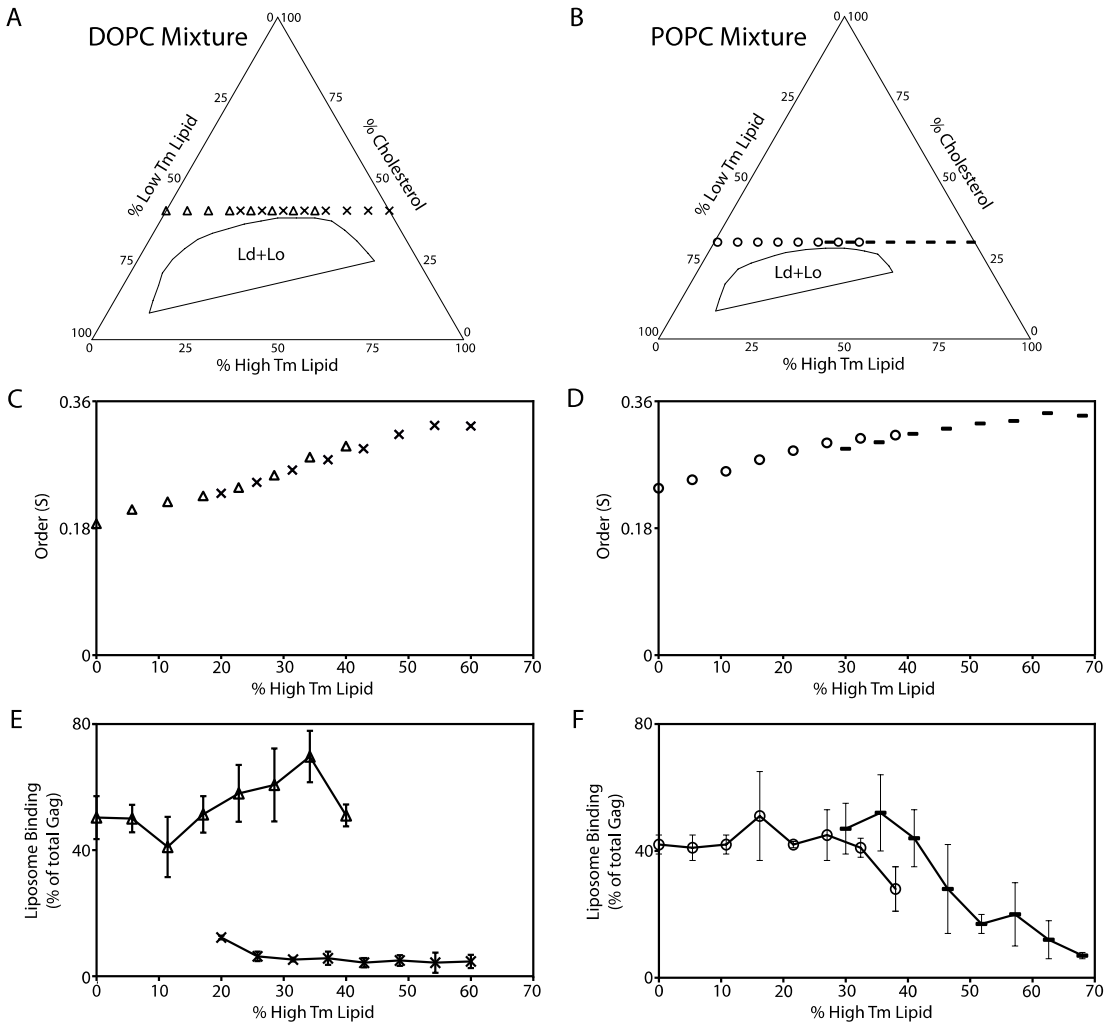
A
DOPC Mixture
% Low Tm Lipid
% Cholesterol
% High Tm Lipid
Ld+Lo
B
POPC Mixture
% Low Tm Lipid
% Cholesterol
% High Tm Lipid
Ld+Lo
C
Order (S)
% High Tm Lipid
D
Order (S)
% High Tm Lipid
E
Liposome Binding
(% of total Gag)
% High Tm Lipid
F
Liposome Binding
(% of total Gag)
% High Tm Lipid

Fig. 3.3 Membrane order has complex influence on HIV-1 Gag-liposome binding at fixed PS and cholesterol concentrations. HIV-1 Gag and flotation analyses were as described in Fig. 1. **A** and **B**, phase diagrams situate the DOPC and POPC mixtures tested relative to the Ld + Lo phase coexistence region. **A**. The left-most triangle symbol crossing the Low Tm Lipid axis represents a composition of low Tm lipids DOPC/DOPS/cholesterol (40%/20%/40%). Each triangle moving sequentially to the right has an additional 5.7% DOPC replaced with 5.7% of the high Tm lipid DSPC. The right-most X symbol represents a composition of high Tm lipids DSPC/DPPS/cholesterol (40%/20%/40%). Each X moving sequentially to the left has 5.7% DSPC replaced by 5.7% of the low Tm DOPC. Note that the boundaries of the four-component phase diagrams containing PS have not been determined, but are shown here based on the published three-component phase diagrams (19), in order to provide a guide to the expected phase behavior of the four-component PS-containing mixtures. **B**. As in A, except with POPC lipids instead of DOPC lipids. The left starting point for the low Tm lipids POPC/POPS/cholesterol (38%/30%/32%) is marked by a circle, with each sequential point having 5.4% POPC replaced by 5.4% of the high Tm lipid DSPC. The right starting point for the high Tm lipids DSPC/DPPS/cholesterol (38%/30%/32%) is marked by a dash, with each sequential point having 5.4% DSPC replaced with 5.4% of the low Tm lipid POPC. All compositions yield a single phase (i.e. not coexistence of the two phases, Ld+Lo). Lipid order increases from the left to right (Ld to Lo) as the percentage of high Tm lipid increases. **C** and **E**, ESR and Gag binding measurements for the DOPC-containing liposomes. **D** and **F**, ESR and Gag binding measurements for the POPC-containing liposomes. The symbols in **C** and **D** are the same as those in **A** and **B**. Error bars represent standard deviation for at least three replicas for each data point.

DOPC-Mixture	% DSPC	% DOPC	% DOPS	% Chol
Ld-1	0	40	20	40
Ld-2	5.7	34.3	20	40
Ld-3	11.4	28.6	20	40
Ld-4	17.1	22.9	20	40
Ld-5	22.8	17.2	20	40
Ld-6	28.5	11.5	20	40
Ld-7	34.2	5.8	20	40
Ld-8	40	0	20	40

DOPC-Mixture	% DSPC	% DOPC	% DPPS	% Chol
Lo-1	0	40	20	40
Lo-2	5.8	34.2	20	40
Lo-3	11.5	28.5	20	40
Lo-4	17.2	22.8	20	40
Lo-5	22.9	17.1	20	40
Lo-6	28.6	11.4	20	40
Lo-7	34.3	5.7	20	40
Lo-8	40	0	20	40

POPC-Mixture	% DSPC	% POPC	% POPS	% Chol
Ld-1	0	38	30	32
Ld-2	5.4	32.6	30	32
Ld-3	10.8	27.2	30	32
Ld-4	16.2	21.8	30	32
Ld-5	21.6	16.4	30	32
Ld-6	27	11	30	32
Ld-7	32.4	5.6	30	32
Ld-8	38	0	30	32

POPC-Mixture	% DSPC	% POPC	% DPPS	% Chol
Lo-1	0	38	30	32
Lo-2	5.6	32.4	30	32
Lo-3	11	27	30	32
Lo-4	16.4	21.6	30	32
Lo-5	21.8	16.2	30	32
Lo-6	27.2	10.8	30	32
Lo-7	32.6	5.4	30	32
Lo-8	38	0	30	32

Table 3.1 Compositions of liposomes used in Fig. 3.3. All components of each sample are mole % of total lipids. The DOPC-mixture liposomes, Ld-1 to Ld-8 and Lo-1 to Lo-8 correspond to the triangle and x symbols in Fig 3 respectively. The POPC-mixture liposomes, Ld-1 to Ld-8 and Lo-1 to Lo-8 correspond to the circle and dash symbols in Fig 3 respectively.

ESR measurements showed that increasing the percentage of high Tm lipids increased membrane order, regardless of whether DOPS or DPPS was in the mixtures (Fig. 3.3C, D). Comparing 3.3C with 3.3D, at each high Tm lipid percentage up to ~50%, the DOPC-containing mixture had slightly lower order than did the POPC-containing

mixture, indicating that the saturated acyl chain of POPC confers more order to the mixture despite the lower cholesterol concentration of 32% compared with 40%.

We found that Gag binding in these mixtures was not a function of membrane order. Whereas order increased gradually and monotonically as high Tm lipid concentration increased, Gag binding exhibited dramatic differences. For 20% DOPS in the 40% cholesterol/DOPC/DSPC mixtures (triangle symbols), replacing DOPC with the high Tm DSPC resulted in nearly unchanged Gag binding for the eight LUV compositions (Fig. 3.3E). In stark contrast, for 20% DPPS in the 40% cholesterol/DOPC/DSPC mixtures (x symbols), Gag binding was barely detectable for any replacement of DOPC by DSPC (Fig. 3.3E). This surprising result was reproducible in multiple LUV preparations. Thus, in a variety of membrane environments, including some that are very similar to those resulting in strong Gag binding to DOPS, Gag behaves as if it hardly detects the 20% DPPS at all.

Quite different Gag binding occurred with only subtle changes in lipid composition in the POPC-containing mixtures (Fig. 3.3F): For 30% POPS in 32% cholesterol/POPC/DSPC mixtures (open circle symbols), replacing POPC with DSPC hardly changed Gag binding, which decreased only slightly when DSPC reached 38%.

In contrast, for 30% DPPS in the 32% cholesterol/POPC/DSPC mixtures, Gag binding at first remained high as DSPC replaced POPC, then gradually dropped toward ~0 as the POPC was completely replaced by DSPC (Fig. 3.3F). In remarkable contrast to the behavior of DOPC-containing mixtures at 40% cholesterol where very low Gag binding occurred when the PS was 20% DPPS, high Gag binding was observed in mixtures containing 30% DPPS in POPC-containing mixtures with 32% cholesterol. Thus, Gag binds well to DPPS, but only in mixtures in which the DPPS is in some sense sufficiently "available" to the Gag.

These data show that cholesterol enhancement of HIV-1 Gag-liposome binding is not solely a consequence of a cholesterol-induced increase in membrane order. Instead, the data imply that Gag detects three lipid mixture features besides PS concentration: (i) the ensemble of all acyl chains in the membrane; (ii) the cholesterol concentration; and (iii) the nature of the acyl chains of the negatively charged PS with which Gag interacts.

Response of other retroviral Gag proteins to cholesterol and phospholipid acyl chain type

To determine if the sensing of differences in the content of cholesterol and acyl chains in liposomes is unique to HIV-1 Gag, we tested MLV Gag and RSV Gag proteins in parallel with HIV-1 Gag. MLV Gag also is naturally myristoylated at its N-terminus, but RSV Gag is not lipidated in any way. In order to mimic the differences between Ld and Lo phases, two pairs of LUVs were prepared for each protein: (i) 30% brain PS + egg PC with or without 36% cholesterol; and (ii) 30% PS, but with compositions chosen

close to those of known Ld + Lo phase coexistence (19) and with membrane order characteristic of an Ld mixture or of an Lo mixture.

HIV-1, RSV, and MLV Gag proteins all responded similarly to these LUV mimics of Ld and Lo phases, preferring liposomes containing high cholesterol concentration coupled with acyl chain saturation (Fig. 3.4). Only in the case of the 0% and 36% cholesterol LUVs did RSV Gag bind without significant difference. Thus Gag sensing of the acyl chain composition does not require an N-terminal fatty acid chain. However, the preference for the Lo composition seen here does not indicate that membrane order alone is the explanation. The HIV-1 Gag binding shown in Fig. 3.3E, F makes clear that the nature of the PS acyl chains, the cholesterol concentration, and the acyl chains of other lipids present all have strong influence on Gag binding.

An advantage of the reticulocyte extract is that it simulates a cellular environment, for example by the presence of RNA and proteins. A disadvantage is that unknown components might influence Gag binding. Therefore, we tested the binding of non-radioactively labeled, myristoylated HIV-1 MA protein (myr-MA) that had been purified after expression in *E. coli* (4, 25). Myr-MA behaved similarly to HIV-1 Gag in that the presence of cholesterol strongly enhanced binding to LUVs (Fig. 3.5). And like Gag, purified myr-MA also preferred the LUVs with the Lo composition, corroborating results from the reticulocyte experiments.

PI(4,5)P2-enhanced membrane binding in the presence of cholesterol

Because of the established role of PI(4,5)P2 in membrane binding, we examined the ability of cholesterol to stimulate binding of HIV-1 Gag to LUVs containing PI(4,5)P2.

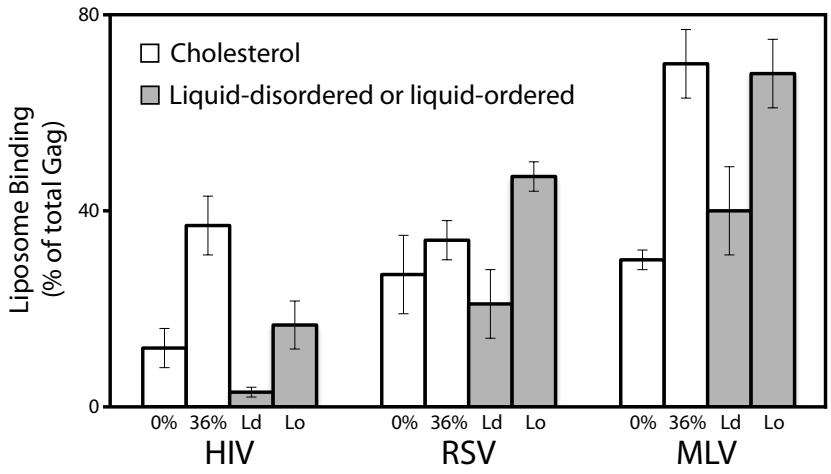

Fig. 3.4 Acyl chain type and presence of cholesterol influence liposome binding of other retroviral Gag proteins. The three Gag proteins were expressed in a reticulocyte lysate and analyzed by flotation as in Fig. 1. RSV, Rous sarcoma virus (alpharetrovirus genus); MLV, murine leukemia virus (gamma retrovirus genus). The lipid compositions were as follows: 0% = 70% eggPC/30% brainPS; 36% = 34% eggPC/30% brainPS/36% cholesterol (white bars); Ld = 10% DSPC/30% POPS/50% POPC/10% cholesterol; Lo = 22% DSPC/30% DPPS/23% POPC/25% cholesterol. The histograms represent at least three replicas; error bars show standard deviation. Order parameter (*S*), as determined via ESR, is 0.156 for the Ld composition, and 0.332 for the Lo composition.

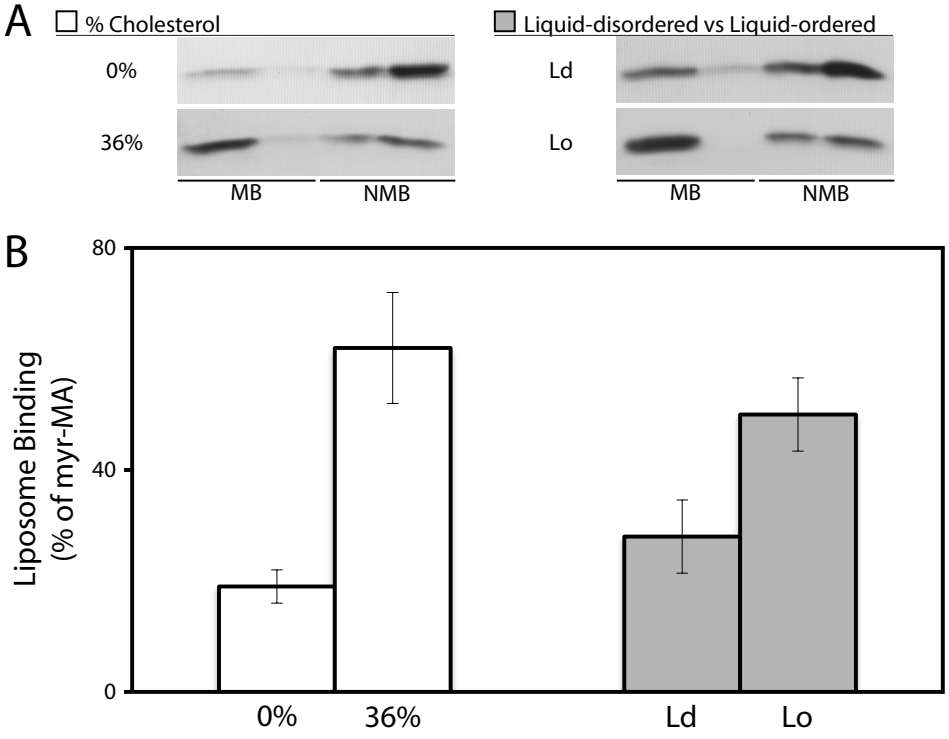

Fig. 3.5 Acyl chain type and presence of cholesterol influence liposome binding of purified HIV-1 MA. Myristoylated MA was purified from an *E. coli* expression system. Fifteen mg of protein was mixed with 50 mg of liposomes containing either 0% cholesterol or 36% cholesterol, or with an Ld or Lo composition, both as defined in Fig. 4. Binding was measured after flotation by SDS-PAGE and Coomassie Blue staining and densitometry. **A**, Representative flotation result showing the stained MA band. **B**, Quantitation. For all of these lipid compositions the concentration of PS was constant (30%). Bars represent the average of no less than three replicas. Error bars represent standard deviation.

Flotation assays were carried out with LUVs prepared with 30% brain PS and egg PC, with or without 36% cholesterol, and with or without 2% PI(4,5)P2, a concentration similar to that found in HIV-1 virion membranes (3). In these binding assays, 2% PI(4,5)P2 was sufficient to elicit a three-fold increase in Gag binding. Addition of cholesterol boosted Gag binding by a further two-fold (Fig. 3.6). Thus the cholesterol enhancement appears to be effective for membrane association driven not only by PS alone, but also by PS and PI(4,5)P2, which are inferred to be important in vivo.

SUMMARY AND CONCLUSIONS

In order to study how virus particles might bud from plasma membrane rafts, we set out to develop an *in vitro* model for HIV-1 Gag binding to raft-like and non-raft-like membranes. The results show that Gag-membrane interaction is sensitive not only to net negative charge, as known previously, but also to the hydrophobic environment of the bilayer, namely cholesterol content and phospholipid acyl chain type. For example, in binary mixtures of PS/PC, the Gag protein strongly prefers DOPS to POPS, and it prefers higher over lower cholesterol content in diverse phospholipid mixtures. Nevertheless, Gag does not detect membrane order *per se*, as inferred from comparison of Gag binding with membrane order, as measured by ESR. The cholesterol enhancement effect behaves as if cholesterol makes more PS available for binding to Gag. To our knowledge, this is the first systematic study of the effects of the hydrophobic core of a membrane on the binding of the internal structural protein of an enveloped virus. Although the mechanisms underlying the effects observed appear to

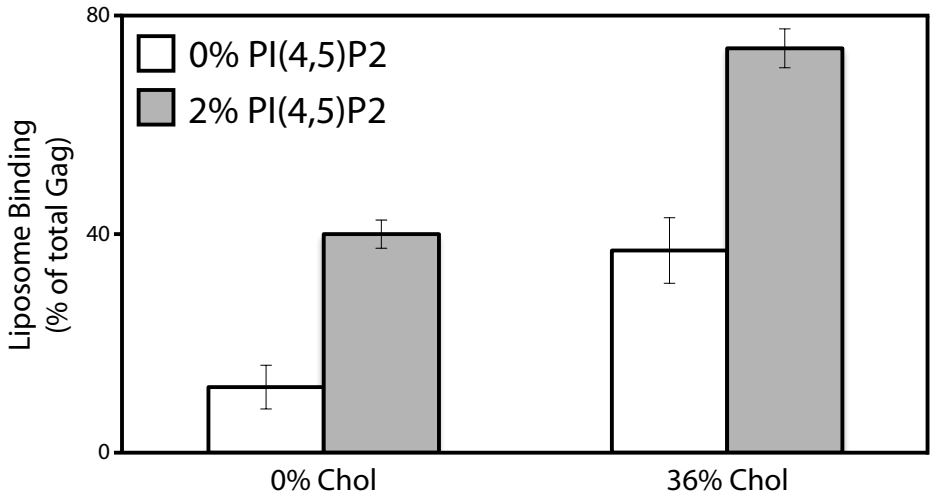

Fig. 3.6 Cholesterol enhancement of HIV-1 Gag binding to membranes containing PI(4,5)P2. Gag protein was synthesized and analyzed by flotation as in Fig. 1. White bars, binding to liposomes containing 0 or 36% cholesterol (data taken from Fig. 4). Grey bars, binding to liposomes with 2% PC being substituted with 2% PI(4,5)P2. The data represent the average of no less than three flotations with error bars representing the standard deviations.

be complex, they may be central to understanding the membrane specificity of viral budding.

ACKNOWLEDGEMENTS

We thank the National Biomedical Center for Advanced ESR Technology at Cornell University and Boris Dzikovski for help in ESR data collection and analysis. We also thank Christina Wang and Susan Duan for helpful discussions. This work was supported by USPHS grant CA20081 to VMV and NSF grant MCB 0842839 to GWF.

CHAPTER 3 REFERENCES

1. Saad J*, et al.* (2006) Structural basis for targeting HIV-1 Gag proteins to the plasma membrane for virus assembly. *Proc Natl Acad Sci U S A* 103(30):11364-11369.

2. Ono A, Ablan SD, Lockett SJ, Nagashima K, & Freed EO (2004) Phosphatidylinositol (4,5) bisphosphate regulates HIV-1 Gag targeting to the plasma membrane. *Proc Natl Acad Sci U S A* 101(41):14889-14894.

3. Chan R*, et al.* (2008) Retroviruses human immunodeficiency virus and murine leukemia virus are enriched in phosphoinositides. *J Virol* 82(22):11228-11238.

4. Dalton AK, Ako-Adjei D, Murray PS, Murray D, & Vogt VM (2007) Electrostatic interactions drive membrane association of the human immunodeficiency virus type 1 Gag MA domain. *J Virol* 81(12):6434-6445.

5. Chukkapalli V, Hogue IB, Boyko V, Hu WS, & Ono A (2008) Interaction between the human immunodeficiency virus type 1 Gag matrix domain and phosphatidylinositol-(4,5)-bisphosphate is essential for efficient gag membrane binding. *J Virol* 82(5):2405-2417.

6. Chan J, Dick RA, & Vogt VM (2011) Rous sarcoma virus gag has no specific requirement for phosphatidylinositol-(4,5)-bisphosphate for plasma membrane association in vivo or for liposome interaction in vitro. *J Virol* 85(20):10851-10860.

7. Waheed AA & Freed EO (2009) Lipids and membrane microdomains in HIV-1 replication. *Virus Res* 143(2):162-176.

8. Ott DE (2008) Cellular proteins detected in HIV-1. *Rev Med Virol* 18(3):159-175 .

9. Aloia RC, Tian H, & Jensen FC (1993) Lipid composition and fluidity of the human immunodeficiency virus envelope and host cell plasma membranes. *Proc Natl Acad Sci U S A* 90(11):5181-5185 .

10. Brugger B*, et al.* (2006) The HIV lipidome: a raft with an unusual composition. *Proc Natl Acad Sci U S A* 103(8):2641-2646 .

11. Pessin JE & Glaser M (1980) Budding of Rous sarcoma virus and vesicular stomatitis virus from localized lipid regions in the plasma membrane of chicken embryo fibroblasts. *J Biol Chem* 255(19):9044-9050 .

12. Quigley JP, Rifkin DB, & Reich E (1971) Phospholipid composition of Rous sarcoma virus, host cell membranes and other enveloped RNA viruses. *Virology* 46(1):106-116 .

13. Nitta T, Kuznetsov Y, McPherson A, & Fan H (Murine leukemia virus glycosylated Gag (gPr80gag) facilitates interferon-sensitive virus release through lipid rafts. *Proc Natl Acad Sci U S A* 107(3):1190-1195 .

14. Zheng YH, Plemenitas A, Fielding CJ, & Peterlin BM (2003) Nef increases the synthesis of and transports cholesterol to lipid rafts and HIV-1 progeny virions. *Proc Natl Acad Sci U S A* 100(14):8460-8465 .

15. Ono A, Waheed AA, & Freed EO (2007) Depletion of cellular cholesterol inhibits membrane binding and higher-order multimerization of human immunodeficiency virus type 1 Gag. *Virology* 360(1):27-35 .

16. Hogue IB, Grover JR, Soheilian F, Nagashima K, & Ono A (2011) Gag induces the coalescence of clustered lipid rafts and tetraspanin-enriched microdomains at HIV-1 assembly sites on the plasma membrane. *J Virol* 85(19):9749-9766 .

17. van Meer G, Voelker DR, & Feigenson GW (2008) Membrane lipids: where they are and how they behave. *Nat Rev Mol Cell Biol* 9(2):112-124 .

18. Wang TY & Silvius JR (2001) Cholesterol does not induce segregation of liquid-ordered domains in bilayers modeling the inner leaflet of the plasma membrane. *Biophys J* 81(5):2762-2773 .

19. Heberle FA, Wu J, Goh SL, Petruzielo RS, & Feigenson GW (2010) Comparison of three ternary lipid bilayer mixtures: FRET and ESR reveal nanodomains. *Biophys J* 99(10):3309-3318 .

20. Dalton A, Murray P, Murray D, & Vogt V (2005) Biochemical characterization of rous sarcoma virus MA protein interaction with membranes. *J Virol* 79(10):6227-6238 .

21. Alfadhli A, Still A, & Barklis E (2009) Analysis of human immunodeficiency virus type 1 matrix binding to membranes and nucleic acids. *J Virol* 83(23):12196-12203 .

22. Winiski AP, McLaughlin AC, McDaniel RV, Eisenberg M, & McLaughlin S (1986) An experimental test of the discreteness-of-charge effect in positive and negative lipid bilayers. *Biochemistry* 25(25):8206-8214 .

23. Huang J, Buboltz, J., Feigenson, G. (1999) Maximum solubility of cholesterol in phosphatidylcholine and phosphatidylethanolamine bilayers. *Biochimica et Biophysica Acta* 1417:89-100.

24. Huang J & Feigenson GW (1999) A microscopic interaction model of maximum solubility of cholesterol in lipid bilayers. *Biophys J* 76(4):2142-2157 .

25. Tang C*, et al.* (2004) Entropic switch regulates myristate exposure in the HIV-1 matrix protein. *Proc Natl Acad Sci U S A* 101(2):517-522 .

26. Buboltz JT & Feigenson GW (1999) A novel strategy for the preparation of liposomes: rapid solvent exchange. *Biochim Biophys Acta* 1417(2):232-245 .

27. Zhao J*, et al.* (2007) Phase studies of model biomembranes: complex behavior of DSPC/DOPC/cholesterol. *Biochim Biophys Acta* 1768(11):2764-2776 .

28. Kingsley PB, Feigenson, G.W. (1979) The synthesis of a predeuterated phospholipid: 1,2-dimyristoyl-sn-glycero-3-phosphocholine-d72. *Chemistry and Physics of Lipids* 24:135-147.

29. Schorn K, Marsh, D. (1997) Extracting order parameters from poder EPR lineshapes for spin-labelled lipids in membranes. *Spectrochimica Acta Part A-Molecular and Biomolecular Spectroscopy* 53(12):2235-2240.

CHAPTER 4

[3]EFFECT OF MULTIMERIZATION ON MEMBRANE ASSOCIATION OF ROUS SARCOMA VIRUS AND HIV-1 MA PROTEINS[3]

In most retroviruses, plasma membrane (PM) association of the Gag structural protein is a critical step in viral assembly, relying in part on interaction between the highly basic Gag MA domain and the negatively charged inner leaflet of the PM. Assembly is thought to begin with Gag dimerization followed by multimerization, resulting in a hexameric lattice. To directly address the role of multimerization in membrane binding, we fused the MA domains of Rous sarcoma virus (RSV) and HIV-1 to the chemically inducible dimerization domain FKBP, or to the hexameric protein CcmK4 from cyanobacteria. The cellular localization of the resulting GFP-tagged chimeric proteins was examined by fluorescence imaging, and the association of the proteins with liposomes was quantified by flotation in sucrose gradients, following synthesis in a reticulocyte extract or as purified proteins. Four lipid compositions were tested, representative of liposomes commonly reported in flotation experiments. By themselves GFP-tagged RSV and HIV-1 MA proteins were largely cytoplasmic, but both hexamerized proteins were highly concentrated at the PM. Dimerization led to partial

---

[3] The following section is reproduced from: Dick, R. A., Kamynina, E., V. M. Vogt. 2013. Effect of multimerization on membrane association of Rous sarcoma virus and HIV-1 MA proteins. (Submitted to J Virol), with modifications to conform to the required format. R.A.D. performed liposome flotation, protein purification, and part of the imaging. E.K. performed part of the imaging.

PM localization for HIV-1 MA. These in vivo effects of multimerization were recapitulated in vitro. In flotation analyses, the intact RSV and HIV-1 Gag proteins were more similar to multimerized MA than to monomeric MA. RNA is reported to compete with acidic liposomes for HIV-1 Gag binding, and thus we also examined the effects of RNase treatment or tRNA addition on flotation. tRNA competed with liposomes in the case of some but not all lipid compositions and ionic strengths. Taken together, our results further underpin the model that multimerization is critical for PM association of retroviral Gag proteins.

INTRODUCTION

Particle assembly and budding are critical steps in the retrovirus life cycle. For most retroviruses the structural protein, Gag, assembles into a budding virus particle on the inner leaflet of the cellular plasma membrane (PM). The matrix domain (MA) at the N-terminus of Gag mediates the PM interaction. Retroviral MAs contain as many as three membrane binding signals that provide membrane interactions as well as specificity. First, all contain a highly basic region that interacts electrostatically with the negatively charged inner leaflet of the PM (55). The inner leaflet of the PM derives its net negative charge from phosphatidylserine (PS) and to a lesser extent phosphatidylinositols (PIPs) (83). Second, most retroviral MAs are myristoylated, a modification that is required for membrane interaction (71). However, the Gag proteins of some retroviruses, such as Rous sarcoma virus (RSV) and equine infectious anemia virus (EIAV), are not myristoylated.

Third, at least some retroviral MAs have phosphatidylinositol (4,5) bisphosphate (PI(4,5)P2) binding pockets. Examples include human immunodeficiency virus type-1 and type-2 (HIV-1, HIV-2), Mason-Pfizer monkey virus (MPMV), and EIAV. Other viruses, RSV, murine leukemia virus (MLV), and human T-lymphotropic virus (HTLV) apparently do not (31, 66, 73, 74). In vivo, HIV-1 and MLV are sensitive to phosphatidylinositol-4,5-bisphosphate (PI(4,5)P2) depletion mediated by 5PtaseIV, in that plasma membrane localization and viral particle release are decreased (13, 15, 39, 41, 58). HTLV and EIAV are less sensitive to PI(4,5)P2 depletion (31, 41). However, EIAV virus-like particle (VLP) release is decreased by expression of synaptojanin 2, a phosphatase with broad specificity (31). *In vivo*, RSV does not respond to 5PtaseIV depletion under conditions that HIV-1 does (13), but under different conditions RSV Gag also is sensitive to 5PtaseIV (56).

In contrast with some *in vivo* results, in liposome binding assays *in vitro* most or all retroviral Gag proteins bind more tightly to membranes in the presence of PI(4,5)P2 as well as other PIPs (13, 16, 18, 27, 39). In such assays it is challenging to ascertain to what degree PIP-enhanced binding is due to electrostatic interactions, and to what degree it is due to specific recognition of the PIP head group. In solution with short chain versions of PI(4,5)P2, HIV-1 MA interacts not only with the phosphorylated inositol head group but also with the 2' acyl chain (74). This observation led to a model for HIV-1 MA and Gag *in vivo*, in which the typically unsaturated, long 2' acyl chain "flips out" of the hydrophobic core of the lipid bilayer and binds instead to a hydrophobic groove in MA (34, 74). Similar observations recently have been reported for short chain versions

of the abundant inner leaflet phospholipids PS and phosphatidylcholine (PC) (84). Recently we demonstrated that HIV-1 Gag binding to liposomes is strongly modulated by membrane cholesterol content and by degree of acyl chain unsaturation, implying that the protein can somehow sense the hydrophobic environment of the membrane (27).

Assembly of the virus particle is driven by Gag-Gag interactions, ultimately resulting in the formation of an incomplete hexameric lattice in the immature virus particle just before its release from the cell (5, 85). Gag multimerization primarily is dependent on interactions of the capsid (CA) portion of Gag, plus short immediately adjoining N-terminal and C-terminal sequences (26, 45, 48, 64). The CA-CA contacts that hold the immature Gag lattice together have not been elucidated at a molecular level, although an 8A model recently has been suggested based on electron cryo-tomographic reconstructions of the MPMV lattice (3). It is unknown if Gag hexamers form in the cytoplasm and are an intermediate in assembly, or alternatively if the hexameric lattice grows by addition of monomers or dimers.

Gag dimers are inferred to be a critical building block of the Gag lattice, as evidenced by diverse studies. For example*, in vitro* assembly requires a nucleic acid (such as a DNA oligonucleotide) that is long enough to bind to two NC domains, or about 16 nt in the case of RSV (53, 54, 86). The function of NC can be replaced by a coiled coil domain that forms dimers (leucine zipper) (1, 2, 19, 42, 87), and in some cases disulfide-mediated crosslinking near the Gag C-terminus also can replace NC (2).

While the role of Gag multimerization in particle assembly has been studied extensively, little is known about how multimerization affects Gag membrane binding. While MA is dispensable for assembly of particles *in vitro* (10-12, 37), *in vivo* assembly of Gag at the PM requires a membrane binding domain--either its own MA or part of it (16, 63), or the MA from another retrovirus (14, 41, 62, 69), or a membrane binding domain from a cellular protein (13, 43, 82). In an extreme example, a deletion of Gag MA that removed the entire highly basic region (HBR) including the PI(4,5)P2 binding pocket, but left the N-terminal myristoylation site, only modestly reduced the number of released extracellular particles (4, 70). By contrast, a Gag mutation that prevented myristoylation abrogated membrane binding and VLP release, although some particles were assembled in the cytoplasm (57). In summary, while a membrane binding domain is not required for Gag assembly it is required for targeted assembly at the PM of cells.

Both RSV and HIV-1 Gag MA domains can interact with RNA (38, 40, 52, 61, 67, 68, 80). At least in HIV-1, MA-RNA interaction can regulate membrane binding (18). In this example, the RNA binding appeared not to be dependent on the overall electrostatic charge of MA, but instead on two lysine residues located near the PI(4,5)P2 binding pocket. When these two amino acids were mutated, MA membrane binding became promiscuous, resulting in an increase in particle release *in vivo* (18). RSV MA binds RNA much more weakly than does HIV-1 MA (K. Musier-Forsyth, personal communication), and hence any role that RNA may play in Gag membrane binding in vivo may not be common to all retroviruses.

Little is known about the interplay between Gag-membrane interaction and Gag-Gag interactions. Previously we showed that dimerization of RSV MA and HIV-1 MA increases membrane binding by an order of magnitude (20, 21). We have now expanded on this observation with *in vivo* and *in vitro* assays of MA proteins that were engineered to be monomeric, dimeric, or hexameric. We have also investigated the effect RNA has on the binding of RSV and HIV-1 Gag to membranes *in vitro*. Overall, the results show that while MA dimerization is sufficient to increase membrane binding under some conditions, the increase is most dramatic upon MA hexamerization.

MATERIALS AND METHODS

DNA vectors

The MA multimers used in this study are shown schematically in Fig. 4.1. All DNA constructs were cloned using common subcloning techniques and were propagated in DH5a cells. RSV and HIV-1 MA were PCR amplified and ligated at an AatII restriction site (added with primers) to either FKBP (Clontech) or Ccmk4 with a DVGSGS or DVTRPEL linker, respectively. The Ccmk4 plasmid was a gift from Owen Pornillos (65). RSV and HIV-1 MA–FKBP and MA–Ccmk4 fusion proteins were PCR amplified and cloned into pET3x for reticulocyte expression using sites NdeI and KpnI (in the backbone of the vector and added to the MA chimeras by PCR). The same chimeras were fluorescently tagged by cloning into pEGFP-N1 (Clontech) using sites EcoRI and AgeI (in the backbone of the vector and added to the insert by PCR). RSV MA and super M-MA (SM-MA) were cloned into pET3x and pEGFP in the same way. The

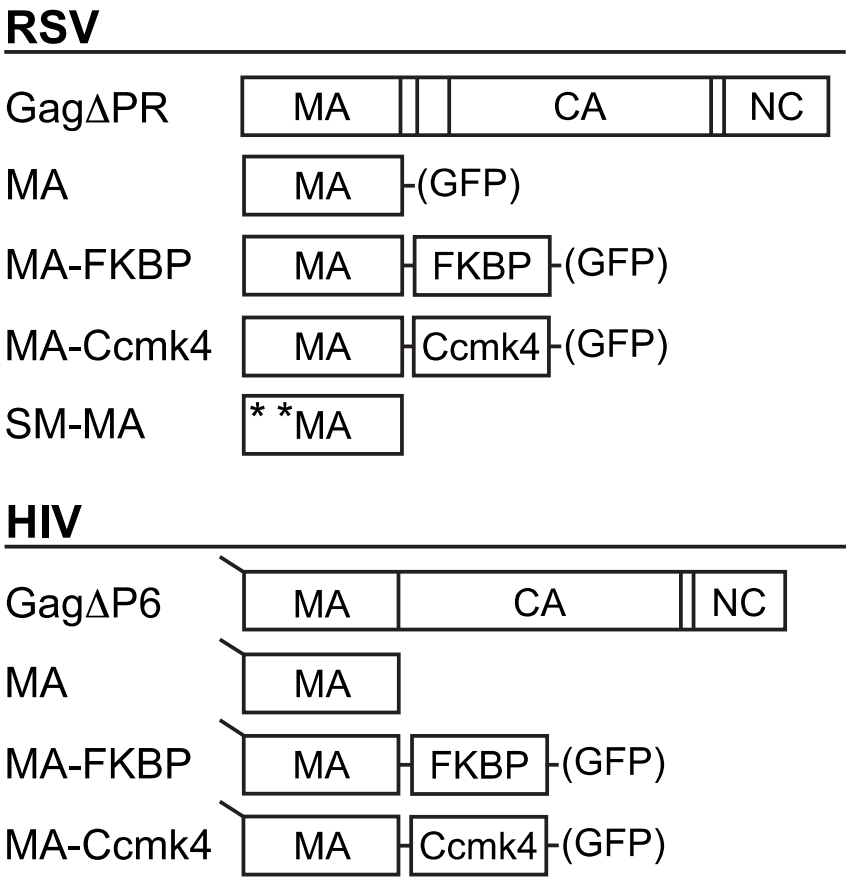

Fig. 4.1 Schematic representations of proteins. RSV and HIV-1 proteins (top and bottom) used in liposome flotation assays. GFP-tagged versions of the proteins expressed in transfected cells are denoted by GFP in parenthesis. All HIV-1 proteins used were myristoylated, as denoted by the line at the N-terminus. The mutations E25K and E70K of Super-M (SM) RSV MA are shown by an asterisk.

plasmid expressing HIV-1 MA (myr-MA) was previously described (21, 81). RSV GagΔPR and HIV-1 GagΔP6 (henceforth referred to as RSV Gag and HIV-1 Gag) were previously described in (13). Super M Gag was a gift from John Wills (9).

Cells, transfection, and imaging

Cell cultures and transfections were performed as previously described (13, 21). QTC (quail) fibroblasts were maintained in Dulbecco modified Eagle medium supplemented with 5% fetal bovine serum, 5% NuSerum (BD Biosciences), 1% heat-inactivated chick serum, standard vitamins, L-glutamine, penicillin, and streptomycin. In brief, QT6 cells were seeded onto glass coverslips 24 h prior to transfection. At 50% confluence cells were transfected with 1ug of DNA per mL of medium with FuGENE HD (Roche) according to the manufacturer's instructions. For cells expressing MA-FKBP-GFP, medium was replaced 16-18 h post transfection with medium with (dimer) or without (monomer) 100 nM homodimerization reagent AP20187 (BB) (Clontech).

Cells were imaged as previously described (13). Briefly, at 20-24 h post transfection cells were fixed with 3.7% formaldehyde in PBS for 15 min and mounted on glass slides with Fluoro-Gel (Electron Microscopy Sciences). Slides were viewed on an Ultraview spinning disc confocal microscope (Perkin-Elmer) with a Nikon 100x Plan-Apochromat oil objective lens. Image analysis was performed using ImageJ software (v1.40g). The strength of fluorescence at the plasma membrane and the cytoplasm was measured at two or three representative locations for each cell using the plot profile function. Cells with low and high expression levels were included. Background was

subtracted and the ratio of plasma membrane to cytoplasmic signal was quantified. Outliers were identified and removed using the *Q* test.

Liposome binding and velocity sedimentation

Large unilamellar vesicles (LUVs) were prepared by the rapid solvent exchange (RSE) method as previously described (6, 27, 88). Briefly, lipids in chloroform were mixed in glass tubes at the stated molar ratios. Excess chloroform was removed by evaporation under a stream of nitrogen to a final approximate volume of 50 uL. Buffer (20 mM HEPES, pH 7.0) was added and the mixture was vortexed under vacuum for 90 seconds and sealed under argon gas, resulting in a final hydrated lipid mixture at 10mg/mL. LUVs were prepared by extruding the lipid mixture at least 41 times through a 100 nm polycarbonate filter (Avanti) on a mini-extruder block heated to 45 °C. LUVs were used within 10 days of preparation.

LUV binding was performed as previously described (13, 15, 20, 21, 27). Briefly, radioactively labeled protein was prepared by translation in the TNT coupled T7 rabbit reticulocyte reaction (Promega) in the presence of [35S]methionine/cysteine (Perkin-Elmer; ExPRE35S35 protein labeling mix). Five uL of reticulocyte reaction was combined with 15 uL binding buffer (20mM HEPES pH 7.0) and 50 ug LUVs (to a concentration of 8.5 mg/mL). The reaction mix was incubated for 10 minutes at 22 °C. The reaction mix was than combined with 75 uL 67% sucrose (20mM HEPES pH 7.0). Next, 80 uL of the resulting sucrose and reaction mix was placed in a TLA-100 tube followed by 120 uL 40% sucrose and 40 uL 4% sucrose. All sucrose was made wt/wt with binding buffer. Centrifugation was performed at 90,000 rpm in a TLA-100 rotor

(Beckman) for one hour. Purified protein flotations were performed with 10 ug of protein in place of the reticulocyte reaction. The binding buffer and sucrose were supplemented with NaCl to a final concentration of 50 mM or 150 mM.

Velocity sedimentation was performed with an eight-step sucrose gradient (20 mM Tris pH 8.0 and 150 mM NaCl), 10-30% (wt/wt), overlaid with approximately 50 ug purified protein in storage buffer (20mM Tris pH 8.0, 150-350mM NaCl, 30% glycerol, 10mM DTT). Gradients were centrifuged in a SW-60 (Beckman) rotor at 45,000 rpm for 20 h. Fourteen, 270 uL fractions were taken and 40 uL of each was subjected to SDS-PAGE on a 17.5% SDS gel. Gels were Coomassie stained for 16 h, destained, and imaged.

Protein purification

Proteins were purified as previously described (20, 21, 27) with some modifications. Briefly, BL21 cultures were grown to an OD600 of 0.4, IPTG was added to a final concentration of 0.5 mM, and cells were collected 4 h later. Pelleted cells were resuspended in lysis buffer (20 mM TrisHCl pH 8.0, 500 mM NaCl, 10 mM DTT, protease inhibitor (Roche, Complete Mini tablet)), lysed by sonication, and cleared by centrifugation in a TLA-110 (Beckman) rotor at 90K for 45 min. Polyethylenimine (PEI) was added to a final concentration of 0.3% to precipitate nucleic acid, which was spun down and removed. Ammonium sulfate was added to 30% saturation to precipitate the protein, followed by centrifugation. The pellet was resuspended in binding buffer (20 mM Tris pH 8.0, 100 mM NaCl, 10 mM DTT). The protein was further purified by cation exchange chromatography (HiTrap SP, Amersham Pharmacia). All purified proteins

were concentrated to 2-5 mg/mL (Millipore, Ultracel -10K), aliquoted, and stored at -80 °C in storage buffer (10-20mM Tris pH 8.0, 150-330 mM NaCl, 10mM DTT, 30% Glycerol). HIV-1 MA (myr-MA) was purified as described (21, 27, 81). BL21 cultures were supplemented with myristic acid (10 mg/L, Sigma) 1 h before induction with IPTG. The MA protein was purified from the supernatant by Ni-NTA resin (Qiagen) followed by cation exchange chromatography (HiTrap SP, Amersham Pharmacia). Mass spectrometry confirmed that the protein was myristoylated.

RESULTS

We examined the effect of MA dimerization and hexamerization on membrane interaction *in vivo* and *vitro*. Chimeric MA proteins that can be induced to dimerize were created by fusion of MA with the FK506-binding protein (FKBP) (44, 72, 76) (Fig. 4.1). Similarly, hexameric MAs were created by fusion with the cyanobacterial carboxysome shell protein Ccmk4 (46, 65). The chimeras were designed so that the MA moieties are oriented with their membrane-binding domains all facing in the same direction, similar to their arrangement in the Gag lattice. For *in vivo* visualization, the chimeras were further fused to GFP (Fig. 4.1). MA dimers and hexamers were compared with MA monomers and with full length Gag in a standard liposome (also referred to as large unilamellar vesicle, LUV) flotation assay, using radiolabeled proteins generated in a reticulocyte extract, or in some cases using purified proteins.

Effect of MA dimerization and hexamerization on sub-cellular localization

Reports of HIV-1 MA cellular localization vary from cytoplasmic (21, 28, 59, 60) to partially membrane associated (77, 89), while fluorescence of RSV MA-GFP is cytoplasmic and nuclear (75) owing to a nuclear localization signal (NLS) in the latter (7, 75). To determine the effect of dimerization on cellular localization of MA, we treated transfected cells expressing chimeric MA proteins with the dimerization chemical AP20187 (here referred to as BB). The amount of BB required to induce a change in MA-FKBP localization was determined empirically in a series of concentration tests (data not shown).

The fluorescence from RSV MA-GFP and MA-FKBP-GFP monomers (-BB) were cytoplasmic and nuclear, as expected (Fig. 4.2A) (75). Inducing dimerization (+BB) did not significantly affect this result. By contrast, the RSV MA-Ccmk4-GFP hexamer was strongly concentrated at the PM, with little fluorescence elsewhere in the cell. To provide a graphical representation of the images, we used the ImageJ plot profile function to count pixel intensity, which is correlated with the fluorescence signal, at the plasma membrane and in the cytoplasm for each chimera tested. Over thirty cells were analyzed for each chimera, with at least two measurements per cell. Ratios of the average fluorescence intensity at the PM and cytoplasm showed that for the RSV MA chimeras, hexamerization increased PM localization by approximately five-fold over the monomers and dimers (Fig. 4.2B).

For HIV-1, monomeric MA-FKBP-GFP was cytoplasmic while the dimerized MA-FKBP-GFP (+BB) was enriched somewhat at the PM. Similar to RSV MA-Ccmk4-GFP,

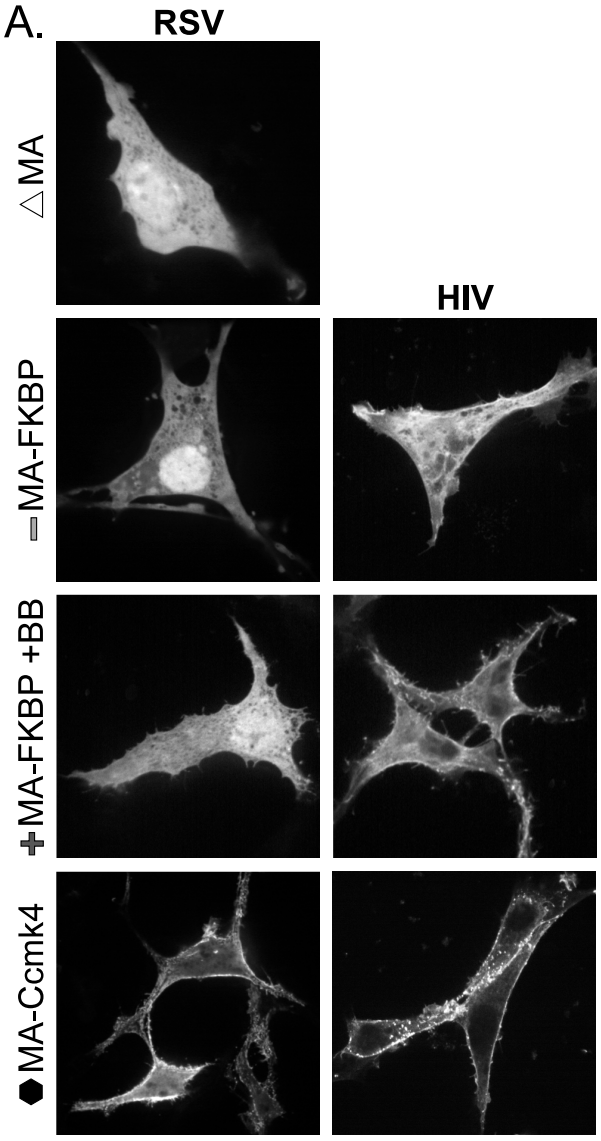
A.
RSV
HIV
△MA
▯MA-FKBP
✚MA-FKBP +BB
⬢MA-Ccmk4
B.
Ratio of Plasma Membrane to Cytoplasm
8
4
0
*
*
*
△
▯
✚
⬢
RSV
HIV

Fig. 4.2 Effect of multimerization on RSV and HIV-1 MA-GFP localization. (A) QT6 cells were transfected with DNAs for either RSV (left) or HIV-1 (right) GFP-tagged MA multimers. MA or MA chimeras are indicated on far left as MA (monomer, triangle), MA-FKBP (monomer, minus), MA-FKBP +BB (dimerized, plus), and MA-Ccmk4 (hexamer, hexagon). Images are of a single confocal section near the mid-body of cells. Images are representative for each protein (n>25). (B) Ratio of plasma membrane to cytoplasmic fluorescent signal. For each cell at least two measurements of signal intensity, at representative locations, were taken as described in Materials and Methods, for a total of at least 50 measurements per protein. *P* values were determined using Student's *t* test for comparisons denoted by horizontal line above two bars. Asterisk indicates $P<0.001$.

the HIV-1 MA-Ccmk4-GFP hexamer was very strongly concentrated at the PM (Fig. 4.2A, B). These results for both viruses suggest that for the full length Gag protein, stable binding to the PM most likely requires multimerization. For HIV-1, dimerization may be sufficient to drive Gag to the PM but for RSV dimerization is not sufficient.

To investigate the possible cell-type specificity of the effects of hexamerization, both RSV and HIV-1 MA-Ccmk4-GFP localization were tested in 293T cells, yielding the same results as observed in QT6 cells (data not shown). As a further control to rule out the possibility that Ccmk4 itself might interact with membranes, we visualized the localization of Ccmk4-GFP. The fluorescence was diffuse and cytoplasmic (data not shown).

Effect of MA dimerization and hexamerization on liposome interaction

We previously reported that dimerization of purified RSV and HIV-1 MA results in an increase in LUV association across a range of lipid concentrations (20, 21). In those studies dimerization was achieved by fusing the MA domain to either a monomeric (mutant W184A/M185A, (35) or a dimeric (Q192A, (25)) version of the HIV-1 CA C-terminal domain (CA_{CTD}). In transfected cells, the GFP-tagged HIV-1 $MACA_{CTD(Q192A)}$ was somewhat concentrated at the PM in 293T cells (21), while the similarly constructed RSV dimer was largely cytoplasmic in avian DF-1 cells (unpublished results), fully consistent with the present results based on FKBP chimera. We re-tested both of the CA_{CTD} chimeras in 293T cells and again observed similar localization. However, when these monomeric and dimeric proteins were translated *in vitro* in a rabbit reticulocyte system and subjected to liposome flotation, the proteins did not behave as reported

previously for the purified proteins. Little difference in flotation between monomeric and dimeric MAs was observed, both for RSV $MACA_{CTD}$ and HIV-1 $MACA_{CTD}$ (data not shown). By comparison with other proteins, we infer that the reticulocyte-generated $MACA_{CTD(W184A/M185A)}$ monomers behave like dimers. Apparently some component in the reticulocyte system affects dimerization or membrane binding for these chimeric proteins.

To address this discrepancy, we employed an independent approach to study the effect of MA dimerization, based on the chemically inducible dimerization domain FKBP (44, 79). When RSV MA by itself and monomeric RSV MA-FKBP were compared, similar flotation results were obtained for all LUV types tested, implying that in this assay MA and MA-FKBP in the absence of BB are functionally equivalent. Similar to the approach used in vivo, a series of flotations was carried out to find the optimal homodimerization reagent concentration to elicit dimerization of MA-FKBP, as measured by augmented liposome flotation (data not shown). BB-induced dimerization led to a two- to three-fold increase in flotation of RSV MA-FKBP (Fig. 4.3A, B), and up to a two-fold increase for HIV-1 MA-FKBP (Fig. 4.3A, C). For the hexamerized MA-CcmK4 chimeras, association with liposomes was three- to five-fold higher than for the monomeric protein for RSV, and about two-fold higher for HIV-1. In summary, though differing in detail, LUV binding of these chimeric monomeric, dimeric, and hexameric MA species to four types of LUVs followed the same trends as observed in cells.

We also compared flotation of full-length RSV and HIV-1 Gag proteins with flotation of the chimeric MA species. Previous work by us and by others had shown that

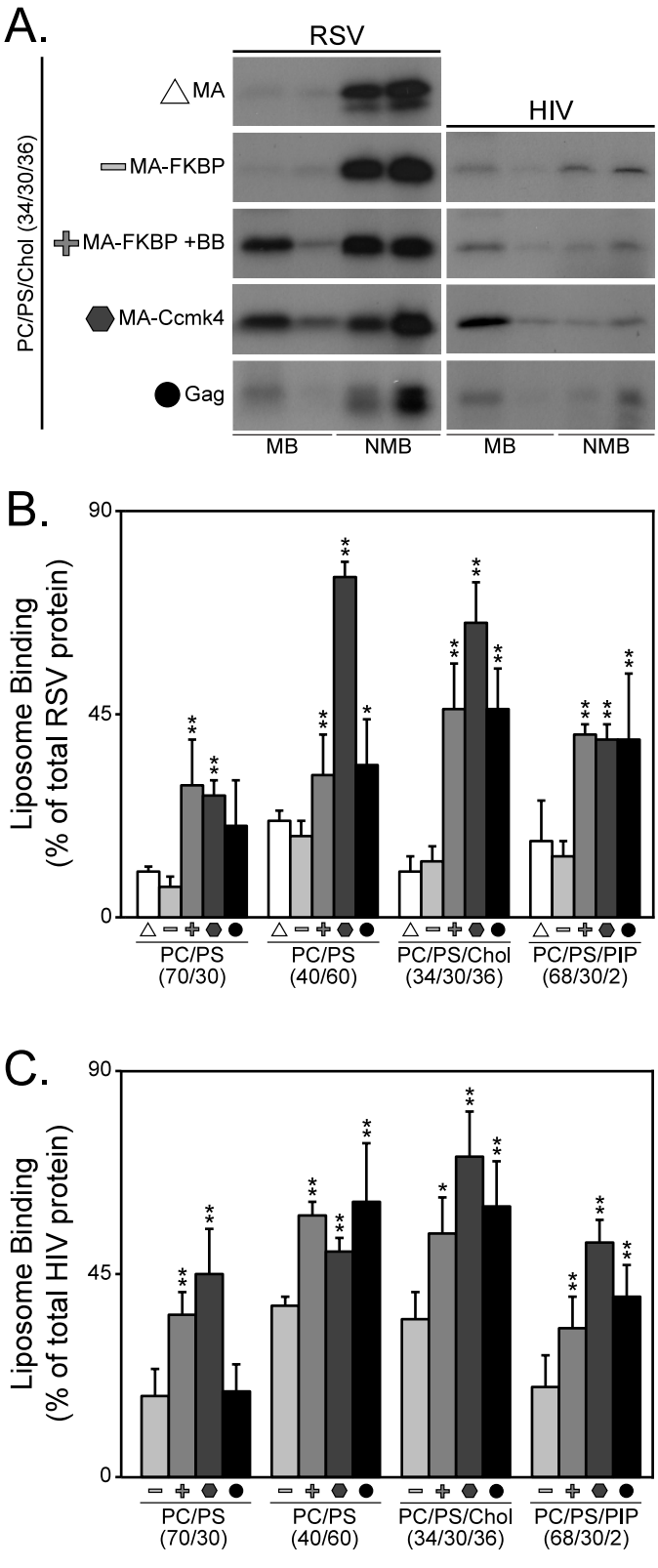
A.
RSV
HIV
MA
MA-FKBP
MA-FKBP +BB
MA-Ccmk4
Gag
PC/PS/Chol (34/30/36)
MB
NMB
MB
NMB
B.
Liposome Binding
(% of total RSV protein)
90
45
0
PC/PS
(70/30)
PC/PS
(40/60)
PC/PS/Chol
(34/30/36)
PC/PS/PIP
(68/30/2)
C.
Liposome Binding
(% of total HIV protein)
90
45
0
PC/PS
(70/30)
PC/PS
(40/60)
PC/PS/Chol
(34/30/36)
PC/PS/PIP
(68/30/2)

Fig. 4.3 Flotation analysis of RSV and HIV-1 MA multimers. Liposomes were made with the following compositions PC/PS (70/30), PC/PS (40/60), PC/PS/Chol (34/30/36), or PC/PS/PI(4,5)P2 (68/30/2). All proteins were radiolabeled in reticulocyte translation reactions. (A) Representative flotation results of MA multimers to PC/PS/Chol liposomes. Symbols denoting multimeric state, the same as Fig. 2. The radioactive protein was scored either as membrane-bound (MB) or non membrane-bound (NMB). (B and C) Percent of total protein found associated with liposomes for both RSV and HIV-1 MA multimers. Error bars represent standard deviations from the mean. *P* values for Student's *t* test for comparison of MA-FKBP monomer to MA-FKBP dimer, MA-Ccmk4 hexamer, and Gag (*, $P<0.05$; **, $P<0.005$).

Gag binding to liposome membranes is augmented by high concentrations of PS, by cholesterol, and by low concentrations of PIPs (13, 16, 27). These findings were qualitatively recapitulated in the present study (Fig. 4.3). In comparisons of Gag with the different MA multimers, Gag behaved like the MA multimers, but with some variation. For example, flotation of HIV-1 Gag with LUVs made with low PS was consistently not higher than flotation of monomeric MA (Fig. 4.3C). Also, flotation of the RSV MA-FKBP monomer was not boosted by cholesterol or PIP2, and similarly flotation of the HIV-1 MA-FKBP monomer was not boosted by PIP2. To explain these results, we speculate that the observed high binding of Gag to LUVs with cholesterol or PIPs may reflect Gag multimerization. Expressed in another way, membranes that support strong binding of Gag may promote Gag multimerization.

Membrane association of purified MA multimers

To further investigate the effect of MA multimerization on membrane association, we purified RSV MA, RSV MA-FKBP, RSV MA-Ccmk4, and HIV-1 myr-MA after expression in *E. coli*. First, to confirm that these proteins were in their predicted multimeric state, sucrose gradient velocity sedimentation was performed. Each protein traveled to a fraction consistent with its predicted size, based on the assumption that the proteins are roughly globular (Fig. 4.4A). Second, the proteins were submitted to flotation analyses like those for radioactive proteins translated *in vitro*. The LUV binding was in agreement with that found for the reticulocyte-translated proteins. For example, the RSV MA-Ccmk4 hexamer associated with all liposome types significantly more than did the MA-FKBP monomer (Fig. 4.4B). Similarly, LUV association of the RSV MA

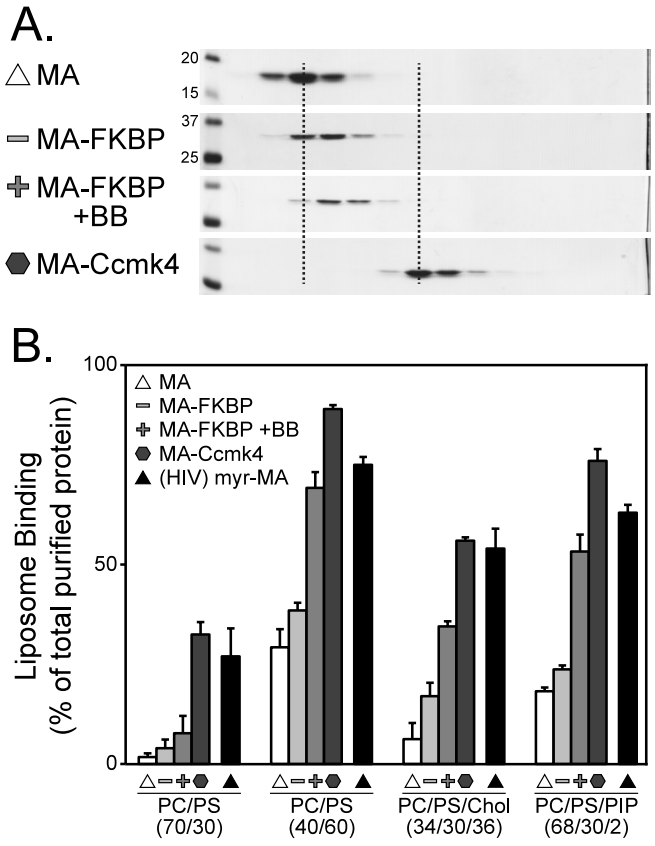

Fig. 4.4 Flotation analysis of purified RSV MA multimers. (A) Velocity sedimentation of RSV MA, MA-FKBP, MA-FKBP +BB, and MA-Ccmk4 proteins. A molecular weight marker is indicated for the MA and MA-FKBP gels; all other gels were run identically. Dotted lines are added to more easily show the shift of MA monomers to dimer and hexamer. (B) Percent of total protein found associated with four liposome types. Symbols indicate protein type, as in Fig. 2. All MA proteins are RSV except HIV-1 myr-MA, which is indicated by the black triangle. Error bars represent standard deviations from the mean.

monomer, dimer, and hexamer was strengthened by high PS, by cholesterol, and by PIP2, as found for the in vitro translated proteins. We conclude that the effects of multimerization and of membrane composition on membrane binding are not substantially altered by the vast excess of rabbit protein present in the in vitro translation mix.

Previously we reported that the relative binding constants of monomeric RSV $MACA_{ctd}$ and monomeric HIV-1 $MACA_{ctd}$ were of similar magnitude, and the same for the dimeric versions of these proteins (20, 21). In contrast, in the present study RSV MA and MA-FKBP on the one hand, and HIV-1 myr-MA on the other, showed significant differences in the flotation. Perhaps this discrepancy arises from the different salt concentrations used in the analyses, 75mM NaCl in the earlier work (20, 21) and 150mM NaCl here.

Effect of RNA on Gag and MA membrane interaction

RNase treatment of a reticulocyte extract in which HIV-1 Gag has been synthesized increases Gag binding to liposomes, suggesting that RNA competes for Gag-membrane interactions (18). To determine if this is a general principle of retroviral Gag- and MA-membrane interaction, we tested the effect of RNase on RSV MA monomer and RSV Gag, compared with HIV-1 MA-FKBP monomer and HIV-1 Gag. RNase treatment for RSV MA, MA-FKBP monomer, and Gag had little effect on membrane binding of these proteins. Enhanced binding was observed only for RSV MA monomers to LUVs with high levels of PS (Fig. 4.5A). By contrast, the LUV binding of HIV-1 MA-FKBP monomer and of HIV-1 Gag was augmented by RNase treatment (Fig.

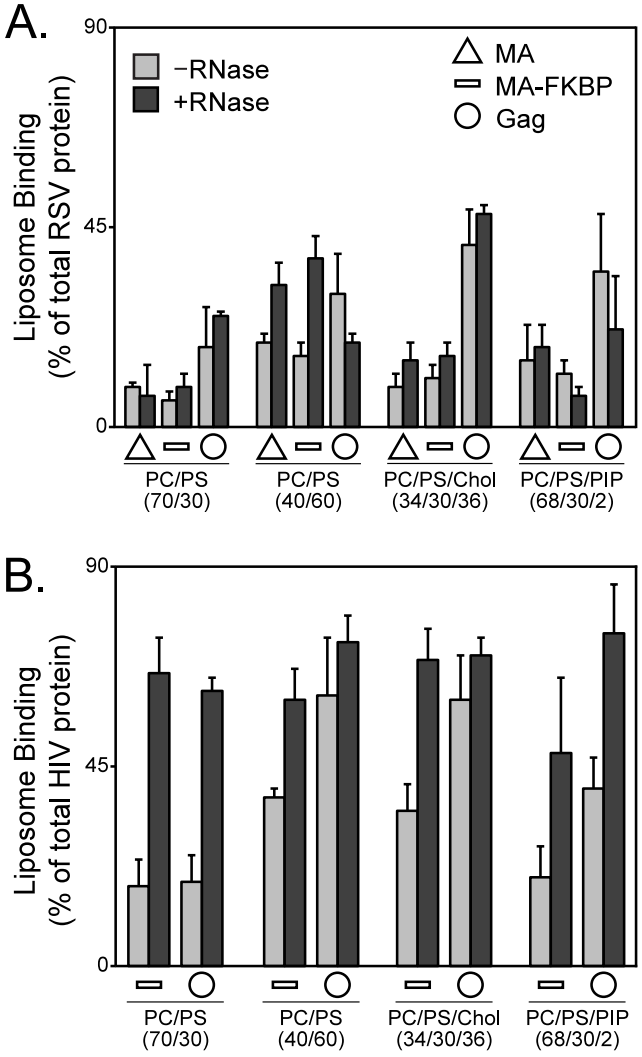

Fig. 4.5 Effect of RNA on liposome binding of reticulocyte-generated RSV MA or RSV Gag. (A, B) Liposome binding of RSV and HIV-1 MA (triangle, not done for HIV-1), MA-FKBP monomer (dash), and Gag (circle) protein to liposomes in the absence of (light gray) or presence of (dark gray) RNase. Error bars represent standard deviations from the mean.

4.5B), as reported previously (18, 41). At low PS, the flotation levels for the HIV-1 proteins increased by about three-fold. At high PS and with the addition of cholesterol, flotation of HIV-1 MA-FKBP monomer increased about two-fold, but of HIV-1 Gag increased only modestly. The small effect of RNase on HIV-1 Gag for these lipid mixtures might be explained by saturation of binding. In our hands, RNase also led to about a two-fold stimulation of flotation of HIV-1 MA-FKBP monomer and of HIV-1 Gag to PIP2-containing liposomes, in contrast to the results of Chukkapalli et al (18), who saw no increase in the presence of PIP2. This discrepancy might be grounded in differences in PIP concentrations. We used a more physiological 2% PIP2 compared with their 7%. In summary, these results suggest that at equivalent protein, salt, and lipid concentrations, RNA does not inhibit the LUV binding of RSV MA and Gag, while it does inhibit LUV binding of HIV-1 MA and Gag.

RSV MA has a net surface charge of plus three, while HIV-1 MA has net surface charge of plus six (55). We speculated that this difference might underlie the observed differences in RNase sensitivity. To explore this idea, we tested the binding of a mutant RSV MA called super-M (SM) to liposomes, with and without RNase treatment. SM-MA carries the two mutations E25K and E70K (8, 9), resulting in a net change in charge of plus four, leading to a total surface charge of plus seven. SM-Gag is known to bind more rapidly to the PM, and as a consequence to bypass trafficking into the nucleus (8, 9). SM-MA floated with LUVs approximately two-fold more extensively than did wt MA when the liposomes had low levels of PS or included cholesterol or included PIP2 (Fig. 4.6). Similar to what was observed for HIV-1 MA-FKBP, RNase increased the binding of

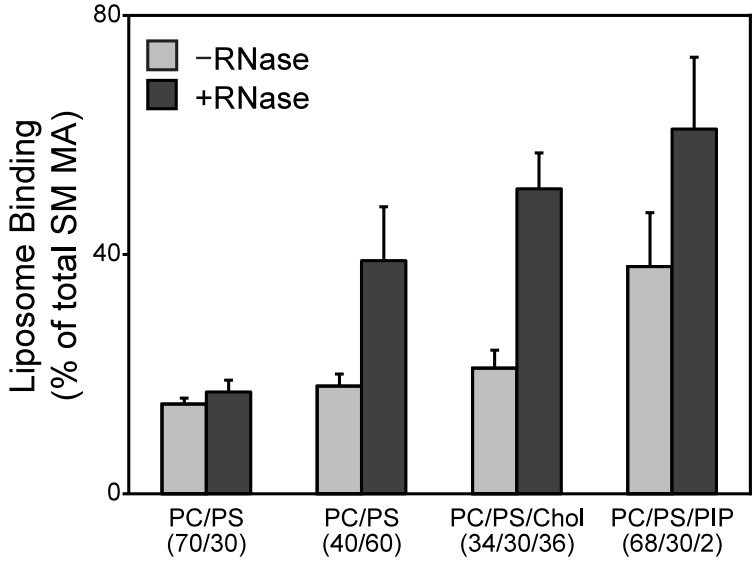

Fig. 4.6 Effect of RNase on Super-M MA. Liposome binding of RSV SM MA to liposomes without (light gray) or with (dark gray) RNase. Error bars represent standard deviations from the mean.

SM-MA to three of the four LUV types tested. From these results taken together, we conclude that in this experimental setting RNA plays less of a role in membrane interaction for wt RSV than for HIV-1, and that this difference is accounted for at least in part by surface charge density.

RNA - membrane competition with purified RSV MA and HIV-1 MA

Considering the basic nature of both RSV and HIV-1 MA, it seemed surprising that RNase treatment of the reticulocyte extract led to different results for the wt RSV and HIV-1 proteins. Therefore, we decided to test for RNA competition in another way, using flotation analysis of purified RSV MA and HIV-1 myr-MA proteins in the presence or absence of added purified tRNA. At 150mM NaCl little or no tRNA effect on flotation of either protein was observed (data not shown). But at 50 mM NaCl, consistent with flotations of RNase-treated reticulocyte translation reactions, addition of tRNA decreased the binding of HIV myr-MA to all LUVs tested (Fig. 4.7B). This decrease was greatest for membranes with low levels of PS. For RSV MA at this salt concentration, addition of tRNA also led to greatly reduced flotation for LUVs with low levels of PS. But unlike for HIV-1 myr-MA, for RSV MA the addition of tRNA did not significantly reduce binding to LUVs with PIP2. The effect of tRNA on protein binding to LUVs prepared with high levels of PS or cholesterol was modest for both HIV-1 and RSV MA. These results suggest that RSV MA binding to membranes with high PS, with cholesterol, or with 2% PIP2 is hardly perturbed by tRNA.

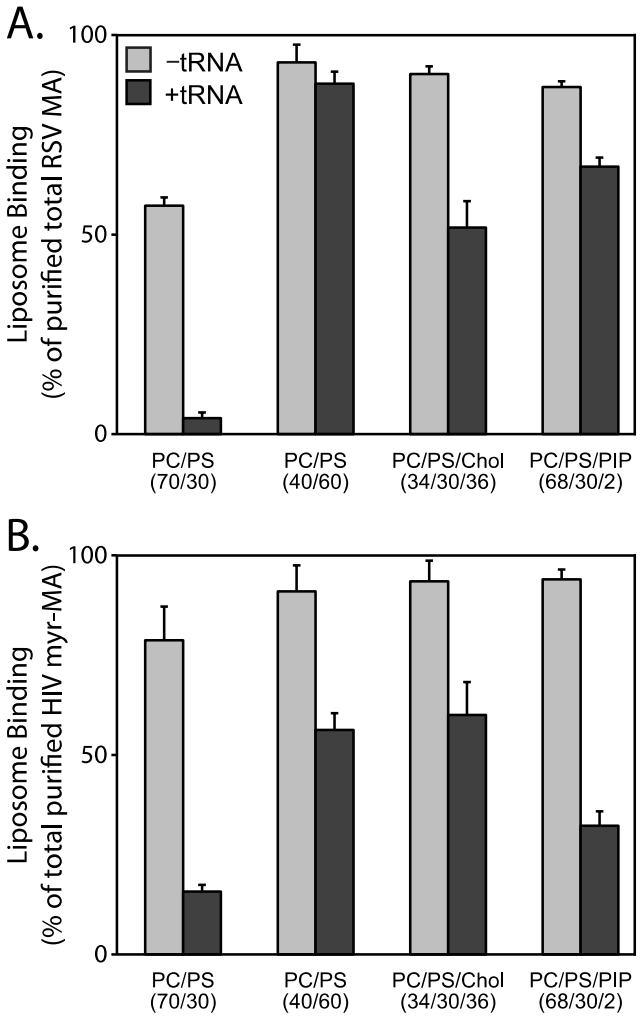

Fig. 4.7 RNA inhibition of purified RSV and HIV-1 MA proteins. (A, B) Liposome binding of purified RSV man and HIV-1 myr-MA proteins to liposomes in the absence (light gray) or presence (dark gray) of tRNA. Error bars represent standard deviations from the mean.

DISCUSSION

We have studied the effect of multimerization on the binding of RSV and HIV-1 MA to membranes *in vivo* and *vitro*. For HIV-1, dimerization of MA-GFP increased fluorescence at the PM, as reported previously (21), while hexamerization led to highly concentrated PM fluorescence. For RSV, dimerization of MA-GFP did not lead to significant PM localization, but hexamerization resulted in highly concentrated PM fluorescence, as for HIV-1. Liposome flotation analyses of MA multimers translated *in vitro* in a reticulocyte extract largely mirrored what was observed in transfected cells. For both viruses, binding of full length Gag protein to liposomes resembled binding by dimeric or hexameric MA. In their interactions with liposomes, RSV and HIV-1 MA proteins in the reticulocyte translation mixes differed in their response to RNase treatment. As had been shown previously for HIV-1 Gag (18), RNase increased the flotation of HIV-1 Gag and MA-FKBP, but had little effect on RSV Gag, MA, and MA-FKBP.

In previous work on binding of full length Gag to liposomes (13, 15, 27), it was assumed, explicitly or tacitly, that Gag remained monomeric, since the Gag concentration in the reticulocyte extract was presumed to be below the Kd for dimerization (~10 uM,(35)). Two scenarios could explain our present results showing that by liposome flotation both HIV-1 and RSV Gag behave more like MA multimers than MA monomers. The first is based on the presence of two highly basic domains in Gag, MA and NC, both of which may interact with membranes. Indeed it is known for HIV-1 Gag (in its non-myristoylated form) that in solution the MA and NC domains are

near each other, making the overall shape of Gag like that of a horseshoe (22, 23). Moreover, from low angle neutron scattering analyses of HIV-1 Gag bound to a tethered membrane, it appears that the horseshoe shape is maintained, implying that both domains contact the membrane simultaneously under the relatively low ionic strength conditions used (23). One domain, presumably NC, can be displaced by addition of nucleic acid or by increase of the ionic strength, leading to an extended Gag conformation. Perhaps related to these observations, HIV-1 NC appears to play a role in localizing Gag to virological synapses in uropods (51). On the other hand, the possible function of HIV-1 NC in membrane binding is called into question by the observation that wt Gag and Gag missing the NC domain bind similarly to PC/PS liposomes (18).

The second possible explanation to account for the similarity of liposome binding by Gag and multimeric MA is that Gag multimerization is promoted by the RNA in the reticulocyte extract, and/or by membranes. For example, in preliminary experiments we confirmed earlier reports that after ultracentrifugation much of HIV-1 Gag was in the pellet, even in the absence of added liposomes (78). By contrast, under the same conditions, most of the RSV Gag remained in the supernatant. To address the questions implied by these observations, it will be important to carefully compare the properties of purified Gag with the properties of *in vitro*-translated Gag in crude extracts.

Comparisons and quantitative interpretations of the various published liposome binding experiments with Gag proteins, including the flotation experiments described here, is hampered by the diversity of experimental conditions used in different labs and

even the same lab. For example, the ionic strength in the liposome-Gag mix before centrifugation as well as in the sucrose gradients has not been constant for the several published papers. Nor have the methods for liposome preparation and for centrifugation been identical. In our own work presented here, to facilitate processing of the large number of flotation experiments analyzed, we used very small (0.25mL) sucrose gradients, similar to those described by Dalton et al (20, 21, 27). In an earlier publication we used 4 mL gradients and longer centrifugation times, which may explain why some of the results are quantitatively, though not qualitatively, different. It would be very useful to develop a liposome binding assay that is more rapid and quantitative than flotation, and that has a greater dynamic range.

Both *in vivo* (13, 16, 18, 39, 41, 56) and *in vitro* (13, 16, 17, 27, 39, 41, 73, 74) PIPs stimulate PM interaction of retroviral Gag or MA proteins, but these several observations are difficult to interpret in a unified manner. For example, on the one hand the specificity of the HIV-1 MA binding pocket for short chain PI(4,5)P2 is well established (74), and depletion of PI(4,5)P2, the major PIP species at the PM, compromises HIV-1 Gag PM association (13, 16, 41). But on the other hand, HIV-1 Gag shows only very modest specificity for PI(4,5)P2 by flotation analysis (13, 16). It remains to be established to what degree PIP stimulation of membrane binding *in vitro* is due only to electrostatics.

In the experiments described here, we observed that the addition of 2% PI(4,5)P2 to liposomes enhanced binding of HIV-1 Gag more than it did the binding of monomeric or the multimeric chimeric species of MA. To explain this effect, we

speculate that PI(4,5)P2 promotes multimerization of HIV-1 Gag. This hypothesis is based in part on the effects of the PIP head group analogs on *in vitro* assembly of HIV-1 Gag. A non-myristoylated, MA-deleted version of Gag (missing residues 16-99) assembles into normal immature particles in the presence of nucleic acid (10). However, full length non-myristoylated HIV-1 Gag assembles into tiny aberrant particles. This defect can be corrected by addition of inositol hexakisphosphate (IP6) or IP5 (10). Tight interaction of IP6 with Gag requires both the MA and NC domains (24), and this interaction appears to promote a Gag monomer-trimer equilibrium. The authors of these studies interpreted the action of IP6 or IP5 in this *in vitro* system to mimic PIPs, perhaps PI(4,5)P2 or PI(3,4,5)P2. The hypothesis that PIP enhancement of liposome binding at least in part reflects a stimulation of Gag multimerization remains to be tested.

HIV-1 Gag binding to membranes *in vitro* is modulated by nucleic acid. Depletion of RNA from reticulocyte reactions by RNase treatment, or by mutation of the two lysine residues in MA that are inferred to be RNA binding residues (18), results in enhanced flotation (17, 18, 41). We have extended the study of this RNase effect to the chimeric HIV-1 MA species and to RSV. It seems surprising that in contrast to HIV-1 Gag and MA, RSV Gag and the chimeric RSV MA species hardly respond to RNase treatment of the reticulocyte lysate. The simplest explanation of these differences between the two viruses is based on the observation that the interaction of RSV MA with RNA is much weaker than that of HIV MA (K. Musier-Forsythe, personal communication). These differences may be grounded in part in the different surface potential of the MA domain,

with HIV-1 MA having a net positive surface charge of +6 compared with +3 for RSV MA (55). The importance of surface charge in this context is suggested by the observation that the super M mutant form of RSV MA, with a surface charge of +7, was similar to HIV-1 MA in the effect of RNase treatment on liposome flotation. Alternatively or in addition, HIV-1 MA has been inferred to have a specific RNA binding surface that requires specific lysine residues (18), which might be absent in RSV, even though RSV MA also can bind to RNA (80). It remains challenging to understand how RSV Gag is targeted to the PM despite both a lesser surface charge and a lack of myristoylation. We hypothesize that while both RSV and HIV-1 rely on multimerization for stable PM interaction, RSV requires higher order multimerization than does HIV-1.

For all retroviruses surprisingly little is known about the multimeric state of Gag between the time it is synthesized as a monomer on cytoplasmic polysomes and the time it becomes associated with a budding virus particle at the PM. Prior to assembly, HIV-1 Gag becomes complexed with cellular proteins, for example ABCE1 (also called HP68) (30, 47) or AP3 (29), and RSV Gag may enter similar complexes (50), but the stoichiometry of Gag molecules in these structures has not been established. In order to understand the mechanism of assembly, it will be important to determine the multimeric status of retroviral Gag proteins before they reach the plasma membrane. Two studies have addressed this issue. Based on in vivo crosslinking, Kutluay et al (49) concluded that the most abundant HIV-1 species in the cytoplasm is monomeric. Fogarty et al (32) came to a similar conclusion using multiphoton microscopy coupled with quantitative fluorescence fluctuation analysis of Gag-GFP (33, 36). With this

technology it is possible to estimate the actual molar concentration of Gag-GFP in the cystoplasm. In that experimental setting, PM binding of HIV-1 Gag-GFP as well as limited multimeric forms of Gag were observed only after the cytoplasmic concentration reached a critical concentration, approaching micromolar (Lou Mansky, personal communication). What these techniques are not able to answer unambiguously is whether Gag multimers that form in the cytoplasm then quickly become PM-bound, or alternatively Gag molecules are recruited as monomers to assembly sites on the PM. More sophisticated dynamic analyses will be needed to address these questions.

ACKNOWLEDGEMENT

This work was supported by USPHS grant CA20081-34 and its continuation as GM107013-35.

CHAPTER 4 EFERENCES

1. **Accola, M. A., B. Strack, and H. G. Gottlinger.** 2000. Efficient particle production by minimal Gag constructs which retain the carboxy-terminal domain of human immunodeficiency virus type 1 capsid-p2 and a late assembly domain. J Virol **74:**5395-402.

2. **Alfadhli, A., T. C. Dhenub, A. Still, and E. Barklis.** 2005. Analysis of human immunodeficiency virus type 1 Gag dimerization-induced assembly. J Virol **79:**14498-506.

3. **Bharat, T. A., N. E. Davey, P. Ulbrich, J. D. Riches, A. de Marco, M. Rumlova, C. Sachse, T. Ruml, and J. A. Briggs.** 2012. Structure of the immature retroviral capsid at 8 A resolution by cryo-electron microscopy. Nature **487:**385-9.

4. **Borsetti, A., A. Ohagen, and H. G. Gottlinger.** 1998. The C-terminal half of the human immunodeficiency virus type 1 Gag precursor is sufficient for efficient particle assembly. J Virol **72:**9313-7.

5. **Briggs, J. A., J. D. Riches, B. Glass, V. Bartonova, G. Zanetti, and H. G. Krausslich.** 2009. Structure and assembly of immature HIV. Proc Natl Acad Sci U S A **106:**11090-5.

6. **Buboltz, J. T., and G. W. Feigenson.** 1999. A novel strategy for the preparation of liposomes: rapid solvent exchange. Biochim Biophys Acta **1417:**232-45.

7. **Butterfield-Gerson, K. L., L. Z. Scheifele, E. P. Ryan, A. K. Hopper, and L. J. Parent.** 2006. Importin-beta family members mediate alpharetrovirus gag nuclear entry via interactions with matrix and nucleocapsid. J Virol **80:**1798-806.

8. **Callahan, E., and J. Wills.** 2003. Link between genome packaging and rate of budding for Rous sarcoma virus. J Virol **77:**9388-98.

9. **Callahan, E., and J. Wills.** 2000. Repositioning basic residues in the M domain of the Rous sarcoma virus gag protein. J Virol **74:**11222-9.

10. **Campbell, S., R. Fisher, E. Towler, S. Fox, H. Issaq, T. Wolfe, L. Phillips, and A. Rein.** 2001. Modulation of HIV-like particle assembly in vitro by inositol phosphates. Proc Natl Acad Sci U S A **98:**10875-9.

11. **Campbell, S., and A. Rein.** 1999. In vitro assembly properties of human immunodeficiency virus type 1 Gag protein lacking the p6 domain. J Virol **73:**2270-9.

12. **Campbell, S., and V. M. Vogt.** 1997. In vitro assembly of virus-like particles with Rous sarcoma virus Gag deletion mutants: identification of the p10 domain as a morphological determinant in the formation of spherical particles. J Virol **71:**4425-35.

13. **Chan, J., R. A. Dick, and V. M. Vogt.** 2011. Rous sarcoma virus gag has no specific requirement for phosphatidylinositol-(4,5)-bisphosphate for plasma membrane association in vivo or for liposome interaction in vitro. J Virol **85:**10851-60.

14. **Chen, B. K., I. Rousso, S. Shim, and P. S. Kim.** 2001. Efficient assembly of an HIV-1/MLV Gag-chimeric virus in murine cells. Proc Natl Acad Sci U S A **98:**15239-44.

15. **Chukkapalli, V., I. Hogue, V. Boyko, W. Hu, and A. Ono.** 2008. Interaction between the human immunodeficiency virus type 1 Gag matrix domain and phosphatidylinositol-(4,5)-bisphosphate is essential for efficient gag membrane binding. J Virol **82:**2405-17.

16. **Chukkapalli, V., I. B. Hogue, V. Boyko, W. S. Hu, and A. Ono.** 2008. Interaction between the human immunodeficiency virus type 1 Gag matrix domain and phosphatidylinositol-(4,5)-bisphosphate is essential for efficient gag membrane binding. J Virol **82:**2405-17.

17. **Chukkapalli, V., J. Inlora, G. C. Todd, and A. Ono.** 2013. Evidence in Support of RNA-Mediated Inhibition of Phosphatidylserine-Dependent HIV-1 Gag Membrane Binding in Cells. J Virol **87:**7155-9.

18. **Chukkapalli, V., S. J. Oh, and A. Ono.** 2010. Opposing mechanisms involving RNA and lipids regulate HIV-1 Gag membrane binding through the highly basic region of the matrix domain. Proc Natl Acad Sci U S A **107:**1600-5.

19. **Crist, R. M., S. A. Datta, A. G. Stephen, F. Soheilian, J. Mirro, R. J. Fisher, K. Nagashima, and A. Rein.** 2009. Assembly properties of human immunodeficiency virus type 1 Gag-leucine zipper chimeras: implications for retrovirus assembly. J Virol **83:**2216-25.

20. **Dalton, A., P. Murray, D. Murray, and V. Vogt.** 2005. Biochemical characterization of rous sarcoma virus MA protein interaction with membranes. J Virol **79:**6227-38.

21. **Dalton, A. K., D. Ako-Adjei, P. S. Murray, D. Murray, and V. M. Vogt.** 2007. Electrostatic interactions drive membrane association of the human immunodeficiency virus type 1 Gag MA domain. J Virol **81:**6434-45.

22. **Datta, S. A., J. E. Curtis, W. Ratcliff, P. K. Clark, R. M. Crist, J. Lebowitz, S. Krueger, and A. Rein.** 2007. Conformation of the HIV-1 Gag protein in solution. J Mol Biol **365:**812-24.

23. **Datta, S. A., F. Heinrich, S. Raghunandan, S. Krueger, J. E. Curtis, A. Rein, and H. Nanda.** 2011. HIV-1 Gag extension: conformational changes require simultaneous interaction with membrane and nucleic acid. J Mol Biol **406:**205-14.

24. **Datta, S. A., Z. Zhao, P. K. Clark, S. Tarasov, J. N. Alexandratos, S. J. Campbell, M. Kvaratskhelia, J. Lebowitz, and A. Rein.** 2007. Interactions between HIV-1 Gag molecules in solution: an inositol phosphate-mediated switch. J Mol Biol **365:**799-811.

25. **del Alamo, M., J. L. Neira, and M. G. Mateu.** 2003. Thermodynamic dissection of a low affinity protein-protein interface involved in human immunodeficiency virus assembly. J Biol Chem **278:**27923-9.

26. **Demirov, D. G., and E. O. Freed.** 2004. Retrovirus budding. Virus Res **106:**87-102.

27. **Dick, R. A., S. L. Goh, G. W. Feigenson, and V. M. Vogt.** 2012. HIV-1 Gag protein can sense the cholesterol and acyl chain environment in model membranes. Proc Natl Acad Sci U S A **109:**18761-6.

28. **Ding, L., A. Derdowski, J. J. Wang, and P. Spearman.** 2003. Independent segregation of human immunodeficiency virus type 1 Gag protein complexes and lipid rafts. J Virol **77:**1916-26.

29. **Dong, X., H. Li, A. Derdowski, L. Ding, A. Burnett, X. Chen, T. R. Peters, T. S. Dermody, E. Woodruff, J. J. Wang, and P. Spearman.** 2005. AP-3 directs the intracellular trafficking of HIV-1 Gag and plays a key role in particle assembly. Cell **120:**663-74.

30. **Dooher, J. E., B. L. Schneider, J. C. Reed, and J. R. Lingappa.** 2007. Host ABCE1 is at plasma membrane HIV assembly sites and its dissociation from Gag is linked to subsequent events of virus production. Traffic **8:**195-211.

31. **Fernandes, F., K. Chen, L. S. Ehrlich, J. Jin, M. H. Chen, G. N. Medina, M. Symons, R. Montelaro, J. Donaldson, N. Tjandra, and C. A. Carter.** 2010. Phosphoinositides Direct Equine Infectious Anemia Virus Gag Trafficking and Release. Traffic.

32. **Fogarty, K. H., Y. Chen, I. F. Grigsby, P. J. Macdonald, E. M. Smith, J. L. Johnson, J. M. Rawson, L. M. Mansky, and J. D. Mueller.** 2011. Characterization of cytoplasmic Gag-gag interactions by dual-color z-scan fluorescence fluctuation spectroscopy. Biophys J **100:**1587-95.

33. **Fogarty, K. H., W. Zhang, I. F. Grigsby, J. L. Johnson, Y. Chen, J. D. Mueller, and L. M. Mansky.** 2011. New insights into HTLV-1 particle structure, assembly, and Gag-Gag interactions in living cells. Viruses **3:**770-93.

34. **Freed, E. O.** 2006. HIV-1 Gag: flipped out for PI(4,5)P(2). Proc Natl Acad Sci U S A **103:**11101-2.

35. **Gamble, T. R., S. Yoo, F. F. Vajdos, U. K. von Schwedler, D. K. Worthylake, H. Wang, J. P. McCutcheon, W. I. Sundquist, and C. P. Hill.** 1997. Structure of the carboxyl-terminal dimerization domain of the HIV-1 capsid protein. Science **278:**849-53.

36. **Grigsby, I. F., W. Zhang, J. L. Johnson, K. H. Fogarty, Y. Chen, J. M. Rawson, A. J. Crosby, J. D. Mueller, and L. M. Mansky.** 2010. Biophysical analysis of HTLV-1 particles reveals novel insights into particle morphology and Gag stochiometry. Retrovirology **7:**75.

37. **Gross, I., H. Hohenberg, and H. G. Krausslich.** 1997. In vitro assembly properties of purified bacterially expressed capsid proteins of human immunodeficiency virus. Eur J Biochem **249:**592-600.

38. **Gudleski, N., J. M. Flanagan, E. P. Ryan, M. C. Bewley, and L. J. Parent.** 2010. Directionality of nucleocytoplasmic transport of the retroviral gag protein depends on sequential binding of karyopherins and viral RNA. Proc Natl Acad Sci U S A **107:**9358-63.

39. **Hamard-Peron, E., F. Juillard, J. Saad, C. Roy, P. Roingeard, M. Summers, J. Darlix, C. Picart, and D. Muriaux.** 2010. Targeting of murine leukemia virus gag to the plasma membrane is mediated by PI(4,5)P2/PS and a polybasic region in the matrix. J Virol **84:**503-15.

40. **Hearps, A. C., K. M. Wagstaff, S. C. Piller, and D. A. Jans.** 2008. The N-terminal basic domain of the HIV-1 matrix protein does not contain a conventional nuclear localization sequence but is required for DNA binding and protein self-association. Biochemistry **47:**2199-210.

41. **Inlora, J., V. Chukkapalli, D. Derse, and A. Ono.** 2011. Gag Localization and Virus-like Particle Release Mediated by the Matrix Domain of Human T-Lymphotropic Virus Type-1 Gag are Less Dependent on Phosphatidylinositol-(4,5)-bisphosphate than Those Mediated by the Matrix Domain of Human Immunodeficiency Virus Type-1 Gag. J Virol.

42. **Johnson, M. C., H. M. Scobie, Y. M. Ma, and V. M. Vogt.** 2002. Nucleic acid-independent retrovirus assembly can be driven by dimerization. J Virol **76:**11177-85.

43. **Jouvenet, N., S. J. Neil, C. Bess, M. C. Johnson, C. A. Virgen, S. M. Simon, and P. D. Bieniasz.** 2006. Plasma membrane is the site of productive HIV-1 particle assembly. PLoS Biol **4:**e435.

44. **Kay, J. E.** 1996. Structure-function relationships in the FK506-binding protein (FKBP) family of peptidylprolyl cis-trans isomerases. Biochem J **314 (Pt 2):**361-85.

45. **Keller, P. W., M. C. Johnson, and V. M. Vogt.** 2008. Mutations in the spacer peptide and adjoining sequences in Rous sarcoma virus Gag lead to tubular budding. J Virol **82:**6788-97.

46. **Kerfeld, C. A., M. R. Sawaya, S. Tanaka, C. V. Nguyen, M. Phillips, M. Beeby, and T. O. Yeates.** 2005. Protein structures forming the shell of primitive bacterial organelles. Science **309:**936-8.

47. **Klein, K. C., J. C. Reed, M. Tanaka, V. T. Nguyen, S. Giri, and J. R. Lingappa.** 2011. HIV Gag-leucine zipper chimeras form ABCE1-containing intermediates and RNase-resistant immature capsids similar to those formed by wild-type HIV-1 Gag. J Virol **85:**7419-35.

48. **Krausslich, H. G., M. Facke, A. M. Heuser, J. Konvalinka, and H. Zentgraf.** 1995. The spacer peptide between human immunodeficiency virus capsid and nucleocapsid proteins is essential for ordered assembly and viral infectivity. J Virol **69:**3407-19.

49. **Kutluay, S. B., and P. D. Bieniasz.** 2010. Analysis of the initiating events in HIV-1 particle assembly and genome packaging. PLoS Pathog **6:**e1001200.

50. **Larson, D. R., Y. M. Ma, V. M. Vogt, and W. W. Webb.** 2003. Direct measurement of Gag-Gag interaction during retrovirus assembly with FRET and fluorescence correlation spectroscopy. J Cell Biol **162:**1233-44.

51. **Llewellyn, G. N., I. B. Hogue, J. R. Grover, and A. Ono.** 2010. Nucleocapsid promotes localization of HIV-1 gag to uropods that participate in virological synapses between T cells. PLoS Pathog **6:**e1001167.

52. **Lochrie, M. A., S. Waugh, D. G. Pratt, Jr., J. Clever, T. G. Parslow, and B. Polisky.** 1997. In vitro selection of RNAs that bind to the human immunodeficiency virus type-1 gag polyprotein. Nucleic Acids Res **25:**2902-10.

53. **Ma, Y. M., and V. M. Vogt.** 2004. Nucleic acid binding-induced Gag dimerization in the assembly of Rous sarcoma virus particles in vitro. J Virol **78:**52-60.

54. **Ma, Y. M., and V. M. Vogt.** 2002. Rous sarcoma virus Gag protein-oligonucleotide interaction suggests a critical role for protein dimer formation in assembly. J Virol **76:**5452-62.

55. **Murray, P., Z. Li, J. Wang, C. Tang, B. Honig, and D. Murray.** 2005. Retroviral matrix domains share electrostatic homology: models for membrane binding function throughout the viral life cycle. Structure **13:**1521-31.

56. **Nadaraia-Hoke, S., D. V. Bann, T. L. Lochmann, N. Gudleski-O'Regan, and L. J. Parent.** 2013. Alterations in the MA and NC domains modulate phosphoinositide-dependent plasma membrane localization of the Rous sarcoma virus Gag protein. J Virol.

57. **O'Carroll, I. P., F. Soheilian, A. Kamata, K. Nagashima, and A. Rein.** 2013. Elements in HIV-1 Gag contributing to virus particle assembly. Virus Res.

58. **Ono, A., S. Ablan, S. Lockett, K. Nagashima, and E. Freed.** 2004. Phosphatidylinositol (4,5) bisphosphate regulates HIV-1 Gag targeting to the plasma membrane. Proc Natl Acad Sci U S A **101:**14889-94.

59. **Ono, A., D. Demirov, and E. O. Freed.** 2000. Relationship between human immunodeficiency virus type 1 Gag multimerization and membrane binding. J Virol **74:**5142-50.

60. **Ono, A., and E. O. Freed.** 1999. Binding of human immunodeficiency virus type 1 Gag to membrane: role of the matrix amino terminus. J Virol **73:**4136-44.

61. **Parent, L. J., T. M. Cairns, J. A. Albert, C. B. Wilson, J. W. Wills, and R. C. Craven.** 2000. RNA dimerization defect in a Rous sarcoma virus matrix mutant. J Virol **74:**164-72.

62. **Parent, L. J., C. B. Wilson, M. D. Resh, and J. W. Wills.** 1996. Evidence for a second function of the MA sequence in the Rous sarcoma virus Gag protein. J Virol **70:**1016-26.

63. **Perez-Caballero, D., T. Hatziioannou, J. Martin-Serrano, and P. D. Bieniasz.** 2004. Human immunodeficiency virus type 1 matrix inhibits and confers cooperativity on gag precursor-membrane interactions. J Virol **78:**9560-3.

64. **Phillips, J. M., P. S. Murray, D. Murray, and V. M. Vogt.** 2008. A molecular switch required for retrovirus assembly participates in the hexagonal immature lattice. EMBO J **27:**1411-20.

65. **Pornillos, O., B. K. Ganser-Pornillos, B. N. Kelly, Y. Hua, F. G. Whitby, C. D. Stout, W. I. Sundquist, C. P. Hill, and M. Yeager.** 2009. X-ray structures of the hexameric building block of the HIV capsid. Cell **137:**1282-92.

66. **Prchal, J., P. Srb, E. Hunter, T. Ruml, and R. Hrabal.** 2012. The structure of myristoylated Mason-Pfizer monkey virus matrix protein and the role of phosphatidylinositol-(4,5)-bisphosphate in its membrane binding. J Mol Biol **423:**427-38.

67. **Purohit, P., S. Dupont, M. Stevenson, and M. R. Green.** 2001. Sequence-specific interaction between HIV-1 matrix protein and viral genomic RNA revealed by in vitro genetic selection. RNA **7:**576-84.

68. **Ramalingam, D., S. Duclair, S. A. Datta, A. Ellington, A. Rein, and V. R. Prasad.** 2011. RNA aptamers directed to human immunodeficiency virus type 1 Gag polyprotein bind to the matrix and nucleocapsid domains and inhibit virus production. J Virol **85:**305-14.

69. **Reed, M., R. Mariani, L. Sheppard, K. Pekrun, N. R. Landau, and N. W. Soong.** 2002. Chimeric human immunodeficiency virus type 1 containing murine leukemia virus matrix assembles in murine cells. J Virol **76:**436-43.

70. **Reil, H., A. A. Bukovsky, H. R. Gelderblom, and H. G. Gottlinger.** 1998. Efficient HIV-1 replication can occur in the absence of the viral matrix protein. EMBO J **17:**2699-708.

71. **Resh, M. D.** 1999. Fatty acylation of proteins: new insights into membrane targeting of myristoylated and palmitoylated proteins. Biochim Biophys Acta **1451:**1-16.

72. **Rollins, C. T., V. M. Rivera, D. N. Woolfson, T. Keenan, M. Hatada, S. E. Adams, L. J. Andrade, D. Yaeger, M. R. van Schravendijk, D. A. Holt, M. Gilman, and T. Clackson.** 2000. A ligand-reversible dimerization system for controlling protein-protein interactions. Proc Natl Acad Sci U S A **97:**7096-101.

73. **Saad, J., S. Ablan, R. Ghanam, A. Kim, K. Andrews, K. Nagashima, F. Soheilian, E. Freed, and M. Summers.** 2008. Structure of the myristylated human immunodeficiency virus type 2 matrix protein and the role of phosphatidylinositol-(4,5)-bisphosphate in membrane targeting. J Mol Biol **382:**434-47.

74. **Saad, J., J. Miller, J. Tai, A. Kim, R. Ghanam, and M. Summers.** 2006. Structural basis for targeting HIV-1 Gag proteins to the plasma membrane for virus assembly. Proc Natl Acad Sci U S A **103:**11364-9.

75. **Scheifele, L. Z., R. A. Garbitt, J. D. Rhoads, and L. J. Parent.** 2002. Nuclear entry and CRM1-dependent nuclear export of the Rous sarcoma virus Gag polyprotein. Proc Natl Acad Sci U S A **99:**3944-9.

76. **Schreiber, S. L.** 1991. Chemistry and biology of the immunophilins and their immunosuppressive ligands. Science **251:**283-7.

77. **Spearman, P., R. Horton, L. Ratner, and I. Kuli-Zade.** 1997. Membrane binding of human immunodeficiency virus type 1 matrix protein in vivo supports a conformational myristyl switch mechanism. J Virol **71:**6582-92.

78. **Spearman, P., and L. Ratner.** 1996. Human immunodeficiency virus type 1 capsid formation in reticulocyte lysates. J Virol **70:**8187-94.

79. **Spencer, D. M., T. J. Wandless, S. L. Schreiber, and G. R. Crabtree.** 1993. Controlling signal transduction with synthetic ligands. Science **262:**1019-24.

80. **Steeg, C. M., and V. M. Vogt.** 1990. RNA-binding properties of the matrix protein (p19gag) of avian sarcoma and leukemia viruses. J Virol **64:**847-55.

81. **Tang, C., E. Loeliger, P. Luncsford, I. Kinde, D. Beckett, and M. F. Summers.** 2004. Entropic switch regulates myristate exposure in the HIV-1 matrix protein. Proc Natl Acad Sci U S A **101:**517-22.

82. **Urano, E., T. Aoki, Y. Futahashi, T. Murakami, Y. Morikawa, N. Yamamoto, and J. Komano.** 2008. Substitution of the myristoylation signal of human immunodeficiency virus type 1 Pr55Gag with the phospholipase C-delta1

pleckstrin homology domain results in infectious pseudovirion production. J Gen Virol **89:**3144-9.

83. **van Meer, G., D. R. Voelker, and G. W. Feigenson.** 2008. Membrane lipids: where they are and how they behave. Nat Rev Mol Cell Biol **9:**112-24.

84. **Vlach, J., and J. S. Saad.** 2013. Trio engagement via plasma membrane phospholipids and the myristoyl moiety governs HIV-1 matrix binding to bilayers. Proc Natl Acad Sci U S A.

85. **Wright, E. R., J. B. Schooler, H. J. Ding, C. Kieffer, C. Fillmore, W. I. Sundquist, and G. J. Jensen.** 2007. Electron cryotomography of immature HIV-1 virions reveals the structure of the CA and SP1 Gag shells. EMBO J **26:**2218-26.

86. **Yu, F., S. M. Joshi, Y. M. Ma, R. L. Kingston, M. N. Simon, and V. M. Vogt.** 2001. Characterization of Rous sarcoma virus Gag particles assembled in vitro. J Virol **75:**2753-64.

87. **Zhang, Y., H. Qian, Z. Love, and E. Barklis.** 1998. Analysis of the assembly function of the human immunodeficiency virus type 1 gag protein nucleocapsid domain. J Virol **72:**1782-9.

88. **Zhao, J., J. Wu, F. A. Heberle, T. T. Mills, P. Klawitter, G. Huang, G. Costanza, and G. W. Feigenson.** 2007. Phase studies of model biomembranes: complex behavior of DSPC/DOPC/cholesterol. Biochim Biophys Acta **1768:**2764-76.

89. **Zhou, W., and M. D. Resh.** 1996. Differential membrane binding of the human immunodeficiency virus type 1 matrix protein. J Virol **70:**8540-8.

CHAPTER 5

PERSPECTIVES

My work, and the work of many others, has identified key principles involved in the binding of Gag to the inner leaflet of the plasma membrane. These principles include electrostatics, fatty acid modification of MA, multimerization of Gag, interaction with lipids such as PI(4,5)P2, and the ability of MA to sense the hydrophobic core of the membrane. However, there remains a great deal that we don't understand about these key signals. What are some of the critical questions and issues that remain and how should we begin to address them?

STANDARDIZING BINDING ASSAYS

Traditionally *in vitro* membrane binding studies employ a flotation assay, similar to the one used in the studies presented here. However, not all flotation assays are created equal, which is likely the source of a number of discrepancies between studies. These differences include the size of the sucrose gradient, ranging from 250 uL to 5 mL, the type of rotor used, fixed angle vs swinging bucket, and the ionic strength of both the binding reaction and the sucrose gradient. Arguably the most important difference between studies is the method used to prepare liposomes. In some studies liposomes have been prepared by gentle rehydration and sonication, which results in multilamellar membrane sheets and vesicles of varying size. Other studies extrude rehydrated membranes resulting in uniformly sized unilamellar vesicles. Individually each of the

above-mentioned methodological differences may have a small effect on the outcome of an experiment, but collectively these differences may add up resulting in striking incongruencies between studies. At a minimum it will be important for the field to take these experimental variations into consideration when comparing results. Ideally, adoption of more standardized methods of measuring protein membrane interactions should take place.

MOVING FORWARD: HOW TO STUDY PROTEIN MEMBRANE INTERACTIONS MORE PRECISELY?

A number of alternative ways to measure protein membrane interactions can be used. I will describe a few of them briefly, as well as some of the advantages and disadvantages of each.

Fluorescence correlation microscopy

Fluorescent correlation spectroscopy (FCS) can be used to measure the diffusion rate of small, fluorescently labeled molecules, proteins for example, in solution (15). Compared to a 100 nanometer LUV (a standard size) the diffusion of a protein is extremely rapid. However, if the protein is bound to an LUV, its diffusion rate will be dramatically decreased and the difference in diffusion rate can be measured. Two advantages of this method are that the measurements require only small amounts of material, and the measurements are many times more rapid than the traditional flotation method. A disadvantage of this method is that if the protein aggregates, it may be

difficult to tell if a slow moving fluorophore is a protein aggregate, or protein bound to an LUV.

Using GUVs to study protein membrane interactions

Unlike liposomes, which are too small to see microscopically, GUVs can be used to observe binding of proteins to a membrane. One advantage of this method is that GUVs can exhibit macroscopic phase behavior (coexisting liquid-ordered and liquid-disordered phases). If a membrane binding protein of interest binds preferentially to the liquid-ordered or the liquid-disordered phase, the preference could be detected. Alternatively, if protein binding to a GUV induces the formation of a phase, this may also be detected. GUVs have been used successfully to show that multimeric HIV-1 MA binds preferentially to the liquid-disordered phase (9), and to show the sequence with which ESCRT proteins bind to sites of Gag assembly (1). A major hurdle of using GUVs to study electrostatic protein-membrane interactions is that phase diagrams for PS containing lipid mixtures do not exist. This makes the interpretation of results difficult. For example, if a protein binds preferentially to the liquid-disordered phase, is it binding because of the membrane behavior or because PS is enriched in the liquid-disordered phase? One drawback to using GUVs to study protein-membrane interactions is that GUVs are difficult and time intensive to prepare, which means that only a limited number of binding conditions can be tested in an economical amount of time.

Total internal reflection fluorescence microscopy and supported bilayers

Supported bilayers are prepared by depositing vesicles onto a solid support, such as a glass slide. These vesicles can form a unilamellar bilayer, which is supported by a

thin (5-10Å) layer of water (11). One downside of supported bilayers is the significant hydrodynamic coupling between the slide and the inner leaflet of the bilayer, which can influence the phase behavior of the membrane (11).

Total internal reflection fluorescence (TIRF) microscopy is a method used to excite and visualize fluorophores at or near the plasma membrane of cells grown on slides or coverslips (17). The fluorophores are excited by an evanescent field, which occurs when light passes from a high refractive medium, such as glass, to a low refractive medium, such as a cell (17). Because TIRF only excites fluorophores within a couple hundred nanometers of the membrane-coverslip interface, the background fluorescence is very low. Using TIRF on a supported bilayer is similar to using TIRF to study a cell. The evanescent field only excites fluorescently tagged protein, Gag-GFP for example, near the bilayer surface. If binding of Gag to the supported bilayer results in Gag multimerization it should be possible to detect this by TIRF. The multimerized Gag, or Gag puncta, on a supported bilayer could be representative of an assembly, analogous to what occurs at the plasma membrane of cells during the late stage of the viral life cycle. If the membrane supports Gag assembly, the effects of different lipid components and mixtures on the rate of assembly could be tested. For example, does PI(4,5)P2 enhance binding of Gag as measured by liposome flotation assays, or does PI(4,5)P2 promote assembly of Gag?

One drawback of this system is that some lipid mixtures do not form stable supported bilayers. PE-based membranes, for example, form a bilayer that, in the presence of protein, becomes unstable (personal communication, Gerald Feigenson

and Hirsh Nanda). It is possible that alternative bilayer supports may allow for the use of PE-based supported bilayers. However, if the negative effect of PE on the stability of a supported bilayer cannot be remedied, it may be possible to perform similar measurements using PE based GUVs.

INNER LEAFLET PLASMA MEMBRANE LIPID MIXTURES

Many Gag-membrane binding studies use a lipid mixture that is not representative of the lipids found in the inner leaflet of the plasma membrane, and therefore developing a model inner leaflet lipid mix should be a priority. For example, model membranes are typically made with the neutral outer leaflet lipid PC instead of the neutral inner leaflet lipid PE. The very large differences in head group size of PC and PE could dramatically alter the binding of protein. In addition, cholesterol is frequently not included in model membrane mixes, and neither are lipids that represent smaller fractions of the membrane such as sphingomyelin, plasmalogen-PE, and PI. Not only is a model inner leaflet lipid mix rarely used to study protein-membrane interactions, there is essentially no information on the phase behavior of such a lipid mixture. In conclusion, an inner leaflet lipid mixture should be developed and characterized followed by an analysis of the amount of protein binding this lipid mixture supports. These inner leaflet mixes should also be used in the previously described FCS, TIRF-microscopy supported bilayer, and GUV methods.

CHARACTERIZING PIP BEHAVIOR

While we know that HIV-1 Gag membrane binding is sensitive to the presence of PI(4,5)P2 in membranes (2, 3, 13), and *in vitro* as little as 2% PI(4,5)P2 can increase Gag membrane binding by ten fold (7), we understand surprisingly little about how PIPs behave in membranes. It is never explicitly stated in publications but PIPs are generally presented as freely diffusing, evenly distributed lipids that do not demonstrate any phase behavior. However, the opposite may be true. Evidence is emerging from studies of model membranes, that PIPs cluster in membranes (10, 14). Strong intermolecular and intramolecular hydrogen bond networks drive the formation of the PIP clusters, and under certain conditions these clusters represent a separate membrane phase (10, 14). These PIP clusters may serve as specialized binding sites for retroviral Gag proteins. If PIP clustering proves to be a biologically relevant type of lipid organization, characterizing it will be extremely important. It will be necessary to determine the concentration at which PIP clusters form, and what the PIP concentration is in the clusters. Also, how does the propensity to cluster depend on other types of lipids present in the membrane? Finally, what effect does protein binding to the membrane have on PIP clustering?

GAG CONFORMATION AND NUCLEOCAPSID MEMBRANE BINDING

The binding of Gag to the inner leaflet of the plasma membrane is mediated by Gag's MA domain, but could the positively charged C-terminal NC domain also be involved? Size exclusion chromatography (SEC) and small angle X-ray scattering

(SAXS) of HIV-1 Gag show the Gag polyprotein to be in a compact, horseshoe conformation (4). This conformation is also observed for dimers of Gag (5). These conformation studies raise the possibility that both the MA and NC domain interact with the cellular plasma membrane prior to or during virion assembly.

Low angle neutron reflectometry (LANR) shows that, at low ionic strength (50mM NaCl) both the MA and NC domains of HIV-1 Gag interact with the plasma membrane (5). The addition of a short oligonucleotide, too short to induce assembly of Gag into VLPs, results in the extension of the Gag protein (5). This extended structure is interpreted as MA bound to the membrane and NC bound to the oligonucleotide (5). By contrast, MLV Gag in solution is in a rod-like extended conformation (6), but LANR studies suggest that when bound to membranes, the protein also is in a horseshoe conformation with both MA and NC domains interacting with the supported bilayer (personal communication, Hirsh Nanda). Taken together these observations have led to a model in which both ends of Gag bind to the PM. Upon the binding of vgRNA to NC, which outcompetes NC binding to the PM, Gag takes on an assembly competent extended conformation. One major downside of this model is that the studies that led to it were done with a purified HIV-1 Gag that is non-myristoylated (4, 5), because the myristoylated form of Gag cannot be purified in substantial amounts. But myristoylation is critical for membrane binding and virion assembly *in vivo* (12).

Moving forward it will be critical to determine if other retroviral Gag proteins exhibit membrane-binding behavior similar to that of HIV-1 Gag. RSV Gag would be an

excellent candidate for these studies because it is not naturally myristoylated and it can be purified in concentrated form (unpublished data).

If NC shows membrane binding behavior at physiological salt concentrations it will be important to determine if NC binding is enhanced to membranes containing PI(4,5)P2. NC has characteristics similar to the poly-lysine domain of the myristoylated alanine-rich C kinase substrate (MARCKS), a very well studied protein, and so it may be useful to consider the membrane binding properties of the MARCKS peptide. One characteristic of the highly basic MARCKS peptide is its ability to cluster PI(4,5)P2 in membranes (8, 18-20). If NC also clusters PI(4,5)P2, Gag binding may set up a membrane domain where other Gag proteins preferentially bind. This positive feedback could promote virion assembly.

NEUTRON SCATTERING STUDIES OF PROTEIN MEMBRANE INTERACTIONS

What happens to the membrane when a protein binds to it? One way to begin to answer this question employs neutron scattering techniques. Neutrons are uniquely suited for studying lipids and membranes. Unlike X-rays, which interact with the electron cloud surrounding the nucleus, neutrons interact with atomic nuclei (16). Small angle neutron scattering (SANS) is similar to small angle x-ray scattering (SAXS). However, SANS is especially sensitive to hydrogen and deuterium. Molecules containing increasing percentages of hydrogen–for example proteins, membranes, and water–have increasing scattering length densities (SLD) (16). The different SLDs of proteins and lipids can be contrast matched to the aqueous environment by replacing

water with deuterated water (16). For example, contrast-matching protein to the aqueous solution, between 40-45% D_20, effectively makes the protein invisible. This is useful because it allows for the identification of patterns generated by lipids only, even in the presence of protein. SANS could be used to determine the effect of Gag binding to a membrane, such as changes to the lipid packing of the membrane.

SUMMARY

In this chapter I have briefly described some of the remaining questions about retroviral Gag protein binding to membranes. I have also suggested a number of approaches that could be taken to begin to answer these questions. None of these approaches is without downsides, but if they are used in concert, those downsides can be minimized.

The binding of any protein to a membrane involves a limited number of principles. So the study of one protein-membrane interaction may shed light on how other proteins interact with membranes. Therefore future work in this field may have broad implications to cellular biology in general.

CHAPTER 5 REFERENCES

1. **Carlson, L. A., and J. H. Hurley.** 2012. In vitro reconstitution of the ordered assembly of the endosomal sorting complex required for transport at membrane-bound HIV-1 Gag clusters. Proc Natl Acad Sci U S A **109:**16928-33.

2. **Chan, J., R. A. Dick, and V. M. Vogt.** 2011. Rous sarcoma virus gag has no specific requirement for phosphatidylinositol-(4,5)-bisphosphate for plasma membrane association in vivo or for liposome interaction in vitro. J Virol **85:**10851-60.

3. **Chukkapalli, V., I. B. Hogue, V. Boyko, W. S. Hu, and A. Ono.** 2008. Interaction between the human immunodeficiency virus type 1 Gag matrix domain and phosphatidylinositol-(4,5)-bisphosphate is essential for efficient gag membrane binding. J Virol **82:**2405-17.

4. **Datta, S. A., J. E. Curtis, W. Ratcliff, P. K. Clark, R. M. Crist, J. Lebowitz, S. Krueger, and A. Rein.** 2007. Conformation of the HIV-1 Gag protein in solution. J Mol Biol **365:**812-24.

5. **Datta, S. A., F. Heinrich, S. Raghunandan, S. Krueger, J. E. Curtis, A. Rein, and H. Nanda.** 2011. HIV-1 Gag extension: conformational changes require simultaneous interaction with membrane and nucleic acid. J Mol Biol **406:**205-14.

6. **Datta, S. A., X. Zuo, P. K. Clark, S. J. Campbell, Y. X. Wang, and A. Rein.** 2011. Solution properties of murine leukemia virus gag protein: differences from HIV-1 gag. J Virol **85:**12733-41.

7. **Dick, R. A., S. L. Goh, G. W. Feigenson, and V. M. Vogt.** 2012. HIV-1 Gag protein can sense the cholesterol and acyl chain environment in model membranes. Proc Natl Acad Sci U S A **109:**18761-6.

8. **Gambhir, A., G. Hangyas-Mihalyne, I. Zaitseva, D. S. Cafiso, J. Wang, D. Murray, S. N. Pentyala, S. O. Smith, and S. McLaughlin.** 2004. Electrostatic sequestration of PIP2 on phospholipid membranes by basic/aromatic regions of proteins. Biophys J **86:**2188-207.

9. **Keller, H., H. G. Krausslich, and P. Schwille.** 2012. Multimerizable HIV Gag derivative binds to the liquid-disordered phase in model membranes. Cell Microbiol.

10. **Kooijman, E. E., K. E. King, M. Gangoda, and A. Gericke.** 2009. Ionization properties of phosphatidylinositol polyphosphates in mixed model membranes. Biochemistry **48:**9360-71.

11. **Kuhner, M., R. Tampe, and E. Sackmann.** 1994. Lipid mono- and bilayer supported on polymer films: composite polymer-lipid films on solid substrates. Biophys J **67:**217-26.

12. **O'Carroll, I. P., F. Soheilian, A. Kamata, K. Nagashima, and A. Rein.** 2012. Elements in HIV-1 Gag contributing to virus particle assembly. Virus Res.

13. **Ono, A., S. D. Ablan, S. J. Lockett, K. Nagashima, and E. O. Freed.** 2004. Phosphatidylinositol (4,5) bisphosphate regulates HIV-1 Gag targeting to the plasma membrane. Proc Natl Acad Sci U S A **101:**14889-94.

14. **Redfern, D. A., and A. Gericke.** 2005. pH-dependent domain formation in phosphatidylinositol polyphosphate/phosphatidylcholine mixed vesicles. J Lipid Res **46:**504-15.

15. **Rusu, L., A. Gambhir, S. McLaughlin, and J. Radler.** 2004. Fluorescence correlation spectroscopy studies of Peptide and protein binding to phospholipid vesicles. Biophys J **87:**1044-53.

16. **Schoenborn, B. P.** 1976. Neutron scattering for the analysis of membranes. Biochim Biophys Acta **457:**41-55.

17. **Trache, A., and G. A. Meininger.** 2008. Total internal reflection fluorescence (TIRF) microscopy. Curr Protoc Microbiol **Chapter 2:**Unit 2A 2 1-2A 2 22.

18. **Wang, J., A. Gambhir, G. Hangyas-Mihalyne, D. Murray, U. Golebiewska, and S. McLaughlin.** 2002. Lateral sequestration of phosphatidylinositol 4,5-bisphosphate by the basic effector domain of myristoylated alanine-rich C kinase substrate is due to nonspecific electrostatic interactions. J Biol Chem **277:**34401-12.

19. **Wang, J., A. Gambhir, S. McLaughlin, and D. Murray.** 2004. A computational model for the electrostatic sequestration of PI(4,5)P2 by membrane-adsorbed basic peptides. Biophys J **86:**1969-86.

20. **Zhang, W., E. Crocker, S. McLaughlin, and S. O. Smith.** 2003. Binding of peptides with basic and aromatic residues to bilayer membranes: phenylalanine in the myristoylated alanine-rich C kinase substrate effector domain penetrates into the hydrophobic core of the bilayer. J Biol Chem **278:**21459-66.